U.PORTO

FMUP FACULDADE DE MEDICINA
UNIVERSIDADE DO PORTO

UNDERSTANDING THE MECHANISMS OF ACETYL-L-CARNITINE THROUGH NEUROPROTECTION AFTER METHAMPHETAMINE ADMINISTRATION

SÍLVIA FERNANDES

TESE DE DOUTORAMENTO APRESENTADA

À FACULDADE DE MEDICINA DA UNIVERSIDADE DO PORTO EM

NEUROCIÊNCIAS – RAMO NEUROCIÊNCIAS EXPERIMENTAIS

DISSERTAÇÃO DE CANDIDATURA AO GRAU DE DOUTOR EM NEUROCIÊNCIAS APRESENTADA À FACULDADE DE MEDICINA DA UNIVERSIDADE DO PORTO

Orientação: Professora Doutora Maria Teresa Burnay Summavielle

Sílvia Patrícia Morim Fernandes

UNDERSTANDING THE MECHANISMS OF ACETYL-L-CARNITINE THROUGH NEUROPROTECTION AFTER METHAMPHETAMINE ADMINISTRATION

Artigo 48º, § 3º

“A Faculdade não responde pelas doutrinas expandidas na dissertação.”

(Regulamento da Faculdade de Medicina do Porto – Decreto-Lei nº19337, 21 de Janeiro de 1931).

CORPO CATEDRÁTICO
DA FACULDADE DE MEDICINA DA UNIVERSIDADE DO PORTO

Professores Efetivos

ALBERTO MANUEL BARROS DA SILVA
ALTAMIRO MANUEL RODRIGUES COSTA PEREIRA
ANTÓNIO ALBINO COELHO MARQUES ABRANTES TEIXEIRA
DANIEL FILIPE LIMA MOURA
DEOLINDA MARIA VALENTE ALVES LIMA TEIXEIRA
FRANCISCO FERNANDO ROCHA GONÇALVES
ISABEL MARIA AMORIM PEREIRA RAMOS
JOÃO FRANCISCO MONTENEGRO ANDRADE LIMA BERNARDES
JOAQUIM ADELINO CORREIA FERREIRA LEITE MOREIRA
JOSÉ AGOSTINHO MARQUES LOPES
JOSE CARLOS NEVES DA CUNHA AREIAS
JOSÉ EDUARDO TORRES ECKENROTH GUIMARÃES
JOSE HENRIQUE DIAS PINTO DE BARROS
JOSE MANUEL LOPES TEIXEIRA AMARANTE
JOSE MANUEL PEREIRA DIAS DE CASTRO LOPES
MANUEL ALBERTO COIMBRA SOBRINHO SIMOES
MANUEL JESUS FALCAO PESTANA VASCONCELOS
MARIA AMELIA DUARTE FERREIRA
MARIA DULCE CORDEIRO MADEIRA
MARIA FÁTIMA MACHADO HENRIQUES CARNEIRO
MARIA LEONOR MARTINS SOARES DAVID
PATRÍCIO MANUEL VIEIRA ARAÚJO SOARES SILVA
RAQUEL ÂNGELA SILVA SOARES LINO
RUI MANUEL ALMEIDA MOTA CARDOSO
RUI MANUEL LOPES NUNES

Professores Jubilados ou Aposentados

ABEL VITORINO TRIGO CABRAL
ALEXANDRE ALBERTO GUERRA SOUSA PINTO
ÁLVARO JERONIMO LEAL MACHADO DE AGUIAR
AMÂNDIO GOMES SAMPAIO TAVARES
ANTONIO AUGUSTO LOPES VAZ
ANTÓNIO CARLOS DE FREITAS RIBEIRO SARAIVA
ANTÓNIO CARVALHO ALMEIDA COIMBRA
ANTÓNIO FERNANDES OLIVEIRA BARBOSA RIBEIRO BRAGA
ANTÓNIO JOSÉ PACHECO PALHA
ANTÓNIO MANUEL SAMPAIO DE ARAÚJO TEIXEIRA
BELMIRO DOS SANTOS PATRICIO
CÂNDIDO ALVES HIPÓLITO REIS
CARLOS RODRIGO MAGALHÃES RAMALHÃO
CASSIANO PENA DE ABREU E LIMA
DANIEL SANTOS PINTO SERRÃO
EDUARDO JORGE CUNHA RODRIGUES PEREIRA
FERNANDO TAVARELA VELOSO
FRANCISCO DE SOUSA LÉ
HENRIQUE JOSÉ FERREIRA GONÇALVES LECOUR DE MENEZES
JORGE MANUEL MERGULHAO CASTRO TAVARES
JOSÉ CARVALHO DE OLIVEIRA
JOSÉ FERNANDO BARROS CASTRO CORREIA
JOSÉ LUÍS MEDINA VIEIRA
JOSÉ MANUEL COSTA MESQUITA GUIMARÃES
LEVI EUGÉNIO RIBEIRO GUERRA
LUÍS ALBERTO MARTINS GOMES DE ALMEIDA
MANUEL ANTÓNIO CALDEIRA PAIS CLEMENTE
MANUEL AUGUSTO CARDOSO DE OLIVEIRA
MANUEL MACHADO RODRIGUES GOMES
MANUEL MARIA PAULA BARBOSA
MARIA DA CONCEIÇÃO FERNANDES MARQUES MAGALHÃES
MARIA ISABEL AMORIM DE AZEVEDO
MÁRIO JOSÉ CERQUEIRA GOMES BRAGA
SERAFIM CORREIA PINTO GUIMARÃES
VALDEMAR MIGUEL BOTELHO DOS SANTOS CARDOSO
WALTER FRIEDRICH ALFRED OSSWALD

JÚRI NOMEADO PARA A PROVA DE DOUTORAMENTO

Presidente:

Doutora Deolinda Maria Valente Alves Lima Teixeira, Professora Catedrática da Faculdade de Medicina da Universidade do Porto

Vogais:

Doutora Ana Paula Pereira da Silva Martins, Investigadora Auxiliar da Faculdade de Medicina da Universidade de Coimbra

Doutor António José Braga Osório Gomes Salgado, Investigador Principal da Escola de Ciências da Saúde da Universidade do Minho

Doutora Amélia Duarte Ferreira, Professora Catedrática da Faculdade de Medicina da Universidade do Porto

Doutor Rui Manuel Bento de Almeida Coelho, Professor Associado da Faculdade de Medicina da Universidade do Porto

Doutora Maria Teresa Burnay Summavielle, Investigadora Principal do Instituto de Biologia Molecular e Celular da Universidade do Porto - orientadora da Tese

AGRADECIMENTOS / AKNOWLEDGEMENTS

"Life is like riding a bike. To keep your balance, you must keep moving."

Albert Einstein

Chega assim à reta final uma das etapas mais árduas da minha vida. O processo foi longo e cheio de obstáculos, mas uma vez perto do fim, começo a achar que cada obstáculo ultrapassado fez deste fim uma conquista ainda melhor. Durante estes mais de cinco anos que durou este processo, várias foram as pessoas que direta ou indiretamente me acompanharam...

Em primeiro lugar tenho de agradecer à Teresa Summavielle. A Teresa acompanha-me como orientadora desde que entrei no "mundo da ciência", perfazendo agora sete anos… Agradeço à Teresa os conselhos, o conhecimento que me transmitiu, as críticas para fazer mais e melhor e as discussões, mas também a amizade! Obrigada por tudo, Teresa!

Quero agradecer aos elementos do laboratório de Biologia da Adição, aos que ainda lá estão e aos que a vida lhes mudou o rumo, mas estiveram comigo desde o início…Quero agradecer à Joana Bravo, a minha conselheira e amiga, sempre com uma palavra assertiva, pelos maus e pelos bons momentos. Obrigada pela evolução que me proporcionou desde o primeiro dia enquanto estagiária até aos dias de hoje. Agradeço à Juliana Alves, por me ter integrado no laboratório e por me acompanhar desde então; agradeço à Ana Magalhães pelas experiências partilhadas e ao Pedro Melo pelo apoio. Agradeço à Danira Damiani o bom humor e amizade; agradeço à Lídia Cunha a companhia e partilha de momentos; agradeço à Joana Lapa, pela ajuda e boa disposição e agradeço à Andrea Lobo a partilha de experiências e companhia. Agradeço ao elemento mais novo do grupo – a Sofia Salta, que já conheço há uns anos e que veio mais tarde integrar o grupo. À Sofia agradeço toda a ajuda, esforço e dedicação, e o facto de ter sido o meu braço direito e pilar nos últimos meses.

Por falar em pilar, não posso deixar de agradecer à Escola Superior de Tecnologia de Saúde – o meu local de trabalho e meu financiamento. Um agradecimento especial para a Prof. Doutora Regina, por todo o apoio, flexibilidade e, acima de tudo, compreensão. Sem este apoio seria impossível coordenar a minha profissão com o Doutoramento. Muito obrigada! Agradeço também à Filipa Vieira, por todo o apoio em tudo e por ser a melhor colega de trabalho que se pode ter!

Quero agradecer à Mafalda Sousa – a companheira deste Doutoramento! O primeiro ano não foi fácil em termos de gestão de tempo entre o trabalho e as aulas. Como nada acontece por acaso, conheci a Mafalda, a matemática! Obrigada Mafalda pela partilha de conhecimentos, pelas parcerias, pela visão pragmática e simples das coisas! Obrigada principalmente pela amizade que nasceu e que ultrapassou a barreira do doutoramento.

Quebrou-se uma barreira e criou-se um canal que nos vai unir para sempre (a minha afilhada Leonor)!

Agradeço também aos meus pais e família. Apesar de não acompanharem diretamente aquilo que faço, apoiaram-me e desejaram como eu que este Doutoramento acontecesse! Sem eles eu não seria eu, por isso muito obrigada pai e mãe! Às minhas irmãs agradeço o apoio; à Helena agradeço a partilha de momentos menos bons, alguns desafabos e a amizade…; à Isabel agradeço o apoio e a sobrinha linda que me deu. Continua a ser o resultado mais bonito da família!

Agradeço igualmente à Clara Melo, pela partilha de experiências e críticas construtivas do meu trabalho, e a amizade!

E por último, agradeço ao Miguel. Por tudo, por ser quem é e me ter moldado o carácter. Fez-me crescer enquanto pessoa e acompanhou de perto todos os meus passos neste Doutoramento, tendo dado a força e conselhos para que eu nunca desistisse! Obrigada por tudo, Miguel!

Agradeço à Escola Superior de Tecnologia da
Saúde e ao Instituto Politécnico do Porto,

Despacho IPP/P-056/2014, de 1 de agosto,
Programa de Formação Avançada de Docentes
do Instituto Politécnico do Porto 2014/2015

Em obediência ao disposto no Decreto-Lei nº 388/70, Artigo 8.º, ponto 2, declaro que efetuei o planeamento e execução das experiências, observação e análise de resultados e participei ativamente na redação de todas publicações que fazem parte integrante desta dissertação:

I - Fernandes S, Salta S, Bravo J, Silva AP and Summavielle T. Acetyl-L-carnitine prevents methamphetamine-induced structural damage on endothelial cells via ILK related MMP-9 activity. Molecular Neurobiology (*in press, DOI: 10.1007/s12035-014-8973-5*).

II - Fernandes S, Salta S and Summavielle T. Methamphetamine promotes α-tubulin deacetylation in endothelial cells: the protective role of Acetyl-L-Carnitine. Toxicology Letters, 2015, 234 (131-138); *DOI: 10.1016/j.toxlet.2015.02.011*.

A reprodução destas publicações foi feita com autorização das respetivas editoras.

TABLE OF CONTENTS

LIST OF ABBREVIATIONS AND ACRONYMS

5-HT – Serotonin
AJs - Adherens Junctions
ALC – Acetyl-L-Carnitine
ATP – Adenosine Triphosphate
BB-94 – Batimastat
BBB – Blood-Brain Barrier
bEnd.3 – Transformed brain derived endothelioma cell line
BHE – Barreira Hematoencefálica
BMVEC - Brain Microvascular Endothelial Cells
CAT - Carnitine acetyltransferase
CNS - Central Nervous System
CoA – Coenzyme A
COX - Cyclooxygenase
DA – Dopamine
DAT - Dopamine Transporter
ECs – Endothelial Cells
eNOS - Endothelial Nitric Oxyde Synthase
GAPDH – Glyceraldehyde 3-Phosphate Dehydrogenase
GFAP - Glial Fibrillary Acidic Protein
GLUT – Glucose Transporter Protein
GPx – Glutathione Peroxidase
GSK-3ß - Glycogen synthase Kinase-3ß
GUSB – Beta-Glucuronidase
IBMC - Instituto de Biologia Molecular e Celular
ICAM-1 – Intercellular Adhesion Molecule 1
IFN – Interferon
IGF-1 – Insulin Growth Factor 1
IL – Interleukin
ILK – Integrin Linked Kinase
iNOS – inducible Nitric Oxide Synthase
JAM – Junctional Associated Molecules
JNK1/2 - Jun Terminal Kinase 1/2
JO – Junções de Oclusão
LC – L-Carnitine
MAGUK - Membrane-Associated Guanylate Kinase Homologues
MA – Metanfetamina

MAPK - Mitogen-Activated Protein Kinase

MDMA – 3,4-methylenedioxymetham-phetamine (ecstasy)

METH - Methamphetamine

MLCK – Myosin Light Chain Kinase

MMPs – Matrix Metalloproteinases

nNOS – Neuronal Nitric Oxide Synthase

NO – Nitric Oxide

OCTN2 - Organic Cation/Carnitine Transporter 2

PBMC - Peripheral Blood Mononuclear Cells

PI3K-AKT – Phosphatidylinositol 3-kinase/Akt pathway

PKC - Protein Kinase C

RNS – Reactive Nitrogen Species

ROCK – Rho-Associated Protein Kinase

ROS – Reactive Oxygen Species

SERT - Serotonin Transporter

SOD – Superoxide Dismutase

TEER – Transendothelial Electrical Resistance

TJs – Tight Junctions

TNF-α - Tumor Necrosis Factor-alpha

TSA – *Trichostatin*

VCAM-1 - Vascular Cell Adhesion Molecule 1

Y27632 – Fasudil

ZO-1 – Zonnula Occludens 1

INTRODUCTION

“The biggest obstacles in our lives are the barriers our mind creates…”

(unknown author)

1. Blood-Brain Barrier

The central nervous system (CNS) microenvironment requires an appropriate homeostasis for the neuronal function, which is preserved by the blood–brain barrier (BBB). The primary role of the BBB is the regulation of brain microenvironment by restricting ionic, fluid and cell movements between the blood and brain, as represented in **Fig.1**, while contributing to supply essential nutrients and remove secretion and excretion products (Deli 2007).

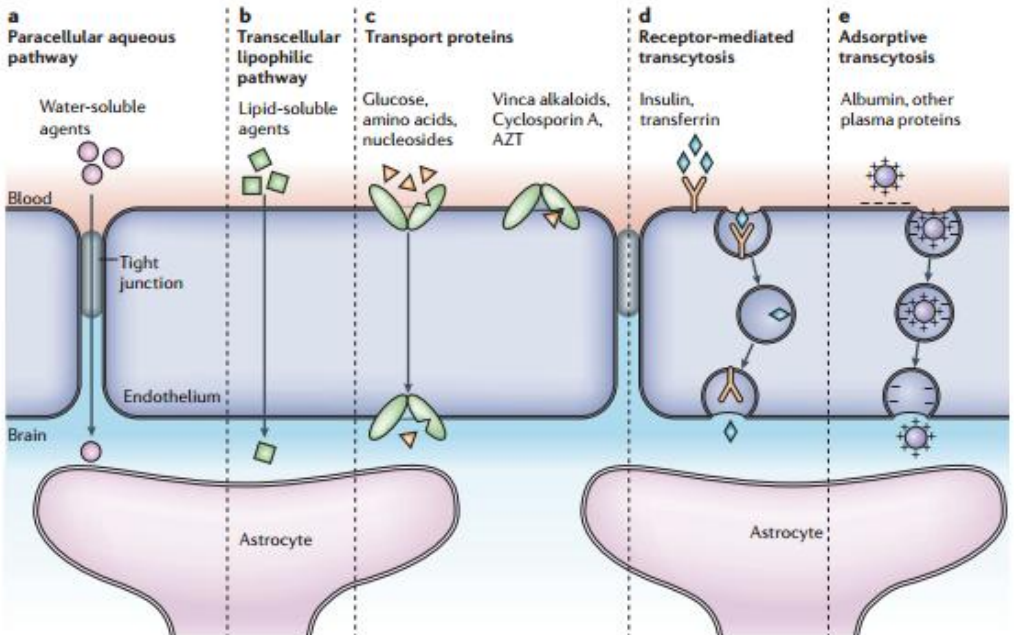

Fig.1 Molecules flux across the blood–brain barrier (BBB). Schematic diagram of the endothelial cells showing the main routes for molecular traffic across the BBB. The tight junctions (**a**) restrict penetration of water-soluble compounds, including polar drugs. In **b** is represented the effective diffusive route for lipid-soluble agents and in **c**, transport proteins (carriers) for glucose, amino acids, purine bases, nucleosides, choline and other substances are represented. Specific receptor mediated-endocytosis and transcytosis are responsible for the transport of specific molecules (**d**). In **e** native plasma proteins are poorly transported, although cationization can increase their uptake by adsorptive-mediated endocytosis and transcytosis. Most CNS drugs enter via route **b**. *Adapted from Abbott NJ, 2006.*

The BBB is part of the neurovascular unit and can be modulated by the crosstalk between brain endothelial cells (ECs), perivascular microglia, astrocytes, pericytes and neurons (Bradbury 1993), represented in **Fig.2** The barrier-conferring properties of the BBB are the ECs of the brain capillaries. However, associated pericytes, astrocytes and the surrounding the basement membrane also play an additional structural and regulatory role (Balda, Whitney et al. 1996; Chen, Hori et al. 2011; Toborek M., Seelbach et al. 2013).

The BBB is composed of specialized non-fenestrated brain microvascular endothelial cells (BMVECs) tightly connected in an impermeable monolayer devoid of transcellular pores (Yamamoto, Ramirez et al. 2008; Reynolds, Mahajan et al. 2011; Toborek M., Seelbach et al. 2013). Epithelial cells contain also other specialized membrane domains at the lateral

membranes for intercellular adhesion - adherens junctions (AJs), desmosomes and Gap Junctions. In these domains, cadherin, and desmoglein/desmocollin were identified as major integral membrane proteins (Brown, Morris et al. 2007). The presence of tight junctions (TJs) at the apical part is responsible for the regulation and proper maintenance of BBB integrity (András, Hong et al. 2003; Yamamoto, Ramirez et al. 2008; Reynolds, Mahajan et al. 2011; Toborek M., Seelbach et al. 2013), as well as for the restriction of paracellular flux and the maintenance of polarity of enzymes and receptors on luminal and abluminal membrane domains (Deli 2007), shown in **Fig.3**.

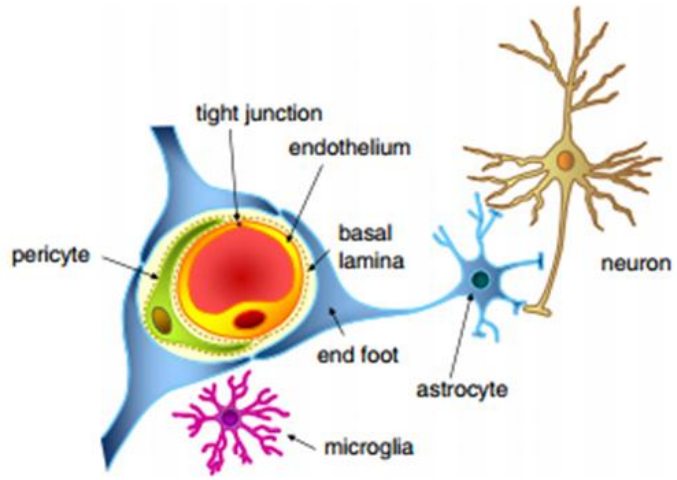

Fig.2 Neurovascular unit components. The barrier is formed by microvascular endothelial cells, surrounded by basal lamina and astrocytic endfeet, which are essential to provide the cellular link to the neurons. The figure also shows pericytes and microglial cells surrounding neurovascular unit. Source: *Adapted from Abbott NJ, 2013.*

Brain endothelial cells are distinct from the other endothelial cells because they are endowed with particular characteristics: very low levels of transcellular endocytosis; expression of specific transporters in a polarized manner; and formation of a low permeability physical barrier between the blood and the brain due to the presence of TJs between adjacent endothelial cells (Brown, Morris et al. 2007; Reynolds, Mahajan et al. 2011). TJs are specialized membrane domains that seal the intercellular spaces in epithelia and endothelia and thus contributing to the permeability barrier between luminal and interstitial compartments. TJs confer also selectivity to the transepithelial flux of molecules and ions through the intercellular spaces between epithelial cells (Balda, Whitney et al. 1996; Zoia, L et al. 2000). TJs are composed of claudins and occludin, intracellular accessory proteins (*Zonnula occludens* - ZO-1 to ZO-3), as well as junctional associated molecules (JAM) (Zoia, L et al. 2000; Yamamoto, Ramirez et al. 2008; Chen, Hori et al. 2011; Toborek M., Seelbach et al. 2013).

Occludin (65-kDa protein) was the first TJ identified and it is highly expressed in BMVECs, consistently found along the cell borders of brain endothelium (Yamamoto, Ramirez et al. 2008; Kashiwamura, Sano et al. 2011). Occludin is composed of four transmembrane domains with the carboxyl and amino terminals oriented to the cytoplasm and two extracellular

loops spanning the intercellular space. The extracellular loops interact with similar loops of occludin in the neighboring cells to form TJs. The role played by the N-terminal domain of occludin is not known but the C-terminal domain interacts with intracytoplasmic proteins, including *ZO-1*, *ZO-2*, and *ZO-3* (Yamamoto, Ramirez et al. 2008; Rao 2009; Chen, Hori et al. 2011). The amount of occludin in endothelial cells of the nervous system is higher that on the other endothelial cells, suggesting a particularly active role in BBB function (András, Hong et al. 2003; Yamamoto, Ramirez et al. 2008).

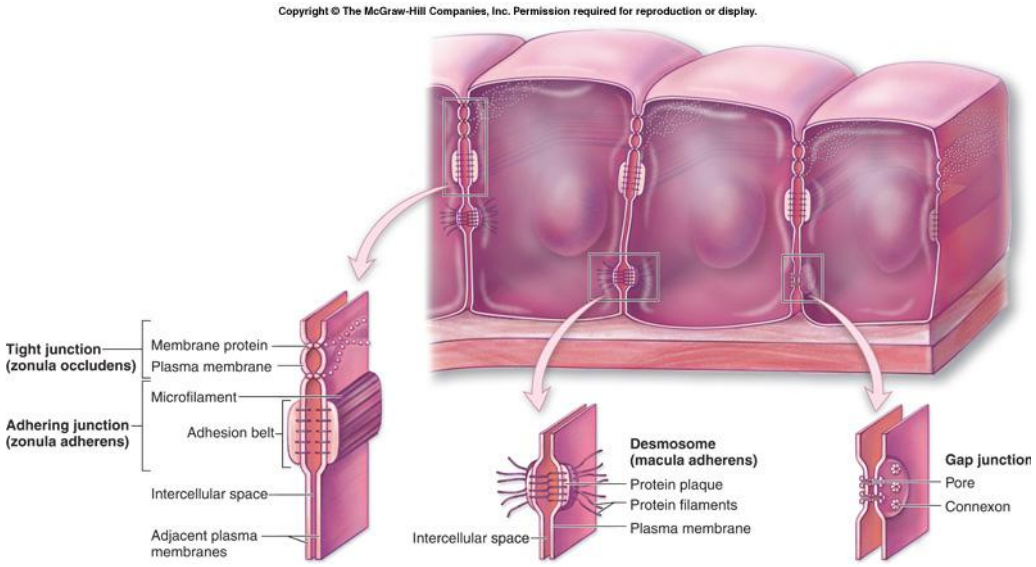

Fig.3 Protein complexes regulation Blood-Brain Barrier permeability. Tight Junctions are represented in the most apical part of the lateral membrane of adjacent cells. Adhering junctions, desmosomes and Gap Junctions are also represented, progressively located in a more basal part of the endothelial cell membrane. So*urce:http://keepinapbiologyreal.wikispaces.com/Extracellular+Components*

Claudins (24-kDa) are also major structural and functional elements of TJs in endothelial cells, and they have been shown to be a critical determinant of BBB permeability (András, Hong et al. 2003; Yamamoto, Ramirez et al. 2008). Up to 24 claudins have been identified in mammals, sharing a high sequence homology in the first and fourth transmembrane domains. Endothelial cell borders are enriched in claudins, both in and outside the CNS. Claudins express high tissue and cell-type specificity and claudins-3 and 5 are the most abundant in the brain endothelium. The interaction of the extracellular loops of claudins ensures the tightness of the contact between the cells of the monolayer (Yamamoto, Ramirez et al. 2008). Claudins are involved in both paracellular sealing and membrane domain differentiation. Within the large family of claudins, claudin-1 and claudin-5 seem to be the most important concerning structure and function of the TJs on BBB. Claudin-5 localizes primarily on the external leaflet of endothelial cell membranes, whereas claudin-1 is associated with the internal membrane leaflet. The tightness of the BBB may depend on the ratio of claudin-1 to claudin-5. Claudin-5 is recognized as endothelial-specific and it is the most important TJ involved in maintaining the BBB function. In mouse brain capillary endothelial cells, claudin-5 was reported

to be the most abundantly expressed at the mRNA level (Liebner, Kniesel et al. 2000; Kashiwamura, Sano et al. 2011). This fact justifies that claudin-5 is also the most studied (Haorah, Knipe et al. 2005; Brown, Morris et al. 2007; Forster, Burek et al. 2008; Mahajan, Aalinkeel et al. 2008; Yamamoto, Ramirez et al. 2008; Abdul Muneer, Alikunju et al. 2011; Kashiwamura, Sano et al. 2011; Martins, Baptista et al. 2011; Schrade, Sade et al. 2012).

The role of each TJ on BBB formation and maintenance is a relevant research topic. Although overexpression of claudins can induce cell aggregation and formation of TJ-like structures, the expression of occludin does not result in TJ formation (Yamamoto, Ramirez et al. 2008). In fact, functional TJs can be formed in the absence of the occludin gene and protein expression (András, Hong et al. 2003). It seems that claudins form the primary makeup of the TJs, and occludin further enhances TJ tightness and plays regulatory processes (Furuse, Hirase et al. 1993; András, Hong et al. 2003; Yamamoto, Ramirez et al. 2008; Rao 2009).

Cytoplasmic accessory proteins *ZO-1*, *ZO-2* and *ZO-3* belong to the family of membrane-associated guanylate kinase homologues (MAGUK) that link TJs to the cytoskeleton. Although the correlation between *ZO-1* and the TJs is strong, former reports indicate that *ZO-1* expression is not correlated with paracellular barrier function (Hawkins and Davis 2005). Among *ZO* accessory proteins, *ZO-1* was first identified as a peripheral membrane protein with a molecular mass of 220-kDa and highly concentrated at TJs in epithelial/endothelial cells, as well as on cardiac muscle cells, fibroblasts and astrocytes. In the brain, *ZO-1* and *ZO-2* function as cross-linkers between occludin and the cytoskeleton. While *ZO* amino-terminal domain bounds directly to the cytoplasmic C-terminal of occludin, the carboxyl-terminal was shown to provide connection to the actin cytoskeleton filaments, both *in vitro* and *in vivo* (Masahiko, Kazumasa et al. 1999; Mahajan, Aalinkeel et al. 2008; Toborek M., Seelbach et al. 2013), that allows the TJ to form a tight seal while still remaining capable of rapid modulation and regulation (Reynolds, Mahajan et al. 2011). Moreover, some findings reveal that *ZO-1* is recruited to normal TJs through direct or indirect interactions not only with occludin but also with claudin (Masahiko, Kazumasa et al. 1999). Interestingly, the stabilization of TJs provided by intracellular proteins such as *ZO*, and transmembrane proteins such as β-dystroglycan, allow the crosslink between the astrocytic endfeet and endothelial cells at the basal lamina (Northrop and Yamamoto 2012). For their peculiar localization, *ZO-1* and *ZO-2* accessory proteins serve as recognition proteins for TJ placement and act as support structures for signaling proteins (Reynolds, Mahajan et al. 2011; Toborek M., Seelbach et al. 2013). Up on that, F-actin filaments are involved in the maintenance of cytoplasmic domains and adhesion, essentially when linked to the accessory proteins of TJs (Matthias, M et al. 2004; Navarro-Costa, Plancha et al. 2012). As such, signaling molecules that directly control actin cytoskeleton organization are of particular significance with regard to TJ function regulation (Matthias, M et al. 2004; Mahajan, Aalinkeel et al. 2008). All together these data allow verifying that cytoskeleton and TJs are strictly related.

1.1 BBB models

In the last three decades, a great number of BBB models based on cell cultures have been developed. Primary cultures of cerebral ECs were firstly used as monolayers for experiments, and later, immortalized cell lines have been established and extensively used for that purpose (Deli 2007). In fact, the difficulty in maintaining primary ECs in culture is a challenge often overtaken by immortalized cell lines utilization, which are easier to culture and maintain and represent a useful material for *in vitro* BBB experiments (Omidi, Campbell et al. 2003; Roux and Couraud 2005; Brown, Morris et al. 2007; Yamamoto, Ramirez et al. 2008; Booth and Kim 2012; Takeshita, Obermeier et al. 2014). Several experiments were carried out using an *in vitro* BBB model to better mimics BBB response to several pathophysiological stimulus (Brown, Morris et al. 2007; Ramirez, Potula et al. 2009; Chen, Hori et al. 2011; Urrutia, Rubio-Araiz et al. 2013). The most common co-culture for BBB integrity assessment is composed by ECs and astrocytes (Mahajan, Aalinkeel et al. 2008; Booth and Kim 2012; Takeshita, Obermeier et al. 2014) although different cell components of BBB may be used for other purposes. Often, assessing relevant signaling cascades from the neurovascular unit that affect BBB properties requires co-culture systems containing glial cells, neurons, or pericytes. These models are valuable tools to study cell–cell interaction in the neurovascular unit, and modulation of BBB permeability in both physiological, pathological, and pharmacological conditions (Deli 2007).

As stated above, ECs and astrocytes co-cultures are the most common combination, allowing to assess the influence of astrocytes modulation over ECs permeability and barrier integrity (Booth and Kim 2012; Takeshita, Obermeier et al. 2014). Astrocytes and microglial cells or astrocyte-produced factors enhance endothelial TJ *in vitro.* These data are further supported by the finding that removal of astroglia from a co-culture of brain ECs led to an increase in permeability for sucrose and peroxidase which occurs without effective loosening of TJs (Abbott, Rönnbäck et al. 2006; Deli 2007).

The tight paracellular barrier is a fundamental characteristic of BBB and the measurement of the transendothelial electrical resistance (TEER) is one of the most straightforward methods to evaluate it. In culture conditions, TEER reflects the junctional permeability for sodium ions. All relevant models must show a sufficient tightness (150–200 $\Omega.cm^2$) to allow the study the permeability or transport of molecules. Considering animal cell lines, the best characterized mouse lines are TM-BBB4 and b.End3 showing higher basal values of TEER (Deli 2007).

Because BBB damage is recognized as an early event in many neurological conditions, understanding BBB signaling has become a relevant research topic, and also a therapeutic target (Abbott 2013). In our work, we are interested in better understand the mechanisms that lead to BBB disruption under exposure to psychostimulant drugs, such as amphetamines (Martins, Baptista et al. 2011; Park, Kim et al. 2013), and in particular how ALC may contribute to preserve BBB integrity (Haorah, Floreani et al. 2011; Muneer, Alikunju et al. 2011).

2. Methamphetamine

Methamphetamine (METH) is a potent stimulant with strong euphoric and reinforcing properties producing short and long-lasting neurotoxic effects. METH is synthetically produced and easily abused (Melega, Cho et al. 2007; ElAli, Urrutia et al. 2012), being the second most commonly used type of illicit substances worldwide, and the most used Amphetamine-type stimulant (**Fig.4**), with 15–16 million estimated users (Crime 2014). A common pattern in METH abuse starts with daily exposure to increasing doses followed eventually by engagement in multiple daily administrations. METH blood levels allow to estimate an intake of about 260 mg in a pattern of 3 to 4 binges per day (Melega, Cho et al. 2007; Ramirez, Potula et al. 2009; Urrutia, Rubio-Araiz et al. 2013), reaching high plasma levels, in an half-life of 12-16h (Melega, Cho et al. 2007; Krasnova and Cadet 2009).

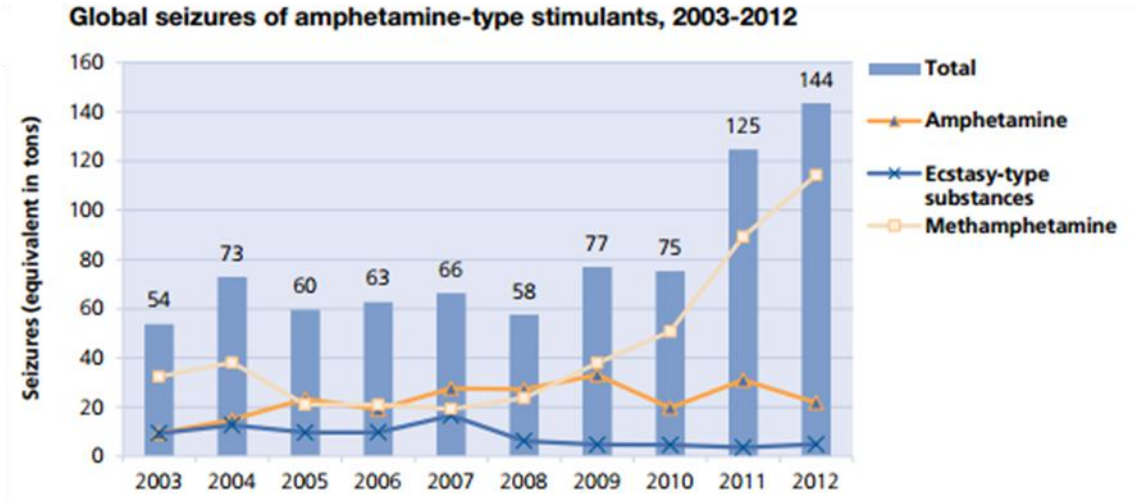

Fig.4. Source: UNODC annual report questionnaire and other official sources.

Note: *Total ATS includes amphetamine, "ecstasy"-type substances, methamphetamine, non-specified ATS, other stimulants and prescription stimulants*

After METH intake, consumers experience a sense of euphoria, hypersexuality, increased productivity and energy, with decreased anxiety. However, both short- and long-term abuse of METH leads to deleterious and long-lasting neurotoxic effects. METH-abuse negative consequences include acute toxicity, altered behavioral and cognitive functions and long-term neurological damage. Consumption of large doses induce more severe consequences including hyperthermia above 41°C, renal and liver failure, cardiac arrhythmias, heart attacks, cerebrovascular hemorrhages, strokes and seizures (Albertson, Derlet et al. 1999). Chronic abuse of METH contributes to attention deficits, anxiety, depression, aggressiveness, social isolation, psychosis, mood disturbances, and psychomotor dysfunction. Neuropsychological deficits in motor skills, and in executive and episodic memory observed after METH intake are a consequence of METH effect at the dopamine rich fronto-striato-cortical loops. In addition, METH abusers show impaired decision-making and impulsivity, which was associated with the

executive aspects of working memory deficits (Gold, Kobeissy et al. 2009; Krasnova and Cadet 2009). METH withdrawal is also associated with anhedonia, irritability, fatigue, impaired social behavior and intense craving for the drug (Krasnova and Cadet 2009).

METH-toxicity has been characterized by the disruption of monoamine production and synaptic integrity (Bowyer, Thomas et al. 2008; Ramirez, Potula et al. 2009; Urrutia, Rubio-Araiz et al. 2013), schematically represented in **Fig.5**. METH-neurotoxicity is characterized by long-term reduction in dopaminergic and serotonergic functions, including depletion of dopamine transporter (DAT), serotonin transporter (SERT), serotonin (5-HT) and dopamine (DA). The *postmortem* analysis of the brain of a METH consumer revealed that DA, tyrosine hydroxylase (TH), and the DAT are reduced. Nowadays, magnetic resonance imaging techniques performed in METH chronic users confirm those brain changes (Imam, El-Yazal et al. 2001; Chandramani Shivalingappa, Jin et al. 2012). In rodents and non-human primates METH was seen to induce long-term depletion of DA metabolism, decreasing the number of high affinity DA uptake sites and reducing the activity of TH in striatum (*caudate* and *putamen*). Moreover, the findings of long-term reduction of dopaminergic markers in animal brains, together with histological signs suggestive of nerve terminal injury following acute exposure, led to the conclusion that METH damages brain dopamine nerve endings (Mirecki, Fitzmaurice et al. 2004; Gold, Kobeissy et al. 2009).

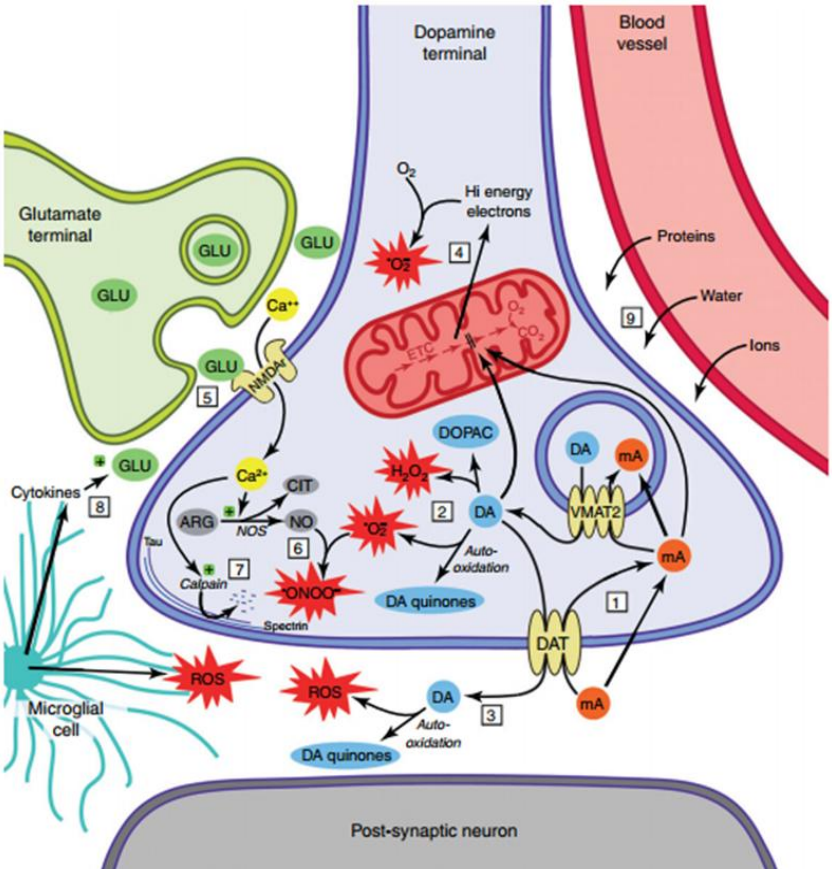

Fig.5 Schematic representation of cellular and molecular events involved in METH-induced neurotoxicity.
mA- methamphetamine; GLU- glutamate; DA- Dopamine; DAT- Dopamine transporter; ROS- Reactive Oxygen Species.
Source: (Marshall and O'Dell 2012)

Although the mechanism underlying METH-induced brain damage in dopamine neurons is not fully understood, oxidative stress is seen as an early event in this mechanism, which could possibly be related with the excessive release or intraneuronal mobilization of dopamine and formation of toxic dopamine-derived oxyradical (Mirecki, Fitzmaurice et al. 2004). Several studies in the literature show a well supported role for oxygen (ROS) and nitrogen-based (RNS) radicals, where ample evidence depicts the importance of peroxynitrite in METH-induced dopaminergic neurotoxicity (Imam, El-Yazal et al. 2001; Jin, Moo et al. 2002; Chandramani Shivalingappa, Jin et al. 2012). METH enters the dopaminergic neuron through DAT and displaces vesicular dopamine (Chandramani Shivalingappa, Jin et al. 2012). The increased content of amines in the cytoplasm leads to high levels of oxidation forming highly reactive dopamine quinones and reactive oxygen species, leading to increased oxidative stress. Besides the toxic effects of METH on monoaminergic terminals, there is evidence of the activation of genes related to cell death which can cause death to the cell by both apoptotic and necrotic mechanisms. METH-induced cell death was observed in the hippocampus, parietal cortex, striatum and in several other brain regions (Gold, Kobeissy et al. 2009). Moreover, METH induces autophagy in neurons which is associated with the formation of ubiquitin-positive, α-synuclein aggregates and multilamellar bodies after METH administration in DA containing neurons (Pasquali, Lazzeri et al. 2008; Ma, Wan et al. 2014).

Chronic exposure to METH can also lead to changes in brain metabolism and energy requirements, which are region specific (Downey and Loftis 2014). Mitochondrial dysfunction has been implicated in the neurodegeneration mechanisms caused by METH. In fact, exposure to METH decreased mitochondrial membrane potential, increased mitochondrial mass and protein nitrosylation, and decreased levels of different subunits from complexes I, III, and IV of the electron transport chain (Chandramani Shivalingappa, Jin et al. 2012). METH exposure significantly inhibits glucose uptake by neurons and astrocytes (Muneer, Alikunju et al. 2011) and the drug neurotoxicity generates a strong and lasting glial response, resulting in astrogliosis and release of inflammatory mediators (Goncalves, Baptista et al. 2010). Moreover, microglial activation has also been reported in the brain of METH abusers using Positron Emission Tomography (PET) imaging techniques (Gold, Kobeissy et al. 2009).

Recently, the brain endothelium has also been shown to be a target of METH toxicity, since it represents a component of major importance in the BBB. However, the effect of METH on the brain endothelium remains largely under-characterized.

2.1 Methamphetamine effects on BBB function

BBB impairment contributes to many pathological states such as inflammation, tumor differentiation (Singh and Harris 2004), epilepsy, Parkinson's and Alzheimer's diseases, multiple sclerosis and ischemia/reperfusion (Forster, Burek et al. 2008).

In the last decades, the effects of METH exposure in BBB have been extensively recorded (Bowyer, Thomas et al. 2008; Mahajan, Aalinkeel et al. 2008; Abdul Muneer, Alikunju et al. 2011; Northrop and Yamamoto 2012; Martins, Burgoyne et al. 2013; Urrutia, Rubio-Araiz et al. 2013). METH exposure impairs glucose transport and uptake in ECs (Abdul Muneer, Alikunju et al. 2011), increases eNOS activation and transcytosis (Martins, Burgoyne et al. 2013; Ma, Wan et al. 2014), decreases BBB tightness along with a decrease in the expression of cell membrane-associated TJs proteins (Ramirez, Potula et al. 2009).

The physiopathological processes involved in some neurological diseases and in METH-induced dysfunction seem to be similar. Fortunately, METH exposure studies in *in vitro* models raise the possibility to explore the mechanisms of action involved. Likewise, possible therapeutic or protective tools can also be explored using these models.

2.1.1 Increased permeability of the BBB

METH-induced increased BBB permeability was consistently reported both *in vivo* and *in vitro* (Bowyer, Thomas et al. 2008; Abdul Muneer, Alikunju et al. 2011; ElAli, Urrutia et al. 2012; Urrutia, Rubio-Araiz et al. 2013). *In vitro*, different models of cell lines and primary ECs were used for the assessment of METH effects and all of them showed a reduced TEER after the drug exposure (Mahajan, Aalinkeel et al. 2008; Ramirez, Potula et al. 2009; Martins, Burgoyne et al. 2013). Evaluation of BBB integrity by the quantification of the transendothelial migration of peripheral blood mononuclear cells (PBMC) across the BBB has also shown a significantly increase in the percentage of PBMC transmigration after METH exposure (Reynolds, Mahajan et al. 2011). *In vivo,* the most frequent approach consists in the measurement of macromolecular tracers that cross the BBB. Using those protein-tracers as well as IgG extravasation, METH was shown to induce marked disruption of BBB causing massive leakage of such molecules across the barrier in the cerebral cortex, hippocampus, thalamus, hypothalamus, cerebellum and amygdale of METH-treated mice (Bowyer, Thomas et al. 2008; Krasnova and Cadet 2009; Conant, Lonskaya et al. 2011; Martins, Baptista et al. 2011).

The decrease in the tightness of ECs monolayers induced by METH occurs in a dose- and time-dependent manner (Ramirez, Potula et al. 2009) and may be caused by decreased expression of cell membrane-associated TJs, concomitant with enhanced ROS production (Ramirez, Potula et al. 2009; Mahajan, Aalinkeel et al. 2012; Park, Kim et al. 2013) and activation of cytoskeleton-related protein expression (Ramirez, Potula et al. 2009; Park, Kim et al. 2013).

2.1.2 Reduction and/or redistribution of TJs

Dynamic regulation of TJs function is fundamental to many physiological processes. TJs disruption drastically alters paracellular permeability which is the hallmark of many pathological states - ischemia/reperfusion, inflammation, tumor differentiation (Singh and Harris 2004). The increased permeability of BBB after METH exposure is accompanied by the reduction and/or redistribution of adhesion molecules – essentially claudin-5 and occludin (Reynolds, Mahajan et

al. 2011; Northrop and Yamamoto 2012; Toborek M., Seelbach et al. 2013). Reduction of TJs is strictly related with BBB increased permeability. Such events were reported in cultured brain microvascular endothelial cells (Ramirez, Potula et al. 2009; Abdul Muneer, Alikunju et al. 2011; Reynolds, Mahajan et al. 2011) and in mouse brain (Bowyer and Ali 2006; Martins, Baptista et al. 2011). METH was shown to reduce the expression of claudin-3, JAMs, ZO-1 and ZO-2 both at the protein and mRNA levels (Mahajan, Aalinkeel et al. 2008). Simultaneously, METH induces the expression of the pro-inflammatory cell adhesion molecules ICAM-1 and VCAM-1 in cerebral microvessels (Toborek M., Seelbach et al. 2013). However, in light of several reports it seems that decrease TJs occurs by the effect of METH on protein turnover rather than on gene expression (Ramirez, Potula et al. 2009). Importantly, immunoreactivity of those proteins after METH exposure is also characterized as fragmented (Toborek M., Seelbach et al. 2013), with formation of gaps (Ramirez, Potula et al. 2009), which contrast with the continuous labeling observed in control conditions. Changes in claudins and occludin are a common outcome of METH exposure. However, several studies show that *ZO-1* or *ZO-2* seem to be unaffected (Ramirez, Potula et al. 2009; ElAli, Urrutia et al. 2012).

Besides disruption and decrease in protein levels, an important finding observed after METH exposure is the translocation/redistribution of TJs. The most frequent pattern described in the literature is the translocation of claudin-5 from the membrane to the cytosol (Ramirez, Potula et al. 2009). Recent studies observed that also occludin shares this pattern after METH exposure through endocytosis in vesicles (Toborek M., Seelbach et al. 2013).

However, there are reports where repeated low doses of METH administered to mice led to increased permeability of cerebral microvessels without disrupting structural proteins (ElAli, Urrutia et al. 2012). Other study showed that primary ECs exposed to low doses of METH display increased TEER without changes in adherens junctions and TJs (Martins, Burgoyne et al. 2013).

2.1.3 Release of pro-inflammatory cytokines and chemokines

There is evidence of BBB disruption in central nervous system (CNS) pathologies characterized by a relevant neuroinflammatory component. In fact, increase of pro-inflammatory cytokines such as tumor necrosis factor (TNF) and interleukins are associated with changes in BBB integrity in several neurological diseases. *In vitro* studies have shown that TNF, interferon-gamma (IFN-γ) and interleukin-1beta (IL-1β) are involved in the disruption of BBB integrity (O'Shea, Urrutia et al. 2014).

The role of neuroinflammation in the BBB structure and function following METH exposure were investigated. Recent data showed that METH-induced neurotoxicity may result from a synergistic response of different cellular entities in which glial cells play an important role. Indeed, METH exposure results in astrogliosis (activation of both astrocytes and microglial cells) along with pro-inflammatory cytokines release (Ladenheim, Krasnova et al. 2000; Ramirez, Potula et al. 2009; Goncalves, Baptista et al. 2010; Northrop and Yamamoto 2012). Microglial activation appears to be an early event in the neurotoxic cascade initiated by METH exposure,

with cytokines release driving at least part of its neurotoxic effects. Importantly, METH seems to induce a substantial microglial response in the areas of the brain that show increased neuronal degeneration after exposure (Friend and Keefe 2013). Some anti-inflammatory drugs afford protection against METH-induced microgliosis and neurotoxicity, but additional investigation needs to be carried out (O'Shea, Urrutia et al. 2014).

Neuroinflammation mediates METH toxicity to monoamine terminals but its role in METH-induced BBB disruption is far from being understood. It was reported that an acute high dose of METH induces an increase in the expression levels of IL-6 mRNA and TNF-α mRNA in some brain regions, soon after exposure (Goncalves, Baptista et al. 2010). Moreover, METH neurotoxicity is attenuated in the IL-6 knockout mice, where a decrease in reactive gliosis marker was observed (Ladenheim, Krasnova et al. 2000). METH also increases the pro-inflammatory cytokine interleukin-1β levels (Krasnova and Cadet 2009). The inflammatory mediator cyclooxygenase (COX) has been implicated in BBB disruption and it was shown increased after METH exposure. Increases in glial fibrillary acidic protein (GFAP) and COX-2 expression in endothelial brain capillaries occurred with BBB disruption a few days after METH exposure in combination with stress (Northrop and Yamamoto 2012). Moreover, nonselective inhibition of COX attenuated TNF-induced BBB disruption. Of note, is still unclear whether reactivity of astrocytes surrounding the capillaries is a cause or a consequence of BBB damage induced by METH. Collectively, these data indicate that ECs respond to the METH-insult by producing inflammatory mediators that can cause damage to the BBB (Northrop and Yamamoto 2012).

Microglia might potentiate METH-related damage by releasing neurotoxic substances such as superoxide radicals and NO (Krasnova and Cadet 2009) and some authors suggested that both oxidative mechanisms and cytokines might exert their effects through modulation of transcriptional factors. However, BBB damage could also result from TJs disruption. There is evidence that TJs and *ZO* are highly sensitive to the microenvironment and *in vitro* respond to inflammatory cytokines by displaying altered subcellular localization and dissociation of the occludin/*ZO* complex (Mahajan, Aalinkeel et al. 2008).

2.1.4 Increased activity and expression of MMP-2/9

Matrix metalloproteinases (MMPs) play significant roles in complex processes, including regulating cell behavior, cell-cell communication and tumor progression. MMPs mediate several proteolytic reactions involving cellular surface elements such as adhesion molecules, receptors and intercellular junction proteins. MMPs belong to a family of proteolytic enzymes of more than 20 members that require the binding of Zn^{2+} for their enzymatic activity (Visse and Nagase 2003; Conant, T Lim et al. 2012; Mizoguchi and Yamada 2013). MMP-9 is up-regulated following various types of insults to the brain, and it has been seen as a marker of neurodegeneration (Liu, Brown et al. 2008). MMP-9 has been observed to play relevant roles both *in vitro* and *in vivo* in different pathological conditions such as brain ischemia and trauma, while the closely related relative MMP-2, does not play a role in those events (Ramirez, Potula

et al. 2009). *In vivo* increased MMP-9 activity was reported in specific brain regions, namely those involved in drug addiction (Mizoguchi, Yamada et al. 2007; Liu, Brown et al. 2008; Martins, Baptista et al. 2011; Urrutia, Rubio-Araiz et al. 2013) but the cellular source of this protease is not exactly known. Neurons and/or microglia as a source have been suggested but a peripheral origin from leukocytes could also be possible. It was demonstrated that ECs secrete MMP-9 in the basal direction, which facilitates the degradation of the basal membrane. Basal membrane degradation has been associated with an increase in vascular permeability and the loss of vascular integrity leading to edema and leukocyte infiltration (Urrutia, Rubio-Araiz et al. 2013).

Chen F et al, 2011 demonstrated that MMP-9 induces significant changes to occludin in ECS both *in vitro* and in mice brains. Moreover, the use of specific monoclonal antibodies against MMP-9 attenuate brain extravasation and edema in some pathological conditions. Experiments with endothelial model bEnd.3 cells allow to conclude that MMP-9 increases BBB permeability, which was attenuated when cells are co-transfected with endogenous MMPs inhibitors (Chen, Hori et al. 2011).

Activation and expression of MMPs is a common mechanism of BBB leakiness, and has been reported after METH exposure (Liu, Brown et al. 2008; Conant, Lonskaya et al. 2011; Martins, Baptista et al. 2011; Reynolds, Mahajan et al. 2011; Conant, T Lim et al. 2012; Urrutia, Rubio-Araiz et al. 2013). Different *in vivo* experiments demonstrate that METH produces an increase in both striatal MMP-9 expression and gelatinolytic activity occurring along with an increase in the degradation of extracellular matrix components and BBB permeability (Liu, Brown et al. 2008; Martins, Baptista et al. 2011; Urrutia, Rubio-Araiz et al. 2013). The same pattern of MMPs activity was observed in neuronal and glial cells of different brain regions after METH exposure (Mizoguchi, Yamada et al. 2007; Conant, T Lim et al. 2012). Recently, MMP-9 was demonstrated to degrade occludin and claudin-5 in focal cerebral ischemia and has also been shown to alter occludin, claudin-5, and *ZO-1* and *ZO-2* in early diabetic retinopathy (Ramirez, Potula et al. 2009).

The use of specific MMPs inhibitors (Batimastat, BB-94) effectively prevented the decrease in extracellular matrix components expression and reducing the BBB disruption induced by METH (Urrutia, Rubio-Araiz et al. 2013). However, the signal transduction pathway associated with MMP-9 mediating TJs alterations remains unknown.

2.1.5 Increased oxidative stress

METH treatment increases excitatory neurotransmission which may result in enhanced oxidative stress by producing highly reactive dopamine quinones and ROS (Imam, El-Yazal et al. 2001; Mahajan, Aalinkeel et al. 2008; Gold, Kobeissy et al. 2009; Chandramani Shivalingappa, Jin et al. 2012; Martins, Burgoyne et al. 2013; Toborek M., Seelbach et al. 2013).

The evidence shows that METH increases oxidative stress in cultured ECs, which leads to activation of signaling cascades resulting in loss of BBB integrity (Ramirez, Potula et al. 2009;

Martins, Burgoyne et al. 2013). Moreover, this increase in oxidative stress results in cytoskeleton re-arrangements and redistribution of TJs proteins (Mahajan, Aalinkeel et al. 2008). Recent data indicated that activation of NADPH oxidase (NOX) is an important source of ROS production in brain ECs exposed to METH (Toborek M., Seelbach et al. 2013). In those conditions, METH exposure induces a pro-oxidant environment quantified by the increase in p66Sch, p47 and gp91 and reduces glutathione levels, as described by *Toborek et al, 2013*. BBB permeability changes induced by oxidative stress can be mediated by Ras and/or Rho signaling acting on TJs. These pathways were demonstrated to play important roles in the regulation of claudin-5, *ZO-1*, and *ZO-2* expression as well as on BBB assembly (Toborek M., Seelbach et al. 2013). On the other hand, results from *Martins T et al, 2013*, showed that METH-induced increased permeability at the BBB involves endothelial Nitric Oxyde Synthase (eNOS) activation and NO generation (Martins, Burgoyne et al. 2013). In fact, eNOS is the main NOS system regulating barrier function and permeability, controlling also other relevant functions such as angiogenesis and inflammatory processes (Fukumura, Gohongi et al. 2001). A similar mechanism was previously described for neuronal dopaminergic toxicity (Imam, El-Yazal et al. 2001), suggesting these drug targets could be similar in both neurons and ECs.

2.1.6 Posttranslational modifications and signaling cascades activation

The hypothesis that posttranslational modifications of TJs occludin and claudin-5 contribute to BBB loss of integrity was considered. The phosphorylation state of occludin regulates its association with the cell membrane and barrier permeability, and multiple phosphorylation sites have been identified on occludin serine (Ser), threonine (Thr) and thyrosine (Tyr) residues (Yamamoto, Ramirez et al. 2008; Rao 2009). Assembly and disassembly of TJs are associated with reversible phosphorylation of occludin on Ser and Thr residues. Occludin dephosphorylation occurs during the disruption of TJs and phosphorylation processes leads to its translocation to cell-cell contacts (Andreeva, Krause et al. 2001; Rao 2009). Intracellular calcium concentration also seems to impact TJs integrity. In this line of evidence, low calcium medium resulted in a rapid reduction of occludin phosphorylation, while calcium replacement leads to TJs reassembly (Andreeva, Krause et al. 2001; Rao 2009). Phosphorylation of TJs may be dynamically regulated by protein kinases and protein phosphatases, where the most feasible are atypical protein kinase C (PKC) isoforms (Andreeva, Krause et al. 2001; Yamamoto, Ramirez et al. 2008; Rao 2009) but protein phosphatases such as PP2A and PP1 are also implicated (Rao 2009).

Moreover, it was found that phosphorylation processes modulate occludin interaction with *ZO* proteins. Altogether these data indicate that Tyr-phosphorylation of occludin is clearly associated with the disruption of TJs, while Ser/Thr-phosphorylation may be required for the assembly of occludin into the TJs complex (Yamamoto, Ramirez et al. 2008; Rao 2009).

After METH exposure in ECs, an increase in RhoA expression was observed (Mahajan, Aalinkeel et al. 2008). Accumulating evidence suggests a role for RhoGTPases in the regulation of BBB integrity through TJs posttranslational modifications. In fact, other studies have

implicated RhoA in TJs functions (Persidsky, Heilman et al. 2006; Mahajan, Aalinkeel et al. 2008). *Yamamoto M et al, 2008* demonstrated the direct phosphorylation of both claudin-5 and occludin by Rho-Associated Protein Kinase (ROCK), which is inhibited by the ROCK-specific inhibitor Y27632. Thus, it was suggested that the suppression of ROCK activity with specific inhibitors could protect the BBB (Yamamoto, Ramirez et al. 2008). Others proposed that after METH exposure, prevention of BBB dysfunction with a ROCK inhibitor occurs through prevention in ROS-induced transmigration of PBMC across an *in vitro* simulation of BBB (Mahajan, Aalinkeel et al. 2008).

There are several molecular pathways that have been involved in METH-induced effects on BBB function. METH-induced oxidative stress can trigger the activation of myosin light chain kinase (MLCK), resulting in enhanced phosphorylation of RhoA, which is known to be associated with loss of TJs integrity (Mahajan, Aalinkeel et al. 2008). Moreover, the increased permeability of the brain endothelium observed both *in vivo* and *in vitro* after METH exposure was also attributed to a significantly decrease in the rate of glucose uptake and in the levels of glucose transporter protein-1 (GLUT1) (Abdul Muneer, Alikunju et al. 2011).

Jun Terminal Kinase 1/2 (JNK1/2) phosphorylation is evident after METH exposure. Blockade of JNK1/2 is known to reduce MMP-9 activity along with prevention of BBB dysfunction, suggesting that the JNK pathway may be involved in the *in vivo* effects of METH on basal lamina and BBB integrity (Urrutia, Rubio-Araiz et al. 2013).

Cytoplasmic integrin-linked kinase (ILK) expression plays also a role in MMP gelatinolytic activity. ILK binds directly to the cytoplasmic domains of β1 integrin and connects integrins to the actin cytoskeleton by interacting with several proteins (such as paxillin and parvin) thus coordinating actin organization (Wu and Dedhar 2001; Rosano, Spinella et al. 2006). There is also evidence that ILK expression stimulates MMP-9 activation, whereas ILK silencing inhibits invasion in several carcinomas (Troussard, Costello et al. 2000; Rosano, Spinella et al. 2006). ILK overexpression and clustering results in the activation of a variety of intracellular signaling processes such as Akt phosphorilation and GSK-3 inhibition, which lead to the activation of the transcription factor AP-1 resulting in the MMP-9 potentiation (Troussard, Costello et al. 2000; Wu and Dedhar 2001). However, the effects of METH on ILK expression were not yet addressed.

2.1.7 Body temperature

One common reported outcome of METH exposure is hyperthermia, which is also an important factor in the mediation of METH toxicity (Albertson, Derlet et al. 1999; Imam, El-Yazal et al. 2001; Bowyer, Thomas et al. 2008; Gold, Kobeissy et al. 2009; Krasnova and Cadet 2009; ElAli, Urrutia et al. 2012). Recently, changes in body temperature induced by METH exposure have also been linked to increased BBB permeability.

Different experiments have shown that the administration of METH or other amphetamine derivatives such as MDMA (ecstasy) led to leakiness of the BBB *in vivo* (Bowyer and Ali 2006; Persidsky, Heilman et al. 2006; Yamamoto and Raudensky 2008). *In vivo* assays

show that METH-induced BBB breakdown appears to be temperature-dependent since the magnitude of tracers diffusion into the brain tissue tightly correlate with the hyperthermia degree. Moreover, when the increase in temperature is prevented these drugs are no longer able to induce BBB disruption at the same extent (Krasnova and Cadet 2009). In agreement, moderate BBB dysfunction observed in the *caudate* and *putamen* after METH treatment was exacerbated by hyperthermia (Bowyer, Thomas et al. 2008). Data strongly suggest that hyperthermia facilitates METH-induced ROS production and that increased oxidation of DA is associated with neurotoxic effects of METH (Ladenheim, Krasnova et al. 2000; Krasnova and Cadet 2009; Downey and Loftis 2014). Morphological changes in epithelial cells of the choroid plexus – an important element of the blood-cerebral spinal fluid barrier - also tightly correlate with METH-induced hyperthermia and BBB permeability (Sharma and Kiyatkin 2009). However, the mechanism leading to the disruption in the BBB was not addressed in these studies.

However, both pharmacological and genetic manipulations can block METH toxicity without influencing the drug-induced thermal responses (Ladenheim, Krasnova et al. 2000; Krasnova and Cadet 2009), thus showing that METH-related changes in body temperature are just a component of the drug toxicity (Krasnova and Cadet 2009).

2.2 Neuroprotection strategies for METH-induced effects

Several approaches have been tested for the treatment and prevention of METH-induced dopaminergic neurotoxicity, essentially by the use of antioxidants. Glutathione peroxidase (GPx) is an antioxidant enzyme that scavenges various peroxides and protects membrane lipids and macromolecules from oxidative damage. Due to METH action over these processes GPx has been studied *in vitro* and *in vivo* in the context of drug exposure. A study reported GPx overexpression in PC12 cells as a protective response against METH cytotoxicity (Imam, El-Yazal et al. 2001). Moreover, therapy with selenium and other antioxidants resulted in positive clinical responses in various neurodegenerative diseases associated with increased oxidative damage (selenium is an essential dietary component for mammals present in the active center of GPx). METH-induced dopaminergic toxicity and the generation of peroxynitrite were significantly avoided both *in vitro* and *in vivo* by selenium supplementation (Imam, El-Yazal et al. 2001). The natural occurring hormone melatonin acts also as a free radical scavenger and antioxidant. *In vivo* and *in vitro* studies showed that melatonin is effective in protecting nuclear DNA, membrane lipids, and possibly cytosolic proteins from oxidative damage thus protecting cells, tissue, and organs. Studies from *Itzhak et al*, showed that this hormone protected the depletion of dopamine and its metabolites in mice after the METH administration. Furthermore, in another study from the same author, a pretreatment with melatonin provided significant protection against METH-induced generation of peroxynitrite and 3-nitrotyrosine in mouse striatum (Itzhak, Martin et al. 1998). Other studies found important neuroprotective effects using NOS inhibitors and peroxynitrites decomposition catalysts in

METH-induced dopaminergic neurotoxicity. Blocking the formation of nitric oxide or decomposition of peroxynitrite could potentially provide a therapeutic intervention in METH-induced dopaminergic neurotoxicity. In this line of evidence, N-acetylcysteine, another antioxidant and free radical scavenger, known to increase intracellular glutathione levels, was used in a mesencephalic dopaminergic neuronal cell model to counteract glutathione depletion caused by METH and to prevent oxidative and nitrative damage (Chandramani Shivalingappa, Jin et al. 2012). Moreover, this antioxidant is able to partially reduce autophagy processes induced by METH treatment, thus demonstrating that alteration of cellular redox status function as a key trigger for several damaging processes (Chandramani Shivalingappa, Jin et al. 2012).

Other approaches to reduce oxidative damage were also used, such as genetic manipulation of target enzymes as valuable tools for METH-damage prevention. In this line of evidence, it was shown that METH-induced dopaminergic neurotoxicity is attenuated in mice overexpressing superoxide dismutase enzymes like CuZnSOD or MnSOD. Similarly, the same authors observed that nNOS knockout mice are also protected against METH-induced peroxynitrite generation (Imam, El-Yazal et al. 2001). Other antioxidants such 6-hydroxy-2,5,7,8-tetramethylchroman-2-carboxylic acid (Trolox) have been intensively used to protect animals and cell models from METH-insult (Ramirez, Potula et al. 2009).

Acetyl-L-carnitine (ALC) was also proposed as a neuroprotective agent with benefits at mitochondrial energetics and function, antioxidant activity, stabilization of membranes, protein and gene expression modulation, and enhancement of cholinergic neurotransmission (Jones, McDonald et al. 2010). Although the exact mechanisms of ALC action is still poorly explored, the next section will highlight some of the benefits of this compound in the brain and how these may be applicable in various clinical situations.

3. Acetyl-L-Carnitine

L-Carnitine (LC), either absorbed from diet or biosynthesized, is incorporated into the total body carnitine pool that comprises both free carnitine and acylcarnitines, which include the acetyl ester - ALC. The carnitine pool of a healthy human weighing 70 kg is about 15-20 g (Marcovina, Sirtori et al. 2013). The largest body storage sites of this pool (95%) are the skeletal and cardiac muscle (Pettegrew, Levine et al. 2000; Marcovina, Sirtori et al. 2013; Onofrj, Ciccocioppo et al. 2013). *In vivo,* ALC is synthesized from L-lysine, L-methionine and vitamin C mostly in liver and kidney but also in intestine and brain (Inano, Sai et al. 2003; Jones, McDonald et al. 2010; Marcovina, Sirtori et al. 2013; Onofrj, Ciccocioppo et al. 2013). Due to its amphiphilic structure, ALC is very mobile through-out the cell (Pettegrew, Levine et al. 2000; Jones, McDonald et al. 2010), and its most widely known function is the transport of long-chain fatty acids into mitochondria for β-oxidation (Sharma and Black 2009; Onofrj, Ciccocioppo et al. 2013). Carnitine acetyltransferase (CAT) is located on the inner mitochondrial membrane as well as in microsomes and peroxisomes and catalyzes the synthesis of ALC. It enters the mitochondrial matrix through an exchange of acylcarnitine/carnitine by carnitine-acylcarnitine translocase, as represented in **Fig.6**. For each acylcarnitine molecule crossing the inner mitochondrial membrane, one molecule of carnitine is shuttled out (Onofrj, Ciccocioppo et al. 2013).

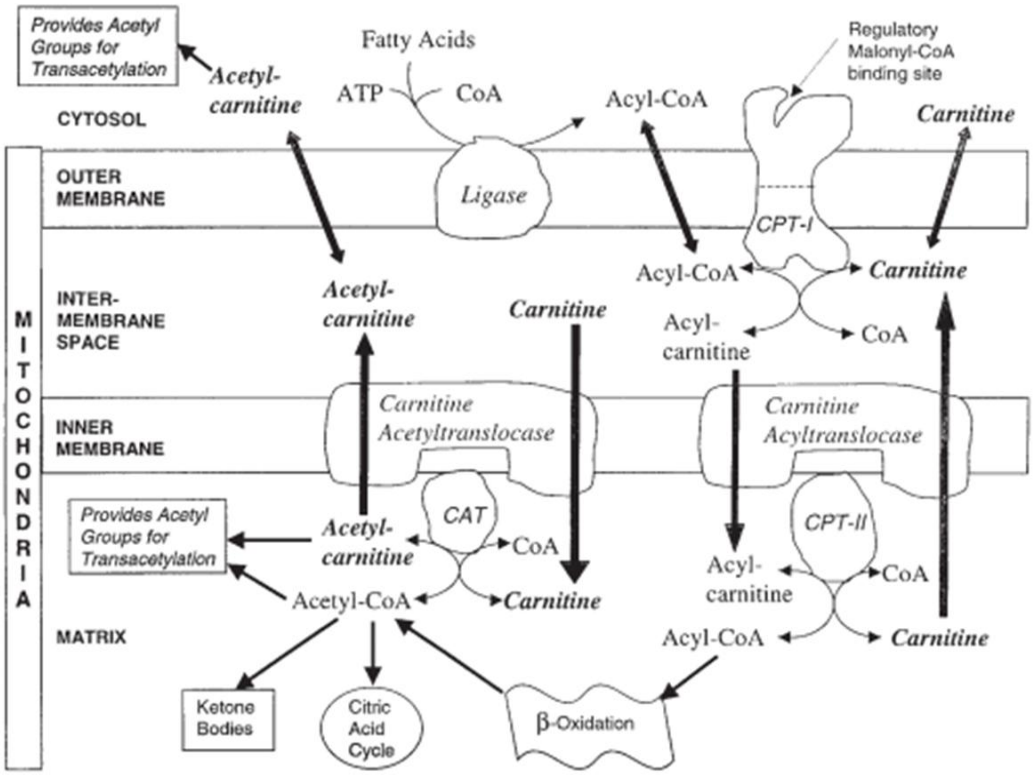

Fig.6 Acetyl-L-carnitine in overall energy metabolism. (CoASH = Coenzyme A). *Adapted from (Pettegrew, Levine et al. 2000)*

The role of carnitine *per se* goes beyond the oxidation of fatty acids since the coenzyme A (CoA)-carnitine relationship is critical for energy metabolism. CoA is required for β-oxidation, for the catabolism of several amino acids, for the detoxification of organic acids and xenobiotics and for the tricarboxylic acid cycle. Decreased carnitine availability induced a reduction of matrix free coenzyme A (CoASH) and a parallel increase of the acyl CoA/CoASH ratio. Consequently, not only the oxidation of fatty acids, but also the utilization of carbohydrates, the catabolism of several amino acids and the detoxification processes may be impaired (Pettegrew, Levine et al. 2000; Sharma and Black 2009; Marcovina, Sirtori et al. 2013). Moreover, ALC has a role in the terminal part of the Krebs cycle where it also facilitates the mitochondrial respiratory chain, acting on complexes I (NADH-reductase ubiquitone) and IV (cytochrome oxidase) (Onofrj, Ciccocioppo et al. 2013). Alterations in dietary conditions change carnitine and acylcarnitine levels in the body. In humans, fasting and diabetic ketosis induce a delayed decrease in plasma carnitine and a rapid increase in both long- and short-chain acylcarnitines, suggesting the overall importance of carnitine in maintaining energy homeostasis (Marcovina, Sirtori et al. 2013).

Some authors suggested that acetyl moiety of ALC (**Fig.7**) can be used to acetylate amine and hydroxil functional groups in peptides and proteins, and possibly modify their structure, function and turnover (Pettegrew, Levine et al. 2000). ALC provides acetyl groups for acetylcholine synthesis, exerting a cholinergic effect and optimizing the balance of energy processes (Madiraju, Pande et al. 2009; Huang, Liu et al. 2012; Onofrj, Ciccocioppo et al. 2013).

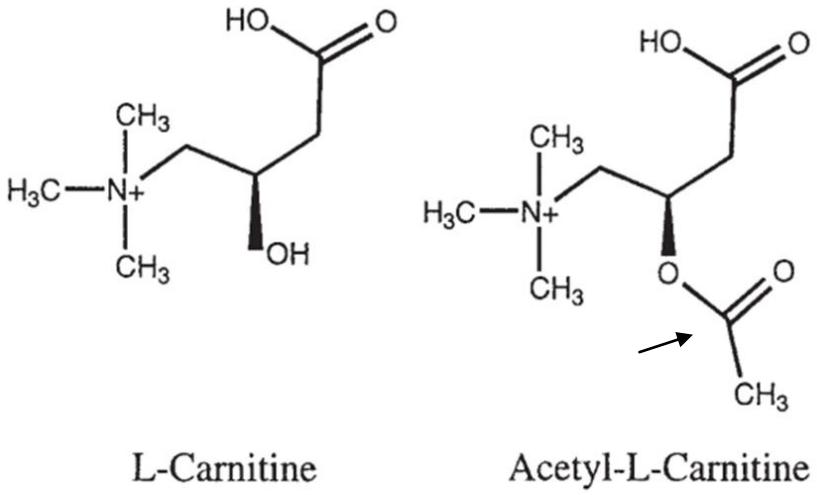

Fig.7 Molecular structure of L-carnitine and acetyl-L-carnitine. Acetyl group (arrow) is proposed to have a role on protein acetylation.
Adapted from (Pettegrew, Levine et al. 2000)

Indeed, ALC has long been reported to affect the cholinergic, serotonergic, dopaminergic, glutamatergic and GABAergic systems, but the mechanisms involved were mostly unknown (Tolu, Masi et al. 2002). Recently, using ^{13}C-ALC, it was demonstrated that the

acetyl moiety of the compound is used as an energy source by both astrocytes and neurons being rapidly incorporated into glutamate and GABA synthesis (Scafidi, Fiskum et al. 2010). This clarifies the direct involvement of ALC in increased glutamine, glutamate and GABA levels, through α-ketoglutarate production, via the tricarboxylic acid cycle. Importantly, biosynthesis of both tyrosine and L-tryptophan, as well as DA and 5-HT precursors, involves either a transamination reaction with glutamate or the participation of glutamine as an amine donor (Stryer 1988), which may explain the action of ALC over monoamine production. Noteworthy, glutamate is also the precursor of glutathione biosynthesis (Griffith and T. 1999), an enzyme frequently implicated in the antioxidant properties of ALC administration.

Thus, ALC can provide high-energy acetyl groups to metabolic pathways improving the overall energy status of the brain, to alter neurotransmitters biosynthesis, and also has the potential to be involved in modulating proteins and gene expression (Jones, McDonald et al. 2010; Marcovina, Sirtori et al. 2013).

3.1 ALC beneficial effects

ALC administration has been seen to be beneficial in a number of disorders characterized by low carnitine concentrations or impaired fatty acid oxidation, including diabetes (Xia, Li et al. 2011; Marcovina, Sirtori et al. 2013), sepsis, and cardiomyopathy (Marcovina, Sirtori et al. 2013). ALC is prescribed for inborn errors of metabolism (Sharma and Black 2009) but also for several neurologic disorders such as Alzheimer and Parkinson diseases, stroke or drug abuse (Pettegrew, Levine et al. 2000; Marcovina, Sirtori et al. 2013).

The neuroprotective action of ALC has been described *in vitro* and *in vivo*. ALC administration has been shown to reduce oxidative stress and mitochondrial alterations counteracting neurologic pathologies. The protective effects of ALC are likely to be achieved through decreased oxidative stress, improvement of mitochondrial function and increased ATP production (Marcovina, Sirtori et al. 2013; Onofrj, Ciccocioppo et al. 2013). Although its antioxidant role has been reported in numerous studies, carnitine and its esters are devoid of direct antioxidant properties. Therefore, other mechanisms are involved in ALC modulation of oxidative stress such as those linked to the positive effects on mitochondrial metabolism and function (Marcovina, Sirtori et al. 2013).

It is known that ALC is able to cross the BBB and is present in high concentrations in the brain, so ALC supplementing can feasibly affect brain metabolism (Pettegrew, Levine et al. 2000; Jones, McDonald et al. 2010; Lee, Choi et al. 2012). In the brain, ALC presents several physiological effects including the modulation of brain energy, neurohormones, neurotrophic factors, synaptic morphology and chemical neurotransmission (Pettegrew, Levine et al. 2000; Inano, Sai et al. 2003; Lee, Choi et al. 2012). Both LC and ALC are transported into the brain in a sodium-dependent manner via a high-affinity carnitine transporter, the organic cation/carnitine transporter 2 (OCTN2). OCTN2 is present in non-neuronal cells such as astrocytes and

especially in brain capillary ECs of human, rat and mouse (Yasuto, Ikumi et al. 2001; Inano, Sai et al. 2003; Lee, Choi et al. 2012). *Kido Yasuto* and collaborators observed that BBB is more permeable to ALC than LC, since ALC is more efficiently transported from circulating blood into the brain across the BBB. According to this and other studies, immortalized ECs are endowed with properties for ALC transport similar to those present *in vivo* and in primary ECs (Yasuto, Ikumi et al. 2001; Lee, Choi et al. 2012).

Within brain cells ALC can be converted by the reversible enzyme CAT into acetyl-CoA and carnitine without ATP utilization (Lee, Choi et al. 2012). In the rat brain, ALC administration led to reduced oxidation of glucose and increased glycogen synthesis. Changes in the activities of specific enzymes involved in the tricarboxylic acid cycle, electron transport chain and amino acid metabolism have also been observed after treatment with ALC (Jones, McDonald et al. 2010).

ALC treatment restores the thalamo-cortical system in rats prenatally exposed to neurotoxic substances such as ethanol and MPP^+ (1-methyl-4-phenylpyridinium) solution (Virmani, Gaetani et al. 2004), promotes acetylcholine synthesis and release protecting cortical neurons from the neurotoxic effects of amyloid fragments and peroxidase (Lee, Choi et al. 2012). ALC significantly prevented mitochondrial oxidative damage and mtDNA deletion with improved expression of respiratory chain components after a 3,4-methylenedioxymetham-phetamine (MDMA or ecstasy) insult (Alves, Binienda et al. 2009). Moreover, ALC administration was reported to ameliorate the spatial memory performance of rats exposed to neonatal anoxia (Pettegrew, Levine et al. 2000) as well as learning-memory function in aged rats (Goo, Choi et al. 2012).

In humans, patients suffering from dementia, major depression, painful neuropathies and Alzheimer's disease seem to benefit from ALC administration. ALC was reported to improve the clinical status of such patients through restoration of cell membranes, brain energy and/or synaptic function (Pettegrew, Levine et al. 2000; Onofrj, Ciccocioppo et al. 2013).

Much of the research on the role of carnitine and its esterified derivative ALC, has been centered in the metabolism. However, there is a great deal of evidence in the literature to support new and multifactorial roles for these compounds. In this sense, in 2000, *Pettegrew* and collaborators suggested that ALC increase in membrane stability could be possibly related with ALC interaction with cytoskeletal proteins as well as by posttranslational regulation of such proteins. Moreover, it was described a role of ALC on enzymatic activity modulation (Pettegrew, Levine et al. 2000), as well as epigenetic modifications (Madiraju, Pande et al. 2009; Huang, Liu et al. 2012; Onofrj, Ciccocioppo et al. 2013).

3.2 ALC preventive effect on BBB function

There is growing evidence that through maintaining the endothelium homeostasis is possible to reduce the incidence or severity of systemic vascular diseases. Although less

explored, protection of the BBB has the potential to delay or prevent the development of neurodegenerative states. Several compounds have been studied in order to reach neuroprotection, including flavonoids, and other polyphenolic agents, and the cytokine erythropoietin. These agents seem to have beneficial effects against *in vivo* and in *in vitro* injury, at the endothelium level, by reducing the level of eNOS and restoring junctional proteins (Abbott, Rönnbäck et al. 2006).

The majority of treatments mentioned so far is designed to seal up and improve the transport function of the BBB. However, another approach consisting in the opening the TJs to facilitate drug delivery to the brain, was also subject of relevant research (Abbott, Rönnbäck et al. 2006).

In the last few years several studies were carried out in order to assess ALC effects on BBB function. However, the mechanisms underlying the protective features reported are very poorly understood.

Recently, some authors reported a link between glucose deprivation and BBB damage due to alcohol and METH exposure both *in vivo* and *in vitro* (Rump, Abdul Muneer et al. 2010; Abdul Muneer, Alikunju et al. 2011; Abdul Muneer, Alikunju et al. 2011; Abdul Muneer, Alikunju et al. 2011; Muneer, Alikunju et al. 2011). In this context, *Muneer PM* and collaborators observed that METH and ethanol-induced inhibition of glucose uptake correlates with a reduction in glucose transporter protein expression (GLUT1 in astrocytes and GLUT3 in neurons). In those studies, ALC counteracts the effect of alcohol on glucose uptake and glucose transporter levels, thus reducing neurotoxicity and neuronal degeneration observed (Muneer, Alikunju et al. 2011). Moreover, both alcohol and METH exposure impaired the BBB TJs proteins claudin-5, occludin and accessory protein *ZO-1* in the brain microvessel, along with increased BBB permeability of sodium fluorescein and Evans Blue (Rump, Abdul Muneer et al. 2010; Abdul Muneer, Alikunju et al. 2011). Again, ALC prevented the adverse effects of those neurotoxic agents on glucose uptake, BBB permeability and neuronal degeneration through stabilization of glucose uptake and GLUT1 protein level. These authors suggested that ALC stabilized glycosylation of GLUT1 protein by donating an acetyl group to glucosamine, enhancing the activity of acetylglucosamine in the neurovascular compartment (Rump, Abdul Muneer et al. 2010; Abdul Muneer, Alikunju et al. 2011).

In another study, ALC was shown to significantly minimize the level of alcohol-induced iNOS/nitrotyrosine formation in neurons and further prevented NOX protein induction in astrocytes and microglia, thereby preventing gliosis in the rat brains exposed to alcohol. These findings indicated that ALC, by providing carnitine and acetyl groups, has therapeutic value as an antioxidant and/or anti-inflammatory agent. Since ALC is not a direct scavenger of free radicals, authors postulate that ALC exerts its antioxidant property by indirect mechanisms such as its ability to maintain mitochondrial membrane transition potential (Rump, Abdul Muneer et al. 2010). Another plausible mechanism for ALC preventing excessive levels of ROS generation is through stabilization of biological antioxidant enzymes and antioxidants such as superoxide dismutase (SOD), catalase, or the intracellular levels of glutathione. In this context, it was

shown afterwards that ALC stabilization of SOD activity correlates with the preservation of both Cu/Zn-SOD1 and Mn-SOD2 protein levels in the human brain ECs, thus preserving brain vascular function (Haorah, Floreani et al. 2011).

The side-effects of ALC administration in the body, namely those affecting the liver and kidney remain unknown, and care should be taken before prescribe it to healthy individuals. Although nothing is currently published concerning ALC toxicity, our previous work shows that an acute hepatic injury can occur in ALC-treated mice. Since ALC is already not only in clinical use as a therapeutic agent for treatment of neurological diseases, but also extensively used to promote weight loss and body building in healthy people, unveiling the ALC molecular mechanism is therefore highly relevant.

4. References

Abbott, N. J. (2013). "Blood-brain barrier structure and function and the challenges for CNS drug delivery." J Inherit Metab Dis **36**(3): 437-449.

Abbott, N. J., L. Rönnbäck, et al. (2006). "Astrocyte–endothelial interactions at the blood–brain barrier." Nature Reviews Neuroscience **7**(1): 41-53.

Abdul Muneer, P. M., S. Alikunju, et al. (2011). "Inhibitory effects of alcohol on glucose transport across the blood-brain barrier leads to neurodegeneration: preventive role of acetyl-L: -carnitine." Psychopharmacology (Berl) **214**(3): 707-718.

Abdul Muneer, P. M., S. Alikunju, et al. (2011). "Methamphetamine inhibits the glucose uptake by human neurons and astrocytes: stabilization by acetyl-L-carnitine." PLoS One **6**(4): e19258.

Abdul Muneer, P. M., S. Alikunju, et al. (2011). "Impairment of brain endothelial glucose transporter by methamphetamine causes blood-brain barrier dysfunction." Mol Neurodegener **6**: 23.

Albertson, T. E., R. W. Derlet, et al. (1999). "Methamphetamine and the expanding complications of amphetamines." Western Journal of Medicine **170**(4): 214.

Alves, E., Z. Binienda, et al. (2009). "Acetyl-L-carnitine provides effective in vivo neuroprotection over 3,4-methylenedioximethamphetamine-induced mitochondrial neurotoxicity in the adolescent rat brain." Neuroscience **158**(2): 514-523.

András, I. E., P. Hong, et al. (2003). "HIV-1 Tat Protein Alters Tight Junction Protein Expression and Distribution in Cultured Brain Endothelial Cells." Journal of Neuroscience Research **74**: 255-265.

Andreeva, A. Y., E. Krause, et al. (2001). "Protein kinase C regulates the phosphorylation and cellular localization of occludin." J Biol Chem **276**(42): 38480-38486.

Balda, M. S., J. A. Whitney, et al. (1996). "Functional Dissociation of Paracellular Permeability and Transepithelial Eletrical Resistance and Disruption of the Apical-Basolateral Intermembrane Diffusion Barrier by Expression of a Mutant Tight Junction Membrane Protein." The Journal of Cell Biology **134**(4): 1031-1049.

Booth, R. and H. Kim (2012). "Characterization of a microfluidic in vitro model of the blood-brain barrier (μBBB)." Lab on a chip **12**(10): 1784-1792.

Bowyer, J. F. and S. Ali (2006). "High doses of methamphetamine that cause disruption of the blood-brain barrier in limbic regions produce extensive neuronal degeneration in mouse hippocampus." Synapse **60**(7): 521-532.

Bowyer, J. F., M. Thomas, et al. (2008). "Brain region-specific neurodegenerative profiles showing the relative importance of amphetamine dose, hyperthermia, seizures, and the blood-brain barrier." Ann N Y Acad Sci **1139**: 127-139.

Bradbury, M. (1993). "The Blood-Brai Barrier." Experimental Physiology(78): 453-472.

Brown, R. C., A. P. Morris, et al. (2007). "Tight junction protein expression and barrier properties of immortalized mouse brain microvessel endothelial cells." Brain Res **1130**(1): 17-30.

Chandramani Shivalingappa, P., H. Jin, et al. (2012). "N-Acetyl Cysteine Protects against Methamphetamine-Induced Dopaminergic Neurodegeneration via Modulation of Redox Status and Autophagy in Dopaminergic Cells." Parkinsons Dis **2012**: 424285.

Chen, F., T. Hori, et al. (2011). "Occludin is regulated by epidermal growth factor receptor activation in brain endothelial cells and brains of mice with acute liver failure." Hepatology **53**(4): 1294-1305.

Conant, K., I. Lonskaya, et al. (2011). "Methamphetamine-associated cleavage of the synaptic adhesion molecule intercellular adhesion molecule-5." J Neurochem **118**(4): 521-532.

Conant, K., S. T Lim, et al. (2012). "Matrix metalloproteinase dependent cleavage of cell adhesion molecules in the pathogenesis of CNS dysfunction with HIV and methamphetamine." Current HIV research **10**(5): 384-391.

Crime, U. N. O. o. D. a. (2014). World Drug Report 2014. New York, United Nations publication, Sales No. E.14.XI.7.

Deli, M. (2007). "Blood–brain barrier models." Handbook of Neurochemistry and Molecular Neurobiology: Neural Membranes and Transport: 29-55.

Downey, L. A. and J. M. Loftis (2014). "Altered energy production, lowered antioxidant potential, and inflammatory processes mediate CNS damage associated with abuse of the psychostimulants MDMA and methamphetamine." Eur J Pharmacol **727**: 125-129.

ElAli, A., A. Urrutia, et al. (2012). "Apolipoprotein-E controls adenosine triphosphate-binding cassette transporters ABCB1 and ABCC1 on cerebral microvessels after methamphetamine intoxication." Stroke **43**(6): 1647-1653.

Friend, D. M. and K. A. Keefe (2013). "Glial reactivity in resistance to methamphetamine-induced neurotoxicity." J Neurochem **125**(4): 566-574.

Forster, C., M. Burek, et al. (2008). "Differential effects of hydrocortisone and TNFalpha on tight junction proteins in an in vitro model of the human blood-brain barrier." J Physiol **586**(7): 1937-1949.

Fukumura, D., T. Gohongi, et al. (2001). "Predominant role of endothelial nitric oxide synthase in vascular endothelial growth factor-induced angiogenesis and vascular permeability." Proc Natl Acad Sci U S A **98**(5): 2604-2609.

Furuse, M., T. Hirase, et al. (1993). "Occludin: a novel integral membrane protein localizing at tight junctions." The Journal of Cell Biology **123**(6): 1777-1788.

Gold, M. S., F. H. Kobeissy, et al. (2009). "Methamphetamine- and trauma-induced brain injuries: comparative cellular and molecular neurobiological substrates." Biol Psychiatry **66**(2): 118-127.

Goncalves, J., S. Baptista, et al. (2010). "Methamphetamine-induced neuroinflammation and neuronal dysfunction in the mice hippocampus: preventive effect of indomethacin." Eur J Neurosci **31**(2): 315-326.

Goo, M. J., S. M. Choi, et al. (2012). "Protective effects of acetyl-L-carnitine on neurodegenarative changes in chronic cerebral ischemia models and learning-memory impairment in aged rats." Arch Pharm Res **35**(1): 145-154.

Griffith, O. W. and M. R. T. (1999). "The enzymes of glutathione synthesis: gamma-glutamylcysteine synthetase." Adv Enzymol Relat Areas Mol Biol. **73**(209).

Haorah, J., N. A. Floreani, et al. (2011). "Stabilization of superoxide dismutase by acetyl-l-carnitine in human brain endothelium during alcohol exposure: novel protective approach." Free Radic Biol Med **51**(8): 1601-1609.

Haorah, J., B. Knipe, et al. (2005). "Alcohol-induced oxidative stress in brain endothelial cells causes blood-brain barrier dysfunction." J Leukoc Biol **78**(6): 1223-1232.

Hawkins, B. T. and T. P. Davis (2005). "The blood-brain barrier/neurovascular unit in health and disease." Pharmacol Rev **57**(2): 173-185.

Huang, H., N. Liu, et al. (2012). "L-carnitine is an endogenous HDAC inhibitor selectively inhibiting cancer cell growth in vivo and in vitro." PLoS One **7**(11): e49062.
Imam, S. Z., J. El-Yazal, et al. (2001). "Methamphetamine-Induced Dopaminergic Neurotoxicity: Role of Peroxynitrite and Neuroprotective Role of Antioxidants and Peroxynitrite Decomposition Catalysts." Ann N Y Acad Sci **939**(1): 366-380.
Inano, A., Y. Sai, et al. (2003). "Acetyl-L-carnitine permeability across the blood–brain barrier and involvement of carnitine transporter OCTN2." Biopharmaceutics & drug disposition **24**(8): 357-365.
Itzhak, Y., J. L. Martin, et al. (1998). "Effect of melatonin on methamphetamine-and 1-methyl-4-phenyl-1, 2, 3, 6-tetrahydropyridine-induced dopaminergic neurotoxicity and methamphetamine-induced behavioral sensitization." Neuropharmacology **37**(6): 781-791.
Jin, C. H., T. T. Moo, et al. (2002). "Methamphetamine-induced Apoptosis in a CNS-derived Catecholaminergic Cell Line." Molecules and Cells **13**(2): 221-227.
Jones, L. L., D. A. McDonald, et al. (2010). "Acylcarnitines: role in brain." Prog Lipid Res **49**(1): 61-75.
Kashiwamura, Y., Y. Sano, et al. (2011). "Hydrocortisone enhances the function of the blood-nerve barrier through the up-regulation of claudin-5." Neurochem Res **36**(5): 849-855.
Krasnova, I. N. and J. L. Cadet (2009). "Methamphetamine toxicity and messengers of death." Brain Res Rev **60**(2): 379-407.
Ladenheim, B., I. N. Krasnova, et al. (2000). "Methamphetamine-induced neurotoxicity is attenuated in transgenic mice with a null mutation for interleukin-6." Molecular pharmacology **58**(6): 1247-1256.
Lee, N. Y., H. O. Choi, et al. (2012). "The acetylcholinesterase inhibitors competitively inhibited an acetyl L-carnitine transport through the blood-brain barrier." Neurochem Res **37**(7): 1499-1507.
Liebner, S., U. Kniesel, et al. (2000). "Correlation of tight junction morphology with the expression of tight junction proteins in blood-brain barrier endothelial cells." Eur J Cell Biol **79**(10): 707-717.
Liu, Y., S. Brown, et al. (2008). "Relationship between methamphetamine exposure and matrix metalloproteinase 9 expression." Neuroreport **19**(14): 1407-1409.
Ma, J., J. Wan, et al. (2014). "Methamphetamine induces autophagy as a pro-survival response against apoptotic endothelial cell death through the Kappa opioid receptor." Cell Death Dis **5**: e1099.
Madiraju, P., S. V. Pande, et al. (2009). "Mitochondrial acetylcarnitine provides acetyl groups for nuclear histone acetylation." Epigenetics **4**(6): 399-403.
Mahajan, S. D., R. Aalinkeel, et al. (2012). "Suppression of MMP-9 expression in brain microvascular endothelial cells (BMVEC) using a gold nanorod (GNR)-siRNA nanoplex." Immunol Invest **41**(4): 337-355.
Mahajan, S. D., R. Aalinkeel, et al. (2008). "Methamphetamine alters blood brain barrier permeability via the modulation of tight junction expression: Implication for HIV-1 neuropathogenesis in the context of drug abuse." Brain Res **1203**: 133-148.
Marcovina, S. M., C. Sirtori, et al. (2013). "Translating the basic knowledge of mitochondrial functions to metabolic therapy: role of L-carnitine." Translational Research **161**(2): 73-84.
Marshall, J. F. and S. J. O'Dell (2012). "Methamphetamine influences on brain and behavior: unsafe at any speed?" Trends Neurosci **35**(9): 536-545.
Martins, T., S. Baptista, et al. (2011). "Methamphetamine transiently increases the blood-brain barrier permeability in the hippocampus: role of tight junction proteins and matrix metalloproteinase-9." Brain Res **1411**: 28-40.
Martins, T., T. Burgoyne, et al. (2013). "Methamphetamine-induced nitric oxide promotes vesicular transport in blood-brain barrier endothelial cells." Neuropharmacology **65**: 74-82.
Masahiko, I., M. Kazumasa, et al. (1999). "Characterization of ZO-2 as a MAGUK Family Member Associated with Tight as well as Adherens Junctions with a Binding Affinity to Occludin and a Catenin." J Biol Chem **274**(26): 5981-5986.
Matthias, B., H. A. M, et al. (2004). "RhoA, Rac 1, and Cdc42 exert distinct effects on epithelial barrier via selective strictural and biochemical modulation on junctional proteins and F-actin." Am J Physiol Cell Physiol **287**: C327-C335.
Melega, W. P., A. K. Cho, et al. (2007). "Methamphetamine Blood Concentrations in Human Abusers: Application to Pharmacokinetic Modeling." Synapse(61): 216–220.
Mirecki, A., P. Fitzmaurice, et al. (2004). "Brain antioxidant systems in human methamphetamine users." J Neurochem **89**(6): 1396-1408.
Mizoguchi, H. and K. Yamada (2013). "Roles of matrix metalloproteinases and their targets in epileptogenesis and seizures." Clin Psychopharmacol Neurosci **11**(2): 45-52.
Mizoguchi, H., K. Yamada, et al. (2007). "Reduction of methamphetamine-induced sensitization and reward in matrix metalloproteinase-2 and -9-deficient mice." J Neurochem **100**(6): 1579-1588.
Muneer, P. A., S. Alikunju, et al. (2011). "Ethanol impairs glucose uptake by human astrocytes and neurons: protective effects of acetyl-L-carnitine." International journal of physiology, pathophysiology and pharmacology **3**(1): 48.
Muneer, P. M. A., S. Alikunju, et al. (2011). "Inhibitory effects of alcohol on glucose transport across the blood-brain barrier leads to neurodegeneration: preventive role of acetyl-L: -carnitine." Psychopharmacology (Berl) **214**(3): 707-718.
Navarro-Costa, P., C. E. Plancha, et al. (2012). Citoesqueleto: composição, organização e significado funcional. Biologia Celular e Molecular. Lidel. Lisboa**:** 286-300.
Northrop, N. A. and B. K. Yamamoto (2012). "Persistent neuroinflammatory effects of serial exposure to stress and methamphetamine on the blood-brain barrier." J Neuroimmune Pharmacol **7**(4): 951-968.
O'Shea, E., A. Urrutia, et al. (2014). "Current preclinical studies on neuroinflammation and changes in blood-brain barrier integrity by MDMA and methamphetamine." Neuropharmacology.
Omidi, Y., L. Campbell, et al. (2003). "Evaluation of the immortalised mouse brain capillary endothelial cell line, b.End3, as an in vitro blood–brain barrier model for drug uptake and transport studies." Brain Res **990**(1-2): 95-112.
Onofrj, M., F. Ciccocioppo, et al. (2013). "Acetyl-L-carnitine: from a biological curiosity to a drug for the peripheral nervous system and beyond." Expert review of neurotherapeutics **13**(8): 925-936.
Park, M., H. J. Kim, et al. (2013). "Methamphetamine-induced occludin endocytosis is mediated by the Arp2/3 complex-regulated actin rearrangement." J Biol Chem **288**(46): 33324-33334.
Pasquali, L., G. Lazzeri, et al. (2008). "Role of autophagy during methamphetamine neurotoxicity." Ann N Y Acad Sci **1139**: 191-196.

Persidsky, Y., D. Heilman, et al. (2006). "Rho-mediated regulation of tight junctions during monocyte migration across the blood-brain barrier in HIV-1 encephalitis (HIVE)." Blood **107**(12): 4770-4780.
Pettegrew, J., J. Levine, et al. (2000). "Acetyl-L-carnitine physical-chemical, metabolic, and therapeutic properties: relevance for its mode of action in Alzheimer's disease and geriatric depression." Molecular Psychiatry **5**: 616-632.
Ramirez, S. H., R. Potula, et al. (2009). "Methamphetamine disrupts blood-brain barrier function by induction of oxidative stress in brain endothelial cells." J Cereb Blood Flow Metab **29**(12): 1933-1945.
Rao, R. (2009). "Occludin phosphorylation in regulation of epithelial tight junctions." Ann N Y Acad Sci **1165**: 62-68.
Reynolds, J. L., S. D. Mahajan, et al. (2011). "Methamphetamine and HIV-1 gp120 effects on lipopolysaccharide stimulated matrix metalloproteinase-9 production by human monocyte-derived macrophages." Immunol Invest **40**(5): 481-497.
Rosano, L., F. Spinella, et al. (2006). "Integrin-linked kinase functions as a downstream mediator of endothelin-1 to promote invasive behavior in ovarian carcinoma." Mol Cancer Ther **5**(4): 833-842.
Roux, F. and P.-O. Couraud (2005). "Rat Brain Endothelial Cell Lines for the Study of Blood–Brain Barrier Permeability and Transport Functions." Cellular and Molecular Neurobiology **25**(1): 41-57.
Rump, T. J., P. M. Abdul Muneer, et al. (2010). "Acetyl-L-carnitine protects neuronal function from alcohol-induced oxidative damage in the brain." Free Radic Biol Med **49**(10): 1494-1504.
Scafidi, S., G. Fiskum, et al. (2010). "Metabolism of acetyl-L-carnitine for energy and neurotransmitter synthesis in the immature rat brain." J Neurochem **114**(3): 820-831.
Schrade, A., H. Sade, et al. (2012). "Expression and localization of claudins-3 and -12 in transformed human brain endothelium." Fluids Barriers CNS **9**: 6.
Sharma, H. S. and E. A. Kiyatkin (2009). "Rapid morphological brain abnormalities during acute methamphetamine intoxication in the rat: an experimental study using light and electron microscopy." J Chem Neuroanat **37**(1): 18-32.
Sharma, S. and S. M. Black (2009). "Carnitine homeostasis, mitochondrial function and cardiovascular disease." Drug Discovery Today: Disease Mechanisms **6**(1): e31-e39.
Singh, A. B. and R. C. Harris (2004). "Epidermal growth factor receptor activation differentially regulates claudin expression and enhances transepithelial resistance in Madin-Darby canine kidney cells." J Biol Chem **279**(5): 3543-3552.
Stryer (1988). Biosinthesys of Amino Acids and Heme. Biochemistry. New York, Ed. W.H. Freeman and Company.
Takeshita, Y., B. Obermeier, et al. (2014). "An in vitro blood-brain barrier model combining shear stress and endothelial cell/astrocyte co-culture." J Neurosci Methods **232**: 165-172.
Toborek M., M. J. Seelbach, et al. (2013). "Voluntary exercise protects against methamphetaminbe-induced oxidative stress in brain microvasculature and disruption of the blood-brain-barrier." Molecular Neurodegeneration **8**(22).
Tolu, P., F. Masi, et al. (2002). "Effects of long-term acetyl-L-carnitine administration in rats: I. increased dopamine output in mesocorticolimbic areas and protection toward acute stress exposure." Neuropsychopharmacology **27**(3): 410-420.
Troussard, A. A., P. Costello, et al. (2000). "The integrin linked kinase (ILK) induces an invasive phenotype via AP-1 transcription factor-dependent upregulation of matrix metalloproteinase 9 (MMP-9)." Oncogene **19**: 5444-5452.
Urrutia, A., A. Rubio-Araiz, et al. (2013). "A study on the effect of JNK inhibitor, SP600125, on the disruption of blood-brain barrier induced by methamphetamine." Neurobiol Dis **50**: 49-58.
Virmani, A., F. Gaetani, et al. (2004). "Role of Mitochondrial Dysfunction in Neurotoxicity of MPP:+: Partial Protection of PC12 Cells by Acetyl-l-Carnitine." Ann N Y Acad Sci **1025**(1): 267-273.
Visse, R. and H. Nagase (2003). "Matrix metalloproteinases and tissue inhibitors of metalloproteinases: structure, function, and biochemistry." Circ Res **92**(8): 827-839.
Wu, C. and S. Dedhar (2001). "Integrin-linked kinase (ILK) and its interactors: a new paradigm for the coupling of extracellular matrix to actin cytoskeleton and signaling complexes." J Cell Biol **155**(4): 505-510.
Xia, Y., Q. Li, et al. (2011). "L-carnitine ameliorated fatty liver in high-calorie diet/STZ-induced type 2 diabetic mice by improving mitochondrial function." Diabetol Metab Syndr **3**: 31.
Yamamoto, B. K. and J. Raudensky (2008). "The role of oxidative stress, metabolic compromise, and inflammation in neuronal injury produced by amphetamine-related drugs of abuse." J Neuroimmune Pharmacol **3**(4): 203-217.
Yamamoto, M., S. H. Ramirez, et al. (2008). "Phosphorylation of claudin-5 and occludin by rho kinase in brain endothelial cells." Am J Pathol **172**(2): 521-533.
Yasuto, K., T. Ikumi, et al. (2001). "Functional relevance of carnitine transporter OCTN2 to brain distribution of L-carnitine and acetyl-L-carnitine across the blood-brain barrier." J Neurochem **79**: 959-969.
Zoia, M., P. D. L, et al. (2000). "Occludin 1B, a Variant of the Tight Junction Protein Occludin." Molecular Biology of the Cell **11**: 627-634.

GOALS

GOALS

The present work aims to explore the mechanisms by which METH-exposure may lead to increased permeability at BBB level, and evaluate the potential of ALC to counteract METH-induced damage. To do so, we have defined the following steps:

1- Investigate early changes in gene expression after METH exposure using a gene array suitable to evaluate cytoskeleton-mediated permeability, to identify research targets. This will be achieved by:
    a. Assessing *in vivo* gene expression of METH-treated mice, using a specific array containing the 84 members of PI3K-AKT signaling pathway;
    b. Defining which pathways are interesting enough to deserve further study in the context on METH-induced permeability;
    c. Validating the array through the individual analysis of particular genes of interest in all treatment conditions.

2- Considering the target genes selected above, assess METH-triggered effects on BBB structure/function using and *in vitro* endothelial cell model exposed to ranging doses of METH. The following parameters will be evaluated:
    a. TJs expression and localization;
    b. Actin and tubulin cytoskeleton arrangement;
    c. Evaluation of specific molecular targets within the pathways previously selected.

3- Unveiling the effects of ALC in preventing METH-induced BBB dysfunction using the same *in vitro* model:
    a. Pretreat cells with ALC before METH exposure in order to:
        i. Assess the ALC protective effects in preventing METH-induced disorganization of cytoskeleton elements;
        ii. Assess the ALC protective mechanism in preventing METH-triggered activation of specific pathways, comparing when possible with other therapeutic approaches.

CHAPTER I

Gene expression after METH exposure in vivo

(unpublished work)

“The scientist is motivated primarily by curiosity and a desire for truth.”

Irving Langmuir

1. Introduction

There is growing evidence that illicit drugs such as METH exert substantial transcriptional and epigenetic modifications in the brain (Betts, Krasnova et al. 2002; Martin, Jayanthi et al. 2012; Cadet, Jayanthi et al. 2013). Gene expression is regulated by epigenetic modifications, which are intimately involved in the development and clinical course of many neurological diseases, such as addiction. In that sense, it was already shown that METH might trigger transcriptional and epigenetic changes that are specific to this drug (Cadet, Jayanthi et al. 2013).

Based on the previously described effects of METH, it is important to address gene expression involvement in the regulation of neuronal responses to stimuli, particularly those that may be implicated in the neuronal responses underlying drug addiction and abuse. In the brain, METH effects are particularly prominent in the striatum, a basal ganglia involved in drug-taking behaviors (Chang, Alicata et al. 2007; Volz, Fleckenstein et al. 2007).

The PI3K/AKT pathway is important not only for the development of many diseases but also for signaling in several mechanisms in normal cells. This pathway plays an important role in numerous cellular functions, such as adhesion, proliferation, differentiation, cellular metabolism, and cytoskeletal reorganization, migration, invasion and survival. Moreover, this pathway acts though integration of signals like insulin, cytokines, growth factors and environmental stresses, mainly for regulating cell proliferation, motility, differentiation and survival (Polivka and Janku 2014). Recently, some evidences strongly suggested the involvement of PI3K-AKT signaling pathway in cytoskeleton-mediated permeability (Bruewer, Hopkins et al. 2004). Since METH has been shown to strongly affect both cytoskeleton structure and permeability events (Ramirez, Potula et al. 2009; Martins, Baptista et al. 2011; Park, Kim et al. 2013), this pathway seems to be to assess METH-induced cytoskeleton and permeability alterations through PI3K-AKT pathway.

Here, we aimed to investigate early changes in gene expression after METH exposure, through assessing *in vivo* gene expression of METH-treated mice, using a specific array containing the 84 members of PI3K-AKT signaling pathway; and analyzing and correlating genes with altered expression that may be involved in METH-related effects. Moreover, we intend to construct an interactome using Ingenuity Pathway Analysis (IPA), QIAGEN software. To validate the array results, we aim to analyze individually gene expression of selected genes in every treatment conditions (saline; METH; ALC; ALC/METH and METH/ALC).

2. Material and methods

2.1 Animal treatment and procedures

Fifteen C57BL/6 mice were divided into 5 groups of treatment (3 animals per group): control saline; METH (3 x 5mg/kg i.p.); METH/ALC (3x5mg/kg i.p., followed by a single i.p. administration of 200 mg/kg of ALC, 30 min after); ALC/METH (3x5mg/kg i.p., preceded in 30 min by a single i.p. administration of 200 mg/kg of ALC), and ALC control. Animals were maintained under a 12h dark/light schedule and were given *ad libitum* food and water access. All experiments were performed respecting the Guidelines of the European Union Council 86/609/EU and 2010/63/EU and the Portuguese law for the care and use of experimental animals (DL n°1095/92) at the Animal Facility of the Instituto de Biologia Molecular e Celular (IBMC), University of Porto. All efforts were made to minimize animal suffering and to reduce the number of animals.

2.2 Brain RNA extraction and RT^2 Profiler PCR Array

Animals were killed 24h after the administration of the different treatments. Brain regions were briefly dissected on ice and frozen on dry ice cooled isopentane. Total RNA from each brain region was extracted using RNeasy® Mini Kit (*Qiagen, Hilden, Germany*). A pool of RNA from each group was prepared and RNA quality was checked by Experion automated electrophoresis system (*Bio-Rad Hercules, CA, USA*). Synthesis of cDNA was performed by Qiagen RT^2 HT First Strand cDNA kit and a total amount of 2,0 µg of RNA was used to screen genes expression of striatum METH-treated animals, compared to control.

This study was carried out using a RT^2 Profiler PCR Array plates approach, that takes advantage of the combination of real-time PCR performance and the ability of microarrays to detect simultaneously the expression of 84 members of PI3K-AKT signaling pathway (# PAMM-058A). This tool comprises 5 housekeeping genes that enable the normalization of data and different internal controls to validate DNA quality. RT^2 SYBR Green Mastermix is used to amplify and quantify genes expression on a cycler (Bio-Rad iQ5 model). Gene relative expression was calculated using $\Delta\Delta C_T$ method, expressed as relative fold change to the control saline treated animals. Gene expression of selected target genes was assessed by traditional RT-PCR and analyzed individually in every treatment conditions.

2.3 Real Time PCR

RT^2 SYBR Green Mastermix was used to amplify and quantify genes expression on a cycler (Bio-Rad iQ5 model), using a total amount of 2.0 µg of RNA from striatum animals, in every treatment conditions. Specific primers were designed using *Beacon* software for gene relative expression and the respective sequences are represented in **Table 1**.

Data were analyzed by ΔΔCT method after normalization to housekeeping gene expression of Glyceraldehyde 3-Phosphate Dehydrogenase (GAPDH) and Beta-Glucuronidase (GUSB).

Table 1 – Primers sequences obtained from *Beacon* software

Gene	Forward sequence (5'-3')	Reverse sequence (5'-3')
IGF1	GCTATGGCTCCAGCATTCG	GCTCCGGAAGCAACACTCA
IGF1R	GGACTGTTCAACGGTAGG	GCTTAGGACTTGGCATCATA
ILK	TGAATGAGCACGGCAATG	TTGTCCACAGGCATCTCT
MMP2	TACTCTGGAGCGAGGATA	GATGTATGTCTTCTTGTTCTTACT3
MMP9	GTCCAACTCACTCACTGT	TCTGACCTGAACCATAACG
RHOA	GCTTGCTCATAGTCTTCAG	CAGGCGGTCATAATCTTC
RAC1	GGACAAGAAGATTATGACAGAT	ACGAGGATGATAGGAGTATT
GAPDH	ACCTGCCAAGTATGATGA	GGAGTTGCTGTTGAAGTC
GUSB	GGTGAAGGTGACAACAACT	CTGAATCCTCGTGCTTATTGA

2.4 Software analysis and interactome construction

Based on the information provided by RT^2 Profiler PCR Array plates the Network Analysis tool of a trial version of IPA software was used in order to assess genes interaction. The interactome construction was done using databases scientific information about mouse brain only.

2.5 Statistical analysis

Results from RT-PCR were represented as mean±SEM. Statistical analysis was performed by one-way ANOVA followed by the *Sidak*'s post hoc test. When data normality was not verified, the Kruskal Wallis test was used. Significance was set at $p<0.05$. All analysis were conducted using the software GraphPad Prism® 6.0 (GraphPad Software, La Jolla CA).

3. Results and Discussion

3.1 PCR Array for *in vivo* gene expression after METH exposure

Among the 84 genes analyzed the relative expression of 24 of them is altered in METH-treated animals when compared to the control, as shown in **Table 2**.

Table 2. Gene expression after METH-exposed mice assessed through RT^2 Profiler PCR Array

Genbank	Symbol	Gene name	$2^{-\Delta Ct}$		Fold Regulation
			METH group	Saline group	METH/ Saline
NM_019655	**ADAR**	Adenosine deaminase, RNA-specific	1,7E-01	1,8E-01	-1,04
NM_009652	**AKT1**	Thymoma viral proto-oncogene 1	5,1E-01	4,2E-01	1,22
NM_007434	**AKT2**	Thymoma viral proto-oncogene 2	9,0E-01	4,9E-01	1,84
NM_011785	**AKT3**	Thymoma viral proto-oncogene 3	9,2E-02	5,0E-02	1,86
NM_007462	**APC**	Adenomatosis polyposis coli	4,8E-01	2,9E-01	1,62
NM_007522	**BAD**	BCL2-associated agonist of cell death	1,9E-01	1,6E-01	1,16
NM_013482	**BTK**	Bruton agammaglobulinemia tyrosine kinase	6,2E-03	5,1E-03	1,22
NM_015733	**CASP9**	Caspase 9	8,6E-02	9,5E-02	-1,10
NM_007631	**CCND1**	Cyclin D1	4,6E-02	2,0E-02	**2,29**
NM_009841	**CD14**	CD14 antigen	2,5E-02	1,4E-02	1,73
NM_009861	**CDC42**	Cell division cycle 42 homolog (S. cerevisiae)	5,0E-01	3,9E-01	1,26
NM_009875	**CDKN1B**	Cyclin-dependent kinase inhibitor 1B	2,1E-01	4,7E-02	**4,37**
NM_007700	**CHUCK**	Conserved helix-loop-helix ubiquitous kinase	3,6E-01	1,8E-01	**2,02**
NM_007788	**CSNK2α1**	Casein kinase 2, α 1 polypeptide	8,9E-01	9,7E-01	-1,09
NM_007614	**CTNNβ1**	Catenin (cadherin associated protein), β 1	6,1E-01	6,4E-01	-1,04
NM_011163	**EIF2αK2**	Eukaryotic translation initiation factor 2-α kinase 2	4,0E-02	3,7E-02	1,07
NM_145625	**EIF4B**	Eukaryotic translation initiation factor 4B	2,0E-01	2,8E-02	**7,00**
NM_007917	**EIF4E**	Eukaryotic translation initiation factor 4E	9,2E-01	8,0E-01	1,16
NM_007919	**EIF4EBP1**	Eukaryotic translation initiation factor 4E binding protein 1	6,4E-03	1,2E-02	-1,90
NM_001005331	**EIF4γ1**	Eukaryotic translation initiation factor 4, γ 1	6,2E-01	6,4E-01	-1,03
NM_007922	**ELK1**	ELK1, member of ETS oncogene family	4,9E-02	1,6E-02	**2,96**
NM_010177	**FAS1**	Fas ligand (TNF superfamily, member 6)	5,6E-03	4,8E-03	1,17
NM_008019	**FKBP1α**	FK506 binding protein 1[a]	4,3E+00	3,5E+00	1,23
NM_010234	**FOS**	FBJ osteosarcoma oncogene	1,9E-01	6,3E-02	**3,01**
NM_019739	**FOXO1**	Forkhead box O1	4,7E-01	7,0E-02	**6,69**
NM_019740	**FOXO3**	Forkhead box O3	3,7E-01	5,5E-01	-1,48
NM_020009	**MTOR**	FK506 binding protein12-rapamycin associated protein 1	1,6E-01	1,6E-01	-1,03
NM_010288	**GJA1**	Gap JUNction protein, α 1	5,0E-01	6,8E-01	-1,36
NM_010345	**GRB10**	Growth factor receptor bound protein 10	1,7E-01	6,2E-02	**2,83**
NM_008163	**GRB2**	Growth factor receptor bound protein 2	3,7E-01	1,7E-01	**2,18**
NM_019827	**GSK3β**	Glycogen synthase kinase 3 β	2,1E-01	2,6E-01	-1,24
NM_008284	**HRAS1**	Harvey rat sarcoma virus oncogene 1	2,1E+00	2,5E+00	-1,16
NM_013560	**HSPB1**	Heat shock protein 1	2,4E-01	2,6E-01	-1,11
NM_010512	**IGF1**	Insulin-like growth factor	9,8E-03	3,3E-02	**-3,32**
NM_010513	**IGF1R**	Insulin-like growth factor I receptor	4,3E-02	4,2E-02	1,02
NM_010562	**ILK**	Integrin linked kinase	4,3E-01	1,8E-01	**2,36**
NM_008363	**IRAK1**	Interleukin-1 receptor-associated kinase 1	5,3E-02	2,4E-02	**2,23**
NM_010570	**IRS1**	Insulin receptor subtrate 1	6,3E-02	9,7E-02	-1,54
NM_010578	**ITGB1**	Integrin β 1 (fibronection receptor β)	3,3E-01	5,1E-01	-1,55
NM_010591	**JUN**	JUN Oncogene	1,8E-02	1,6E-01	**-8,85**
NM_008927	**MAP2K1**	Mitogen-activated protein kinase kinase 1	1,9E+00	1,9E+00	-1,02

Genbank	Symbol	Gene name	$2^{-\Delta Ct}$		Fold Regulation
			METH group	Saline group	METH/ Saline
NM_011949	**MAPK1**	Mitogen-activated protein kinase 1	4,5E+00	3,0E+00	1,50
NM_011951	**MAPK14**	Mitogen-activated protein kinase 14	2,7E-01	1,9E-01	1,47
NM_011952	**MAPK3**	Mitogen-activated protein kinase 3	4,1E-01	2,1E-01	1,96
NM_016700	**MAPK8**	Mitogen-activated protein kinase 8	1,1E-01	3,0E-02	**3,73**
NM_010839	**MTCP1**	Mature T-cell proliferation 1	4,2E-02	2,0E-02	**2,08**
NM_010851	**MYD88**	Myeloid differentiation primary response gene 88	5,6E-03	4,8E-03	1,16
NM_008689	**NFkB1**	Nuclear factor of kappa light polypeptide gene enhancer in B-cells 1, p105	7,6E-02	3,4E-02	**2,20**
NM_010907	**NFkBiα**	Nuclear factor of kappa light polypeptide gene enhancer in B-cells inhibitor, α	1,2E-01	1,9E-01	-1,56
NM_008774	**PABPC1**	Poly(A) binding protein, cytoplasmic 1	2,1E-01	2,9E-02	**7,42**
NM_011035	**PAK1**	P21 (CDKN1A) -activated kinase 1	4,1E-01	7,9E-01	-1,91
NM_011058	**PDGFRα**	Platelet derived growth factor receptor, α polypeptide	1,4E-01	9,3E-02	1,55
NM_172665	**PDK1**	Pyruvate dehydrogenase kinase, isoenzyme 1	1,3E-01	2,8E-01	**-2,15**
NM_133667	**PDK2**	Pyruvate dehydrogenase kinase, isoenzyme 2	1,2E-02	4,8E-03	**2,42**
NM_011062	**PDPK1**	3-phosphoinositide dependent protein kinase-1	4,5E-01	4,4E-01	1,03
NM_008839	**PIK3Cα**	Phosphatidylinositol 3-kinase, catalytic, α polypeptide	2,3E-01	1,4E-01	1,62
NM_020272	**PIK3Cɣ**	Phosphatidylinositol 3-kinase, catalytic, ɣ polypeptide	1,2E-02	5,0E-03	**2,32**
NM_001024955	**PIK3R1**	Pi3k, regulatory subunit, polypeptide 2 (p85 α)	3,3E-01	3,5E-01	-1,04
NM_008841	**PIK3R2**	Pi3k, regulatory subunit, polypeptide 2 (p85 β)	1,0E-01	8,1E-02	1,28
NM_011101	**PRKCα**	Protein kinase C, α	2,5E-01	3,2E-01	-1,24
NM_008855	**PRKCβ**	Protein kinase C, β	3,9E+00	3,7E+00	1,08
NM_008860	**PRKCζ**	Protein kinase C, ζ	1,2E+00	1,7E+00	-1,48
NM_008960	**PTEN**	Phosphatase and tensin homolog	1,2E+00	8,2E-01	1,41
NM_007982	**PTK2**	PTK2 protein tyrosine kinase 2	2,0E-01	2,0E-01	-1,00
NM_011202	**PTPN11**	Protein tyrosine phosphatase, non-receptor type 11	8,2E-01	7,3E-01	1,13
NM_009007	**RAC1**	RAS-related C3 botulinum substrate 1	2,9E+00	1,5E+00	1,96
NM_029780	**RAF1**	V-raf-leukemia viral oncogene 1	2,4E-01	3,2E-01	-1,31
NM_145452	**RASA1**	RAS p21 protein activator 1	3,4E-01	1,7E-01	1,94
NM_011250	**RBL2**	Retinoblastoma-like 2	1,2E-01	3,0E-02	**3,89**
NM_053075	**RHEB**	RAS-homolog enriched in brain	5,9E-01	3,4E-01	1,73
NM_016802	**RHOA**	Ras homolog gene family, member A	5,0E-01	3,5E-01	1,44
NM_009097	**RPS6KA1**	Ribosomal protein S6 kinase polypeptide 1	3,6E-02	1,5E-02	**2,39**
NM_028259	**RPS6kB1**	Ribosomal protein S6 kinase polypeptide 1	5,4E-02	4,0E-02	1,35
NM_011368	**SHC1**	Src homology2 domain-containing transform.protein C1	3,4E-02	4,0E-02	-1,17
NM_009231	**SOS1**	Son of sevenless homolog 1 (Drosophila)	6,6E-02	1,1E-02	**6,02**
NM_020493	**SRF**	Serum response factor	1,3E-01	8,7E-02	1,45
NM_009337	**TCL1**	T-cell lymphoma breakpoint 1	5,6E-03	4,8E-03	1,17
NM_054096	**TIRAP**	Toll-interleukin 1 receptor (TIR) domain-containing adaptor protein	7,6E-03	6,2E-03	1,23
NM_021297	**TLR4**	Toll-like receptor 4	5,6E-03	1,0E-02	-1,82
NM_023764	**TOLLIP**	Toll interacting protein	5,8E-01	3,4E-01	1,71
NM_022887	**TSC1**	Tuberous sclerosis 1	5,3E-02	2,1E-02	**2,53**
NM_011647	**TSC2**	Tuberous sclerosis 2	2,9E-01	2,0E-01	1,47
NM_028459	**WASL**	Wiskott-Aldrich syndrome-like (human)	4,0E-02	5,1E-02	-1,27
NM_011738	**YWHAH**	Tyrosine 3-monooxygenase/tryptophan 5-monooxygenase activation protein, eta polypeptide	1,8E+00	2,4E+00	-1,32
NM_010368	**GUSB**	Glucuronidase, β	1,2E-01	1,0E-01	1,23
NM_013556	**HPRT1**	Hypoxanthine guanine phosphoribosyl transferase 1	2,0E+00	2,8E+00	-1,42
NM_008302	**HSP90αA1**	Heat shock protein 90 α , class B member 1	5,3E-02	5,9E-02	-1,11
NM_008084	**GAPDH**	Glyceraldehyde-3-phosphate dehydrogenase	7,9E+00	6,8E+00	1,15
NM_007393	**ACT b**	Actin, β	9,9E+00	8,8E+00	1,12

We have started by grouping genes with altered expression (shown in **Table.3**) into three main classes according to their function. A group of 12 of those genes exert their function regulating cell cycle, transcription and translation processes; 6 genes are implicated on signaling processes, mainly those regulating extracellular signals, adapter proteins and surface receptors; and 6 genes play an essential role on metabolism. However, some of these genes could play different roles in independent pathways, making their categorization into different groups more complex. A volcano plot of altered genes is represented in **Fig.1**.

Table 3. Gene grouping after expression analysis

Gene		METH/Control Ratio	Function
CCND1	Cyclin D1	2,24	**Cell cycle**
CDKN1B	Cyclin-Dependent Kinase Inhibitor 1B	4,26	
RBL2	Retinoblastoma-Like 2	3,79	
ELK1	Member Of ETS Oncogene Family	2,89	**Transcription**
FOS	FBJ Murine Osteosarcoma Viral Oncogene Homolog	2,93	
FOXO1	Forkhead Box O1	6,52	
JUN	Jun Proto-Oncogen (AP-1)	-9,08	
NFkB1	Nuclear Factor Of Kappa Light Polypeptide Gene Enhancer In B-Cells 1	2,16	
CHUCK	Conserved helix-loop-helix ubiquitous kinase	2,02	
EIF4B	Eukaryotic Translation Initiation Factor 4B	6,83	**Translation**
PABPC1	Poly(A) binding protein, cytoplasmic 1	7,23	
RPS6KA1	Ribosomal Protein S6 Kinase, 90kDa, Polypeptide 1	2,33	
ILK	Integrin-Linked Kinase	2,3	**Signaling**
IRAK1	Interleukin-1 Receptor-Associated Kinase 1	2,17	
MTCP1	Mature T-Cell Proliferation 1	2,02	
PIK3Cγ	Phosphatidylinositol-4,5-Bisphosphate 3-Kinase, Catalytic Subunit Gamma	2,26	
MAPK8	Mitogen-Activated Protein Kinase 8 (JNK)	3,64	
TSC1	Tuberous Sclerosis 1	2,47	
IGF1	Insulin-Like Growth Factor 1	-3,41	**Metabolism**
GRB2	Growth Factor Receptor-Bound Protein 2	2,13	
GRB10	Growth Factor Receptor-Bound Protein 10	2,76	
PDK1	Pyruvate Dehydrogenase Kinase, Isozyme 1	-2,31	
PDK2	Pyruvate Dehydrogenase Kinase, Isozyme 2	2,36	
SOS1	Son Of Sevenless Homolog 1 (Drosophila)	5,87	

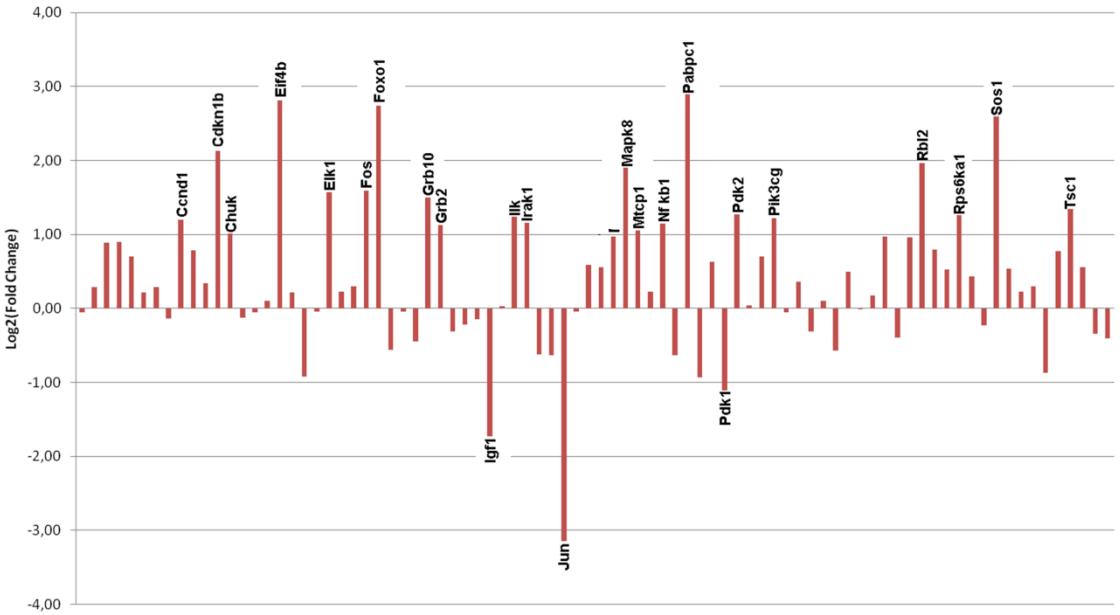

Fig. 1 Volcano plot representation of gene expression fold change of the 84 members of PI3K-AKT signaling pathway, in mice treated with METH. Genes with altered expression are identified.

3.1.1 Cell cycle regulators

Among cell cycle regulators, cyclin D1 (CCND1), cyclin dependent kinase inhibitor 1B (CDKN1B) and retinoblastoma 2 (RBL2) showed important fold changes. CCND1 is a gene that encodes for the regulatory subunit of a holoenzyme responsible for the phosphorylation and inactivation of retinoblastoma protein (pRb), thus promoting progression through the G1-S phase of the cell cycle. CCND1 role on tumorigenesis has been largely explored since it regulates proliferation and differentiation (Barré and Perkins 2007; Stein, Milewski et al. 2013). Both CDKN1B and RBL2, which are important key players on cell cycle progression/arrest, showed an upregulation on METH-treated animals in our study (ckkn1b – 4.37 and RBL2 – 3.89). CDKN1B is a classical negative cell cycle regulator that controls the G1/S-phase transition by binding to and regulating the activity of cyclin-dependent kinases (Stein, Milewski et al. 2013). Interestingly, some studies have explored the importance of CDKN1B in metabolism regulation. Experiments using an animal model of insulin resistance (type 2 diabetes) showed that the deletion of the gene encoding CDKN1B results in ameliorating of hyperglycemia through the stimulation of pancreatic β-cell proliferation (Uchida, Nakamura et al. 2005). In our experiment, we found an upregulation of CDKN1B and a downregulation of insulin-like growth factor (IGF1) after METH-exposure.

There are few studies assessing METH impact on cell cycle (Cadet, Jayanthi et al. 2013; Baptista, Lasgi et al. 2014; Jackson, Shah et al. 2014). In the context of drug abuse, METH has been reported to decrease self-renewal capacity, delaying cell cycle progression in neuronal stem cells. In this study of *Baptista et al,* METH induced a delay in the transition from

Go/G1 to the S phase along with a decrease in cyclin E protein expression, but without any alteration in both cyclin D1 and cyclin A protein levels (Baptista, Lasgi et al. 2014). However, genes of CDK and cyclin family, were already reported to be upregulated after METH exposure (Jackson, Shah et al. 2014).

More recent discoveries point CCND1 as an important regulator of metabolism, cellular adhesion and motility (Fu, Wang et al. 2004). Several studies are consistent with a model in which CCND1 acts as a key sensor and integrator of extracellular environment signals to the core cell cycle machinery (Barré and Perkins 2007), and its activation could be induced by growth factors including epithelial growth factor (Egf) and IGF1 and IGF2 (Holnthoner, Pillinger et al. 2002; Fu, Wang et al. 2004).

As well, other effectors like integrin-linked kinase (ILK) are responsible for the increased levels of transcription and translation of CCND1 via PI3K/AKT pathway. Otherwise, some evidences show that CCND1 has an important role on adhesion, in part mediated by F-actin fibers. The fact that CCND1 regulates cellular adhesion dynamics suggest that this protein regulates cellular substratum interactions and therefore contributes to the invasiveness and/or metastatic phenotype, independently of its effects on cell cycle progression (Fu, Wang et al. 2004).

3.1.2 Transcription and translation regulators

Another altered gene was IKKα, also known as CHUCK (conserved helix-loop-helix ubiquitous kinase). This gene encodes for a protein that belongs to an enzyme complex (IKK) that acts upstream of NFκB (the nuclear factor kappa-light-chain-enhancer of activated B cells) signal transduction cascade. Through phosphorilation processes, IKK dissociates NFκB which migrates to the nucleus and activates the expression of several genes. In the present work, we found an upregulation of NFκB1 (a precursor of NFκB). Although NFκB-independent mechanisms also exist, many authors have described a role for NFκB subunits and IKK in the control of CCND1 expression. This association is evidenced in our study since all these genes were upregulated 24h after the administration of METH (CCND1 – 2.29; CHUCK – 2.02; NFκB1 – 2.20). There are multiple NFκB pathways under the regulation of a large array of stimuli in many cell contexts, resulting in functional differences, such as activation or repression of specific target genes by the same NFκB. In the brain, a role on memory, plasticity and learning has been described (Salles, Romano et al. 2014). In the context of drug-exposure, there is evidence that METH can activate and induce nuclear translocation of NFκB, allowing transcription in microglial cells (Wires, Alvarez et al. 2012).

Besides NFκB, other different genes regulating transcription and translation processes were found in METH-treated animals with a fold change of 2 to 7 times greater than the saline group. ELK1 (member of ETS oncogene family) is a transcription activator that has an important function in events such as long-term memory formation, drug addiction and depression. Some studies showed that activation of ELK1 occurred after exposure to drugs of abuse, initiating a

gene transcription program that is supposed to lead to the long-term effects of repeated exposure to psychostimulants. Moreover, FOS is an immediate early gene, which expression occurs immediately after the stimulus. It can cause both gene repression and gene activation and is involved in important cellular events like proliferation, survival, differentiation but also apoptotic cell death (Burch, Yuan et al. 2004). Our model of METH exposure showed an increase in striatal ELK1 and FOS mRNA levels 24h after administration (ELK1 – 2.96; FOS – 3.01), which is in agreement with the literature reported after drugs of abuse exposure (Betts, Krasnova et al. 2002; Salzmann, Marie-Claire et al. 2003; Mizoguchi, Yamada et al. 2004; Cadet, Jayanthi et al. 2013). It was reported that Elk-1 and CREB transcription factors, both critically involved in immediate-early genes mRNA induction, such as c-FOS, may be phosphorylated by ERK after exposure to psychostimulants, being responsible for persistent drug-induced plasticity (Salzmann, Marie-Claire et al. 2003; Mizoguchi, Yamada et al. 2004).

c-JUN is encoded by the JUN gene and binds to FOS to form dimeric complexes (AP-1) with high affinity for DNA-binding sites. Both c-JUN and its dimeric partners are subject to regulation by diverse extracellular stimuli including pro-inflammatory cytokines, growth factors, oxidative stress and UV radiation, among others (Wisdom, Johnson et al. 1999; Burch, Yuan et al. 2004). Although the response to the stimulus could be initially different, evidence shows that they all regulate c-JUN through the activation of MAPK (Mitogen-Activated Protein Kinase) members, as is the case of MAPK8. Functional data suggest that c-JUN is not merely a target of activation by extracellular stimuli. Instead, it plays a role in mediating the cellular response. Two important biological processes implicate JUN activity: the regulation of cell cycle progression and the anti-apoptotic response. The regulation of c-JUN is complex and distinct biochemical mechanisms underlie its different cellular functions. Concerning cell cycle regulation, c-JUN has the ability to mediate G1 progression by a direct control of CCND1. Cooperating with NFκB, c-JUN protects cells from UV irradiation but it requires proper phosphorilation of specific serines (Wisdom, Johnson et al. 1999). Although the striatal JUN mRNA levels were found unaltered after chronic METH administration (Cadet, McCoy et al. 2009; Saint-Preux, Bores et al. 2013), our acute exposure significantly decreased JUN gene expression (-8.85), while increasing MAPK8 expression (3.73). The biological significance of change remains unknown, essentially because JUN effects seem to be context-dependent and MAPK8 could be activated through different stimulus. *Wisdom et al* proposed that c-JUN could induce the expression of genes that block apoptosis (Wisdom, Johnson et al. 1999), therefore, c-Jun downregulation may be associated with METH-induced apoptotic events. In accordance, *Chetswang et al* observed an increased phosphorilation of c-JUN, hypothesizing that this process is responsible for the Bax and Bcl2 expession, leading to apoptotic death (Chetsawang, Suwanjang et al. 2012). However, different reports show opposite roles for JUN which could mean that the cell-context may determine the outcome of that gene change.

Forkhead Box Protein O1 (Foxo1) is a protein encoded by the gene FOXO1. Foxo1 is a transcription factor involved in the regulation of gluconeogenesis and glycogenolysis by insulin signaling playing also a central role on adipogenesis process. Foxo1 transcriptional activity is

dependent on its phosphorylation state, since this protein is regulated through phosphorylation (Sasaki and Kitamura 2009). In fact, evidence on hepatocarcinomas shows that an overexpression of IGF-1 decreases the phosphorylation levels of proteins like Foxo1, Akt and p70S6K (Hernandez-Breijo, Monserrat et al. 2013). However, the effect of FOXO1 upregulation (6.69) and a downregulation of IGF-1 (-3.32) at the brain level remains unveiled.

Concerning translation regulators, in our experiment both PABPC1 (polyadenylate binding protein 1) and EIF4B (Eukaryotic Translation Initiation Factor 4B) showed gene expression upregulation 24h after METH administration. Both PABPC1 and EIF4B are genes that encode for proteins that regulate and initiate the translation processes. PABPC1 is required for poly(A) shortening and translation initiation and interacts with Eif4 family members that regulate mRNA strand binding to ribosomes (Khan and Goss 2012). The upregulation of these two genes (PABPC1 – 7.42; EIF4B – 7.00) could simply mean that cell machinery is active after the drug stimulus, responding with genetic expression and protein synthesis.

3.1.3 Metabolism players

Growth factors such as EGF, IGF and platelet-derived growth factor (PDGF) and hormone insulin, play a role on mTOR Complex1 regulation through PI3K signaling pathway. The interaction of insulin with the tyrosine kinase receptor leads to the phosphorylation of the receptor, creating on the cell membrane sites for the recruitment of IRS1 (Insulin Receptor Substrate 1) and IRS2 (Insulin Receptor Substrate 2). In turn, specific phosphorylated residues in IRS1 and/or IRS2 function as recognition motifs for the binding of key signaling molecules, such as class I PI3K. This interaction will result in the production of PtdIns (3,4,5)P3 second messengers that bind molecules including PKB/Akt and phosphoinositide-dependent kinase 1 (PDK1). If PtdIns (3,4,5)P3 binds to PDK1, S6k1 is recruited and phosphorylated both by PDK1 and mTOR Complex2. In turn, activated PKB/Akt has several downstream substrates including glycogen synthase kinase-3 (GSK3), FOXO transcription factors and TSC2 of the TSC1–TSC2 complex, which acts as a tumor suppressor complex. TSC2 activation results in its dissociation and degradation of the complex, which releases the small GTPase RAS homologue enriched in brain (RHEB) from the inhibitory state into the GTP-bound active state. It is believed that active RHEB enables mTOR Complex1 signaling to downstream substrates, such as S6K1. When that pathway is activated by growth factors, PKB/Akt can mediate the phosphorylation of several specific substrates, not only those described above, but also caspase 9 and the BCL-2-antagonist of cell death (BAD), culminating in a prosurvival response. Moreover, PTEN (Phosphatase and Tensin Homolog) is a negative regulator of this step and converts PtdIns(3,4,5)P3 into PtdIns(4,5)P2, resulting in a reduced recruitment of PKB/Akt to the cell membrane (Dann, Selvaraj et al. 2007).

In the present study, caspase 9 was seen overexpressed nor PTEN, S6K1 or IRS1 gene expression was altered. Moreover, and in accordance with the observed decreased fold change of PDK1 (-2.15) and more important, IGF-1 downregulation (-8.85), it could mean that insulin pathway is compromised under METH exposure. However, using positron emission

tomography (PET) we evaluated in vivo changes in regional glucose uptake (GU) in the brains of C57BL/6J mice exposed to a single dose of METH (10 mg/kg). Our analysis focused on regions receiving relevant dopaminergic input typically affected by METH, such as the prefrontal cortex (PFC), the striatum and the hippocampus. Interestingly, the dose of METH used led to motor activation, but did not affect GU in any of the evaluated regions (manuscript under preparation).

IGF and EGF receptors are known to phosphorylate a variety of intracellular effector proteins, such as Shc, which generates a recognition site for the SH2 domain of GRB2. GRB2 is an adapter protein with 23 kDa where its SH3 domain mediates the basal state association with SOS, a 170 kDa guanylnucleotide exchange factor for the p21 GTP binding protein Ras. The IGF/EGF-mediated assembly of Shc-GRB2-SOS ternary complex is generally thought to be the major pathway leading to Ras activation. Recent studies have demonstrated that insulin treatment results in a feedback serine/threonine phosphorylation of SOS, which directly correlates with the dissociation of the GRB2-SOS complex. Furthermore, inhibition of this feedback phosphorylation of SOS preserves the interaction between GRB2 and SOS and prolongs the GTP-bound state of Ras. However, other studies provide evidence that alternative pathways to GRB2 may also contribute to SOS-mediated Ras activation (Okada and Pessin 1996). In our study, IGF-1 is strongly downregulated, and both gene levels of GRB2 and SOS-1 are upregulated. However, the lack of differences in the gene expression of SHC or RASA1 (Ras protein activator), do not allow to conclude that RAS could be activated with METH treatment. Moreover, the fact that a variety of cell processes occur through phosphorylation and other by posttranslational modifications make any conclusion based on mRNA levels somewhat fragile.

GRB10 (also known as insulin receptor-binding protein GRB-IB) encodes a growth factor receptor-binding protein that interacts with insulin and insulin-like growth-factor receptors. Overexpression of some isoforms of the encoded protein inhibits insulin/IGF-1 signaling and results in growth suppression. Post-translationally, RPS6Kα1 (Ribosomal Protein S6 Kinase, Polypeptide 1 alpha) also known as S6k, is involved in GRB10 phosphorylation that interacts with the cytoplasmic domain of the autophosphorylated insulin receptor which is then inhibited. In fact, both GRB10 and IRS-1 work by suppressing insulin or IGF-1 signaling upstream of phosphatidylinositol-3-OH kinase PI(3)K, blocking mTOR pathway (Liu, Gan et al. 2013).

Our results showed that S6K (2.39), SOS-1 (6.02), GRB2 (2.83) and GRB10 (2.18) genes are both upregulated on METH-treated animals, which in combination with the IGF-1 (-8.85) downregulation could mean that METH inhibits the insulin-signaling pathway. In line with this hypothesis, RT-PCR for IGF-1 and the respective IGF1 receptor gene expression was performed on striatal samples of METH and ALC/METH treated animals in order to better address it (**see section 1.4**).

3.1.4 Signaling players

Among PI3K-AKT signaling pathway members, several regulators or intermediates of cellular signaling were found with altered gene expression after METH exposure. Most of them could be activated by different stimulus or sub-pathways, which rends the identification of a main target quite hard.

RPS6ka1 is a protein encoded by RPS6Kα1 gene that showed an increased fold change (2.39) expression on METH-treated animals when compared to controls. RPS6ka belongs to a family that has been implicated as signaling intermediates in the cellular response to several growth factors, and due to its kinase catalytic domains it phosphorylates various substrates, including MAPK signaling pathway members (Moller, Xia et al. 1994). The activity of RPS6ka has been generally implicated in controlling cell growth and differentiation. Otherwise, some studies show that RPS6kA interacts with TSC2 (Tuberous Sclerosis 2), a protein encoded by TSC2 gene. TSC2 gene seems not to be altered 24h after the exposure to METH, although its partner TSC1 (also known as hamartin) does. TSC1 protein is known to interact with TSC2 and the complex formed regulates and inhibits the growth factor-stimulated phosphorylation of RPS6Kβ1 (Ribosomal Protein S6 Kinase, Polypeptide 1 beta) and Eif4ebp1 by negatively regulating mTOR Complex 1 signaling (Dann, Selvaraj et al. 2007). Other roles have been identified for TSC1, namely the regulation of the vesicular transport and docking and the involvement on events of ischemia resistance on hippocampal neurons (Papadakis, Hadley et al. 2013). The effective role of TSC1 upregulation is unknown but it may work as a protective mechanism against an injury stimulus like METH.

IRAK1 is a gene that encodes the interleukin-1 receptor-associated kinase 1, one of two putative serine/threonine kinases that become associated with the interleukin-1 receptor (IL1R) upon stimulation. This gene is partially responsible for IL-1-induced upregulation of the transcription factor NFκB. In fact, METH-induced IL-1 mRNA expression is not consensual (Goncalves, Martins et al. 2008) and although NFκB is upregulated in our study (2.20), this could not be sufficient to explain the increased expression of IRAK1 gene (2,23) observed after METH exposure. Importantly, nor toll-interleukin 1 receptor domain-containing adaptor protein (TIRAP), nor toll-like receptor (TLR4) mRNA levels assessed in this array are altered, difficulting the identification of upstream targets for METH action. Recently, new insights on IL-1-induced neuroinflammation of the BBB reveal that integrin β1 is the major adhesion receptor for endothelial cell attachment to extracellular matrix molecules. Moreover, it was found that integrin β1 critically regulates IL-1 β-induced ERK1/2 and NFκB activation, and that integrin activation occurred concomitantly with increased IRAK-1 activation (an hallmark of IL-1 signalling) (Summers, Kangwantas et al. 2013).

MTCP1 (mature T-cell proliferation 1) gene was identified by its involvement in some genetic translocations associated with mature T-cell proliferations, encoding for TCL1 protein, which may be involved in leukemogenesis. The prevailing view of the role of TCL1/MTCP1 proteins in tumorigenesis is related to their involvement in the AKT signal transduction pathway. However, the mechanism by which TCL1 increases Akt activity is not completely known and

remains controversial. Other roles for TCL1 were investigated using animal models, and allowed to verify its role in T- and B-cell growth and survival, including resistance to receptor-induced apoptosis (Despouy, Joiner et al. 2007). This process of cell death through apoptosis is known to occur concomitantly with G1 phase cell-cycle arrest, possibly explaining its involvement with CDKN1B (Le Toriellec, Despouy et al. 2008). The central role of PKC in T-cell physiology is supported by T-cell impairment in PKC-deficient mice associated with impaired activation of its downstream pathways, such as NF-B, ERK and AP-1 (Despouy, Joiner et al. 2007). Nothing is reported about METH effects over MTCP1 expression and data provided by the present study do not allow to take any conclusion.

Recent studies have revealed that cytoplasmic integrin-linked kinase (ILK) and its interactive proteins play important roles in several processes, including cell adhesion, cell shape change, migration, proliferation, survival, and differentiation (Wu and Dedhar 2001). ILK is directly bonded to the cytoplasmic domains of β1 integrin and connects integrins to the actin cytoskeleton by interacting directly with several proteins such as paxillin and parvin, thus, coordinating actin organization (Wu and Dedhar 2001; Rosano, Spinella et al. 2006). ILK overexpression and clustering results in the activation of a variety of intracellular signaling processes such as Akt phosphorilation and GSk3 inhibition, which lead to the activation of the transcription factor AP-1 resulting in the MMP-9 potentiation (Troussard, Costello et al. 2000; Wu and Dedhar 2001). In the present study, GSK3β mRNA levels were evaluated after METH exposure and no significant differences were observed when compared to control group (-1.24). In this context, some studies of METH exposure reveal that GSk3β inhibition leads to a gradual and sustained increase in TJs stability and attenuates BBB dysfunction in brain endothelial cells. In these particular studies, authors observed that GSk3β inhibition increases significantly the half-life of TJs, increasing consistently the amount of occludin and claudin-5 in cell membrane fractions (Rom, Fan et al. 2012; Ramirez, Fan et al. 2013). Moreover, it is well recognized that GSk3 activity is reduced by growth factors, enhancing β-catenin translocation into the nucleus (Holnthoner, Pillinger et al. 2002).

Activation of AP-1 through the phosphorylation of GSk3β seems to be responsible for the ILK-induced expression of MMP-9. Moreover, results from endothelial cells showed that dephosphorylated GSk3β at specific residues suppressed MMP-9 protein, leading to the suppression of cell migration and invasion (Matsui, Assi et al. 2012). The evident upregulation of ILK on METH-treated mice (2.36) needs further study.

Based on the information provided by this array and in combination with the IPA software, Network Analysis tool, an analysis of genes interaction was performed (**Fig.2**). This interactome construction was based in IGF1 and their respective connections, using mouse brain information.

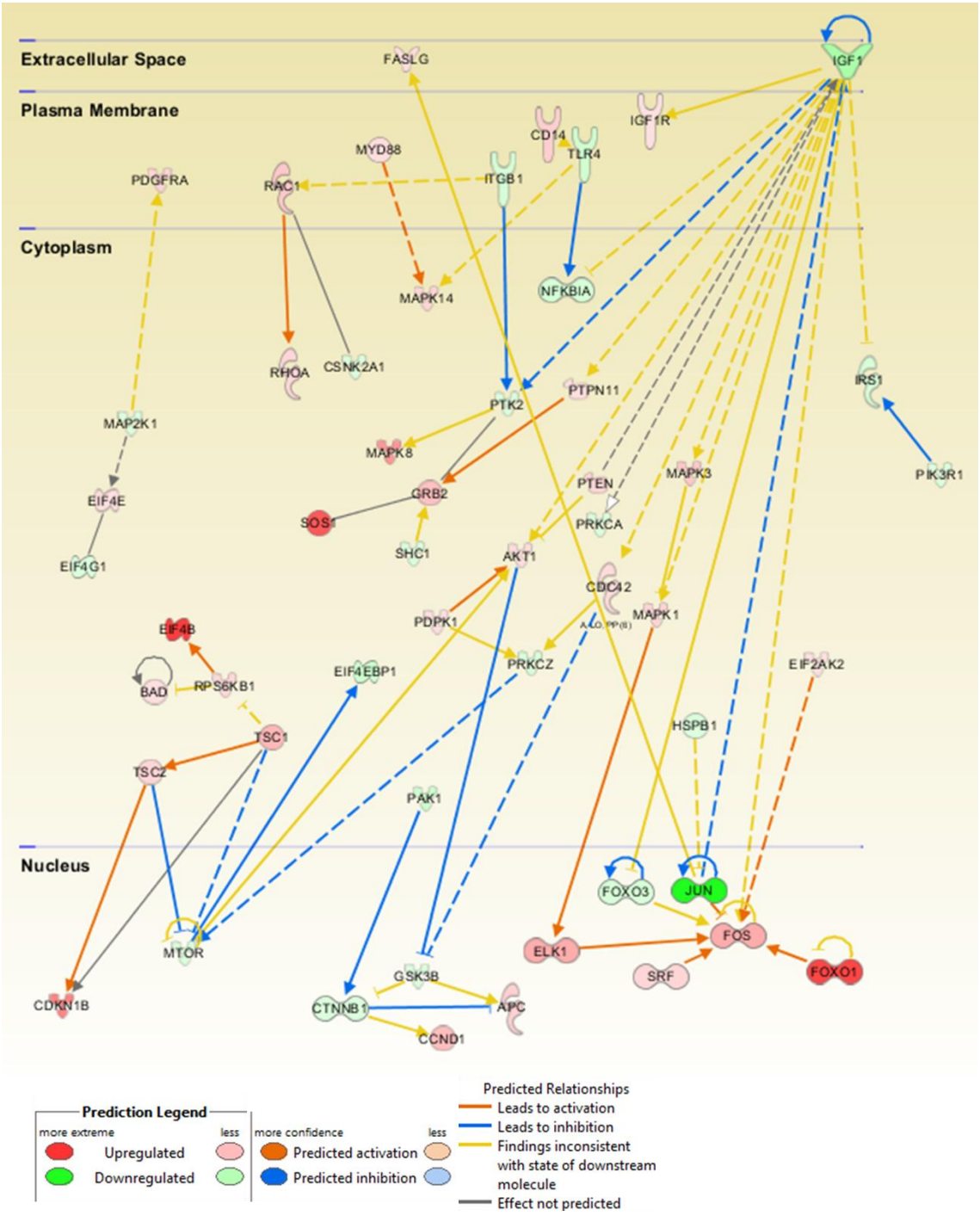

Fig. 2 Interactome representation using IPA Software based on mouse brain information taking in account IGF1 and their respective protein interactions.

3.2 Effects of ALC at gene expression of METH-treated animals

In order to address the protective role of ALC, an individual analysis of relevant gene expression was conducted. Based on the results obtained for METH exposures, a few candidates were selected and validated.

Due to the downregulation of mice IGF1 (-8.85) after METH exposure, we aimed to unveil the putative protective effect of ALC given before and after the drug insult. **Fig.3a** shows that METH significantly decreases IGF1 levels ($p<0.05$). The pretreatment with ALC 200mg/kg, 30 minutes before METH was able to counteract the decreased levels of mRNA ($p<0.05$, METH vs ALC/METH). However, no significant differences were observed when ALC is administered after METH. Moreover, ALC alone is not different from the saline control. Concerning IGF1R, there was also a significant downregulation 24h after METH exposure ($p<0.01$), which was prevented and reverted when ALC was administered ($p<0.001$, METH vs ALC/METH and $p<0.001$, METH vs. METH/ALC) (**Fig.3b**).

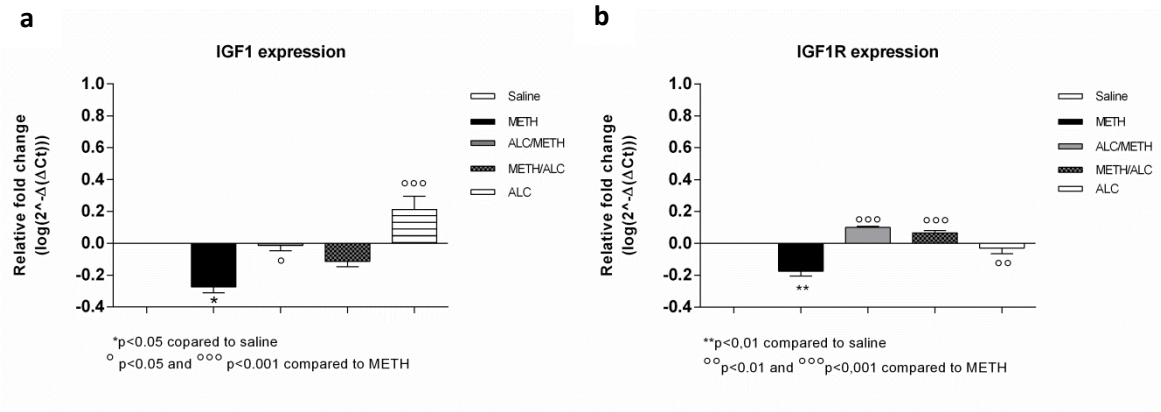

Fig. 3 Representation of mRNA levels assessed through RT PCR for both IGF1 (**a**) and IGF1R (**b**). Data of n=3 were analyzed by ΔΔCT method after normalization to housekeeping gene expression of GAPDH and GUSB.

Regarding RhoGTPases, the literature has evidenced an effect of METH over RhoA and Rac1. In both the PCR array (**Table 2**) and the RT-PCR (**Fig.4**) we observed that METH is not able to alter significantly the levels of either RHOA or RAC1 mRNA levels. Therefore, the METH effect must occur at the level of protein activation rather than at gene expression level, since RhoGTPases are known to be activated posttranslationally.

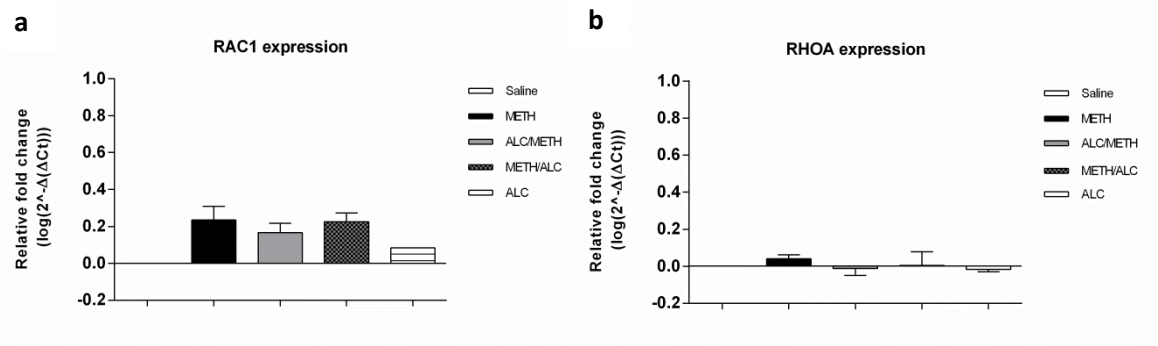

Fig. 4 Representation of mRNA levels assessed through RT PCR for both RAC1 (**a**) and RHOA (**b**). Data of n=3 were analyzed by ΔΔCT method after normalization to housekeeping gene expression of GAPDH and GUSB.

Although ILK was strongly upregulated in the PCR array, RT-PCR results do not allow to confirm this change (**Fig.5a**). However, based on evidence from the literature concerning METH effect on MMPs activity, we assessed MMP9 and MMP2 in the striatum of mice treated with METH and ALC. Our data showed that MMP2 mRNA levels were not altered after METH and/or ALC administration (**Fig.5b**). However, as expected, MMP9 mRNA levels were strongly increased in the mice brain after METH exposure ($p<0.05$). Moreover, we observed that ALC 200mg/kg when given 30 minutes before METH was able to counteract this increase ($p<0.01$) which was not verified when METH is given after METH administration. Of note, ALC *per se* significantly increased MMP9 levels when compared to control (**Fig.5c**). The increased mRNA levels of gelatinases do not necessarily correlate with enzymatic activity augmentation, so further studies are needed to address this question.

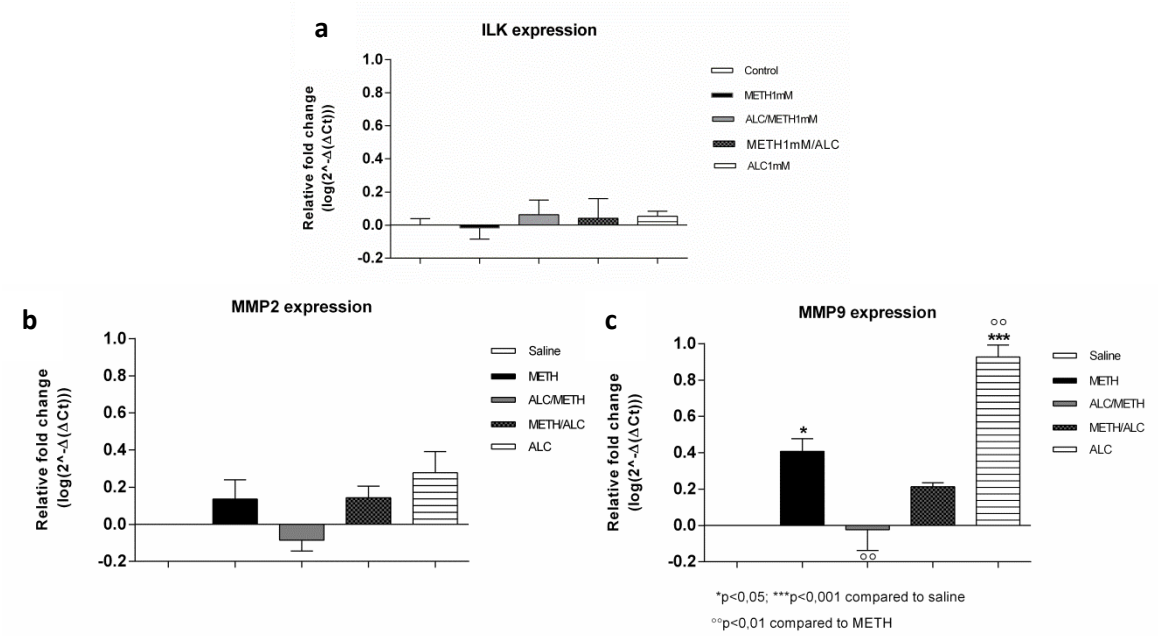

Fig. 5 Representation of mRNA levels assessed through RT PCR for both ILK (**a**), MMP2 (**b**) and MMP9 (**c**). Data of n=3 were analyzed by ΔΔCT method after normalization to housekeeping gene expression of GAPDH and GUSB.

4. Conclusion

Our study was focused on the PI3K-AKT signaling pathway since previous evidence strongly suggested the involvement of METH in cytoskeleton-mediated permeability. The present analysis allowed to verify that METH alters the expression of relevant proteins that could be involved in the signaling pathways that are triggered by METH exposure. Our individual analysis of particular genes of interest contributed to point out which aspects of METH-triggered effects may be prevented by ALC administration. The present results pave the way to define which pathways are interesting enough to deserve further attention. We have identified 3 main targets that are now being addressed in our laboratory: ILK signaling that is addressed in the following chapters; IGF signaling that is being explored in the context of glucose uptake under METH exposure; and RhoGTPases signaling that is being explored for its role in synaptic and dendritic modulation in hippocampal neurons. The data obtained for IGF and for RhoA and Rac1 is out of the scope of the present dissertation and is therefore discussed elsewhere.

Regarding the role of ILK pathway, we are particularly interested in exploring the modulation of MMPs, since there are several reports showing that METH exposure triggers MMP-2/9 release, which seems to play an important role in METH-induced disruption of the BBB function. Of note, nothing is known about METH effect in ILK expression. Based on the present data we reason that METH may increase the catalytic activity of MMPs (as has been described by other authors (Conant, Lonskaya et al. 2011; Martins, Baptista et al. 2011; Urrutia, Rubio-Araiz et al. 2013), and ALC may be effective in preventing these events. As ILK overexpression and clustering has been associated with an increased phenotype of invasiveness in some carcinomas (Wu and Dedhar 2001), whereas ILK silencing inhibits invasion (Troussard, Costello et al. 2000; Rosano, Spinella et al. 2006), we foresee that if ALC successfully prevents a METH-induced MMP activation, then it may also be of use in tumorogenic paradigms. This will be explored in **Chapter 2**.

5. References

Baptista, S., C. Lasgi, et al. (2014). "Methamphetamine decreases dentate gyrus stem cell self-renewal and shifts the differentiation towards neuronal fate." Stem Cell Res 13(2): 329-341.

Barré, B. and N. D. Perkins (2007). "A cell cycle regulatory network controlling NF-kB subunit activity and function." The EMBO Journal 24: 4841-4855.

Betts, E. S., I. N. Krasnova, et al. (2002). "Analysis of methamphetamine-induced changes in the expression of integrin family members in the cortex of wild-type and c-fos knockout mice." Neurotoxicity research 4(7-8): 617-623.

Bruewer, M., A. M. Hopkins, et al. (2004). "RhoA, Rac1, and Cdc42 exert distinct effects on epithelial barrier via selective structural and biochemical modulation of junctional proteins and F-actin." American Journal of Physiology-Cell Physiology 287(2): C327-C335.

Burch, P. M., Z. Yuan, et al. (2004). "An extracellular signal-regulated kinase 1- and 2-dependent program of chromatin trafficking of c-Fos and Fra-1 is required for cyclin D1 expression during cell cycle reentry." Mol Cell Biol 24(11): 4696-4709.

Cadet, J. L., S. Jayanthi, et al. (2013). "Genome-wide profiling identifies a subset of methamphetamine (METH)-induced genes associated with METH-induced increased H4K5Ac binding in the rat striatum." BMC Genomics 14: 545.

Cadet, J. L., M. T. McCoy, et al. (2009). "Methamphetamine preconditioning alters midbrain transcriptional responses to methamphetamine-induced injury in the rat striatum." PLoS One 4(11): e7812.

Chang, L., D. Alicata, et al. (2007). "Structural and metabolic brain changes in the striatum associated with methamphetamine abuse." Addiction 102(s1): 16-32.

Chetsawang, J., W. Suwanjang, et al. (2012). "Calpastatin reduces methamphetamine-induced induction in c-Jun phosphorylation, Bax and cell death in neuroblastoma SH-SY5Y cells." Neurosci Lett 506(1): 7-11.

Conant, K., I. Lonskaya, et al. (2011). "Methamphetamine-associated cleavage of the synaptic adhesion molecule intercellular adhesion molecule-5." J Neurochem 118(4): 521-532.

Dann, S. G., A. Selvaraj, et al. (2007). "mTOR Complex1-S6K1 signaling: at the crossroads of obesity, diabetes and cancer." Trends Mol Med 13(6): 252-259.

Despouy, G., M. Joiner, et al. (2007). "The TCL1 oncoprotein inhibits activation-induced cell death by impairing PKCθ and ERK pathways." Blood 110(13): 4406-4416.

Fu, M., C. Wang, et al. (2004). "Minireview: Cyclin D1: normal and abnormal functions." Endocrinology 145(12): 5439-5447.

Goncalves, J., T. Martins, et al. (2008). "Methamphetamine-induced early increase of IL-6 and TNF-alpha mRNA expression in the mouse brain." Ann N Y Acad Sci 1139: 103-111.

Hernandez-Breijo, B., J. Monserrat, et al. (2013). "Azathioprine desensitizes liver cancer cells to insulin-like growth factor 1 and causes apoptosis when it is combined with bafilomycin A1." Toxicol Appl Pharmacol 272(3): 568-578.

Holnthoner, W., M. Pillinger, et al. (2002). "Fibroblast growth factor-2 induces Lef/Tcf-dependent transcription in human endothelial cells." J Biol Chem 277(48): 45847-45853.

Jackson, A. R., A. Shah, et al. (2014). "Methamphetamine alters the normal progression by inducing cell cycle arrest in astrocytes." PLoS One 9(10): e109603.

Khan, M. A. and D. J. Goss (2012). "Poly(A)-binding protein increases the binding affinity and kinetic rates of interaction of viral protein linked to genome with translation initiation factors eIFiso4F and eIFiso4F.4B complex." Biochemistry 51(7): 1388-1395.

Le Toriellec, E., G. Despouy, et al. (2008). "Haploinsufficiency of CDKN1B contributes to leukemogenesis in T-cell prolymphocytic leukemia." Blood 111(4): 2321-2328.

Liu, P., W. Gan, et al. (2013). "Sin1 phosphorylation impairs mTORC2 complex integrity and inhibits downstream Akt signalling to suppress tumorigenesis." Nat Cell Biol 15(11): 1340-1350.

Martin, T. A., S. Jayanthi, et al. (2012). "Methamphetamine causes differential alterations in gene expression and patterns of histone acetylation/hypoacetylation in the rat nucleus accumbens." PLoS One 7(3): e34236.

Martins, T., S. Baptista, et al. (2011). "Methamphetamine transiently increases the blood-brain barrier permeability in the hippocampus: role of tight junction proteins and matrix metalloproteinase-9." Brain Res 1411: 28-40.

Matsui, Y., K. Assi, et al. (2012). "The importance of integrin-linked kinase in the regulation of bladder cancer invasion." Int J Cancer 130(3): 521-531.

Mizoguchi, H., K. Yamada, et al. (2004). "Regulations of methamphetamine reward by extracellular signal-regulated kinase 1/2/ets-like gene-1 signaling pathway via the activation of dopamine receptors." Molecular pharmacology 65(5): 1293-1301.

Moller, D. E., C. H. Xia, et al. (1994). "Human rsk isoforms: cloning and characterization of tissue-specific expression." American Journal of Physiology - Cell Physiology 266(2): C351-C359.

Okada, S. and J. E. Pessin (1996). "Interactions between Src Homology (SH) 2/SH3 Adapter Proteins and the Guanylnucleotide Exchange Factor SOS Are Differentially Regulated by Insulin and Epidermal Growth Factor." Journal of Biological Chemistry 271(41): 25533-25538.

Papadakis, M., G. Hadley, et al. (2013). "Tsc1 (hamartin) confers neuroprotection against ischemia by inducing autophagy." Nat Med 19(3): 351-357.

Park, M., H. J. Kim, et al. (2013). "Methamphetamine-induced occludin endocytosis is mediated by the Arp2/3 complex-regulated actin rearrangement." J Biol Chem 288(46): 33324-33334.

Polivka, J. and F. Janku (2014). "Molecular targets for cancer therapy in the PI3K/AKT/mTOR pathway." Pharmacology & therapeutics 142(2): 164-175.

Ramirez, S. H., S. Fan, et al. (2013). "Inhibition of glycogen synthase kinase 3beta promotes tight junction stability in brain endothelial cells by half-life extension of occludin and claudin-5." PLoS One 8(2): e55972.

Ramirez, S. H., R. Potula, et al. (2009). "Methamphetamine disrupts blood-brain barrier function by induction of oxidative stress in brain endothelial cells." J Cereb Blood Flow Metab 29(12): 1933-1945.

Rom, S., S. Fan, et al. (2012). "Glycogen synthase kinase 3beta inhibition prevents monocyte migration across brain endothelial cells via Rac1-GTPase suppression and down-regulation of active integrin conformation." Am J Pathol 181(4): 1414-1425.

Rosano, L., F. Spinella, et al. (2006). "Integrin-linked kinase functions as a downstream mediator of endothelin-1 to promote invasive behavior in ovarian carcinoma." Mol Cancer Ther 5(4): 833-842.

Saint-Preux, F., L. R. Bores, et al. (2013). "Chronic co-administration of nicotine and methamphetamine causes differential expression of immediate early genes in the dorsal striatum and nucleus accumbens of rats." Neuroscience 243: 89-96.

Salles, A., A. Romano, et al. (2014). "Synaptic NF-kappa B pathway in neuronal plasticity and memory." J Physiol Paris.

Salzmann, J., C. Marie-Claire, et al. (2003). "Importance of ERK activation in behavioral and biochemical effects induced by MDMA in mice." Br J Pharmacol 140(5): 831-838.

Sasaki, T. and T. Kitamura (2009). "Roles of FoxO1 and Sirt1 in the central regulation of food intake." Endocrine journal 57(11): 939-946.

Stein, J., W. M. Milewski, et al. (2013). "The negative cell cycle regulators, p27(Kip1), p18(Ink4c), and GSK-3, play critical role in maintaining quiescence of adult human pancreatic beta-cells and restrict their ability to proliferate." Islets 5(4): 156-169.

Summers, L., K. Kangwantas, et al. (2013). "Activation of brain endothelial cells by interleukin-1 is regulated by the extracellular matrix after acute brain injury." Mol Cell Neurosci 57: 93-103.

Troussard, A. A., P. Costello, et al. (2000). "The integrin linked kinase (ILK) induces an invasive phenotype via AP-1 transcription factor-dependent upregulation of matrix metalloproteinase 9 (MMP-9)." Oncogene 19: 5444-5452.

Uchida, T., T. Nakamura, et al. (2005). "Deletion of Cdkn1b ameliorates hyperglycemia by maintaining compensatory hyperinsulinemia in diabetic mice." Nature medicine 11(2): 175-182.

Urrutia, A., A. Rubio-Araiz, et al. (2013). "A study on the effect of JNK inhibitor, SP600125, on the disruption of blood-brain barrier induced by methamphetamine." Neurobiol Dis 50: 49-58.

Volz, T. J., A. E. Fleckenstein, et al. (2007). "Methamphetamine-induced alterations in monoamine transport: implications for neurotoxicity, neuroprotection and treatment." Addiction 102(s1): 44-48.

Wires, E. S., D. Alvarez, et al. (2012). "Methamphetamine activates nuclear factor kappa-light-chain-enhancer of activated B cells (NF-kappaB) and induces human immunodeficiency virus (HIV) transcription in human microglial cells." J Neurovirol 18(5): 400-410.

Wisdom, R., R. S. Johnson, et al. (1999). "c-Jun regulates cell cycle progression and apoptosis by distinct mechanisms." The EMBO journal 18(1): 188-197.

Wu, C. and S. Dedhar (2001). "Integrin-linked kinase (ILK) and its interactors: a new paradigm for the coupling of extracellular matrix to actin cytoskeleton and signaling complexes." J Cell Biol 155(4): 505-510.

CHAPTER II

Acetyl-L-carnitine prevents methamphetamine-induced structural damage on endothelial cells via ILK related MMP-9 activity

Molecular Neurobiology (in press)

“Life itself is your teacher, and you are in a state of constant learning.”

Bruce Lee

Mol Neurobiol
DOI 10.1007/s12035-014-8973-5

Acetyl-L-Carnitine Prevents Methamphetamine-Induced Structural Damage on Endothelial Cells via ILK-Related MMP-9 Activity

S. Fernandes · S. Salta · J. Bravo · A. P. Silva · T. Summavielle

Received: 2 August 2014 / Accepted: 29 October 2014

Abstract Methamphetamine (METH) is a potent psychostimulant highly used worldwide. Recent studies evidenced the involvement of METH in the breakdown of the blood-brain-barrier (BBB) integrity leading to compromised function. The involvement of the matrix metalloproteinases (MMPs) in the degradation of the neurovascular matrix components and tight junctions (TJs) is one of the most recent findings in METH-induced toxicity. As BBB dysfunction is a pathological feature of many neurological conditions, unveiling new protective agents in this field is of major relevance. Acetyl-L-carnitine (ALC) has been described to protect the BBB function in different paradigms, but the mechanisms underling its action remain mostly unknown. Here, the immortalized bEnd.3 cell line was used to evaluate the neuroprotective features of ALC in METH-induced damage. Cells were exposed to ranging concentrations of METH, and the protective effect of ALC 1 mM was assessed 24 h after treatment. F-actin rearrangement, TJ expression and distribution, and MMPs activity were evaluated. Integrin-linked kinase (ILK) knockdown cells were used to assess role of ALC in ILK mediated METH-triggered MMPs' activity. Our results show that METH led to disruption of the actin filaments concomitant with claudin-5 translocation to the cytoplasm. These events were mediated by MMP-9 activation in association with ILK overexpression. Pretreatment with ALC prevented METH-induced activation of MMP-9, preserving claudin-5 location and the structural arrangement of the actin filaments. The present results support the potential of ALC in preserving BBB integrity, highlighting ILK as a new target for the ALC therapeutic use.

Keywords Blood-brain-barrier · Methamphetamine · Acetyl-L-carnitine · Tight junctions · Matrix-metalloproteinase-9 · Integrin-linked kinase

Electronic supplementary material The online version of this article (doi:10.1007/s12035-014-8973-5) contains supplementary material, which is available to authorized users.

S. Fernandes · S. Salta · J. Bravo · T. Summavielle (✉)
Addiction Biology Group, IBMC - Instituto de Biologia Molecular e Celular, Universidade do Porto, Rua do Campo Alegre, 823, 4150-180 Porto, Portugal
e-mail: tsummavi@ibmc.up.pt

S. Fernandes
e-mail: silvia.fernandes@ibmc.up.pt

S. Salta
e-mail: sofia.salta@ibmc.up.pt

J. Bravo
e-mail: joana.bravo@ibmc.up.pt

S. Fernandes · S. Salta · T. Summavielle
School of Allied Health Sciences, Polytechnic Institute of Porto (ESTSP-IPP), Porto, Portugal

S. Fernandes
Faculdade de Medicina, Universidade do Porto (FMUP), Porto, Portugal

J. Bravo
Institute de Ciências Biomédicas de Abel Salazar (ICBAS), Universidade do Porto, Porto, Portugal

A. P. Silva
Institute of Biomedical Research on Light and Image (IBILI), Faculty of Medicine, University of Coimbra, Coimbra, Portugal
e-mail: apsilva@cnc.cj.uc.pt

Published online: 03 December 2014

Introduction

Methamphetamine (METH) is a powerful psychostimulant with high abuse liability. Both short- and long-term METH uses lead to long-lasting deleterious effects [1, 2]. METH toxicity is typically characterized by disruption of synaptic integrity and decreased monoamine production [3–5], concomitant with terminal degeneration and neuronal death [2,

6]. METH is increasingly recognized to impact also non-neuronal cells, such as microglia, and astrocytes and the blood-brain-barrier (BBB), causing the release of inflammatory mediators and astrogliosis [1, 3, 7, 8]. The concept of METH-induced damage at the level of the BBB has gained relevance over the last few years, justifying the interest in understanding its consequences at the endothelium [4, 9, 10].

METH-induced permeability at the BBB has been consistently reported both in vivo and in vitro [4, 5, 11]. In mice models, METH was seen to increase permeability and induce massive leakage of macromolecules across the BBB in the cerebral cortex, hippocampus, and other limbic regions [5, 6, 9]. In vitro, BBB increased permeability after METH exposure was accompanied by a reduction and/or redistribution of the tight junction (TJ) proteins [7, 12–14].

The BBB is part of the neurovascular unit and is responsible for maintaining a homeostatic microenvironment for the central nervous system (CNS). Although pericytes, astrocytes, and the surrounding basement membrane play a structural and regulatory role on the neurovascular unit, the endothelial cells (ECs) are the barrier-conferring properties of the BBB [13, 15–17]. Its modulation is essentially a function of the TJ proteins [13, 16, 18–20]. Claudins, essentially claudin-5, ensure the tightness of the contact between the brain capillaries ECs, which is critical in determining BBB permeability [21, 22], while occludin plays a regulatory role and enhances TJ tightness [18]. The endothelial paracellular permeability occurs due to the equilibrium between cytoskeleton contractile forces and adhesive forces produced at the endothelial cell-cell junctions and cell-matrix contacts [14], where actin filaments play an essential role. Functioning as a cross-linker between occludin and the actin cytoskeleton, the protein *ZO-1* is also central to the TJ structure [10, 13, 18, 23].

BBB impairment with TJ dysfunction is a hallmark of many pathological states such as inflammation, tumor differentiation [24], epilepsy, Parkinson's and Alzheimer's disease, multiple sclerosis, and ischemia/reperfusion [25]. Importantly, METH-induced BBB increased permeability was associated with reduction and/or redistribution of TJ proteins [10, 13]. There is also evidence that it can interfere with actin structure and arrangement, which also may lead to compromised TJ function [14, 26]. Although the molecular mechanisms underlying BBB disruption under METH exposure are not fully characterized, the activation of matrix metalloproteinases (MMPs), commonly involved in remodeling and degradation of the neurovascular matrix components and therefore associated with BBB leakiness, has been reported [4, 6, 9, 27].

Investigating the mechanisms that underlie the action of compounds able to counteract these detrimental effects at the level of BBB is of major relevance. Acetyl-L-carnitine (ALC) has been described to protect the BBB function from EtOH-induced inhibition of glucose transport [28] and increased reactive oxygen species (ROS) levels [29]. ALC is a natural occurring compound synthesized from acetyl-CoA and carnitine [30–32], able to cross the BBB essentially through organic cation transport (OCTN2) [33–35], and reaching high concentrations in the brain [30, 34]. When therapeutically administered, ALC is more easily transported across the BBB than L-carnitine, which supports its prescription in acute and chronic neurological disorders [34]. ALC described effects include the modulation of neurotrophic factors and multiple neurotransmitters, as well as mitochondrial stabilization [30, 31], but the mechanisms involved in its action at the BBB level remain elusive.

Here, we used a model of endothelial cells exposed to ranging doses of METH to evaluate the potential protective role of ALC. Based on former reports [28, 36], we hypothesized that ALC could be protective at the BBB level by counteracting the effect of METH in the structural disruption of TJ and consequential loss of adhesive forces. We further hypothesized that ALC could be protective by preventing METH-triggered activation of MMPs.

Material and Methods

In Vitro Model and Cell Culture

The immortalized bEnd.3 cells are derived from mouse brains and known to mimic some of the BBB characteristics [37, 38]. The cell line bEnd.3 was obtained from ATCC (American Type Cell Culture-CRL-2299, Manassas, VA), and cultures were maintained in Dulbecco's Modified Eagle's medium (DMEM) (1×)/Glutamax (GIBCO®, Life Technologies, Paisley, UK), containing 5 % penicillin and streptomycin (GIBCO®, Life Technologies) and 10 % fetal bovine serum (GIBCO®, Life Technologies). Purity of the cell line was checked using an anti-CD31 antibody (Abcam 7388, rat monoclonal, 1:1000), which showed 100 % enrichment of cells on the adhesion marker. For viability assays, cells were cultured in 24-well plates (80,000 cells/well). For immunofluorescence, cells were plated on 24-well plates (80,000 cells/well) containing glass cover slips. To obtain protein extracts, bEnd.3 cells were cultured in petri dishes (one million of cells). Cell culture media was changed every 3 days until cells were confluent.

Drug Regimen

ALC-hydrochloride was kindly provided by Sigma-Tau, S.p.a (Pomezia, Italy). METH hydrochloride was purchased from Sigma-Aldrich (St. Louis, MO, Cat.M-8750).

Immortalized bEnd.3 cells at confluence were treated with 0.25, 0.5, and 1 mM of METH, with or without a pretreatment with 1 mM ALC added 30 min prior to METH. The METH

range of doses tested was predetermined in our laboratory in agreement with previous studies using METH in similar cell models [39]. The selected ALC dose of 1 mM is not toxic for the cells and is within the range of doses previously used in similar works [40]. For zymography studies, cells were treated with 10 nM BB-94 (Batimastat, Tocris Bioscience, Bristol, UK), a broad spectrum MMP inhibitor [41], 15 min prior to METH exposure.

Cell Viability Assay—MTT

Cell viability was determined by 3-(4,5-dimethylthiazol-2yl)-2,5-diphenyl tetrazolium bromide (MTT) assay, which is based on the reduction of yellow tetrazolium salt to purple formazan crystals by metabolically active cells. The reduction of MTT is thought to mainly occur in the mitochondria through the action of succinate dehydrogenase, therefore, providing a measure of mitochondrial function [42]. In these assay, METH concentrations of 0.25, 0.5, and 1 mM were used. Briefly, 24 h after treatment, the cells were added MTT (0.5 mg/mL, Sigma-Aldrich, Steinheim, Germany) and incubated at 37 °C. DMSO (Sigma-Aldrich) was then added to promote the dissolution of MTT-formazan crystals. Absorbance of the purple formazan was measured in duplicate by a microplate reader (Sunrise Tecan™, Mannedorf, Switzerland) at 540-nm wavelength.

Lactate Dehydrogenase Cytotoxic Assay

At 24 h of METH exposure, the LDH release to the extracellular medium was evaluated by a colorimetric assay using the CytoTox96 Non-Radioactive Assay kit (Promega, Madison, WI), according to the manufacturer's instructions. The percentage of LDH release was determined as the ratio between LDH activity in the extracellular medium and total LDH activity obtained after complete cell lysis with Triton X-100. All experiments were carried out in duplicate, using a microplate reader at 490 nm (Sunrise Tecan™).

Immunostaining Procedure

For immunocytochemistry, bEnd.3 cells were cultured on glass cover slips in 24 well plates until 90–100 % confluent. Cells were then treated with 0.5 and 1 mM of METH in the presence or absence of 1 mM ALC (added 30 min before), for 24 h. For F-actin filaments evaluation, cells were washed with phosphate buffered saline (PBS) and fixed with microtubule-protecting buffer (MPB) (65 mM PIPES; 25 mM HEPES; 10 mM EGTA; 3 mM $MgCl_2$) diluted in 4 % paraformaldehyde (pH 6.9), for 10 min. After permeabilization with Triton X-100 0.1 % for 10 min, cells were blocked with 10 % normal goat serum (NGS) for 45 min and incubated at room temperature for 1 h with Alexa488®-conjugated primary antibody (Phalloidin, Life Technologies, A12379, 1:1000). For claudin-5 and occludin, cells were washed with PBS, fixed during 15 min in methanol and permeabilized in 0.1 % Triton X-100 during 10 min. After a blocking of 45 min in 5 % BSA (bovine serum albumin), cells were incubated overnight at 4 °C with respective primary antibodies—Rabbit anti-Claudin-5 (Abcam 53765, 1:200) and Rabbit anti-occludin (Invitrogen #71–1500, 5 μg/mL). For *ZO-1* immunoreaction, a preincubation with a *preextraction* buffer (as described by Balda MS, 1996 [16]) was performed before 96 % ethanol fixation (30 min, on ice). Cells were rehydrated, permeabilized for 10 min with 0.05 % Triton X-100 and blocked for 45 min with 10 % NGS before overnight at 4 °C incubation with primary antibody (Rabbit *ZO-1*, Invitrogen #44–2200, 2.5 μg/mL). For secondary antibody incubation, we used Anti-Rabbit IgG Alexa-Fluor488® Conjugate (Cell Signaling, #4412, 1:1000), for 1 h at room temperature in the dark. Coverslips were then mounted onto glass slides (Fluorescent Mounting Medium, CA, USA) containing 4′,6-diamidino-2-phenylindole (DAPI), and then fluorescence microphotographs were captured using AxioImager Z1 fluorescence microscope (Carl Zeiss, Germany).

Morphometric Analysis

F-actin Analysis

Changes observed on F-actin by immunofluorescence were analyzed by the Directionality plugin of Fiji Software version 2.0. This plugin is used to infer the preferred orientation of structures present in the input image. The final result is a histogram indicating the amount of filaments in a given direction (from −90 to 90°), peaking at the preferred orientation. Measurements were obtained using the Fiji Local Gradient Orientation tool that uses a 5×5 Sobel filter to derive the local gradient orientation [adapted from 43]. To compare different conditions, a minimum of four independent experiments was considered and an average of twelve images were captured blindly. For each condition, an average histogram was built using the mean of the amount of filaments in each bin/orientation. To analyze differences in the directionality of actin filaments, we used the interval of fifteen consecutive degrees containing the higher number of filaments for each condition.

Claudin-5 Analysis

Analysis of claudin-5 immunofluorescence images was made using the Fiji Software version 2.0. A total of four independent experiments were performed. From each coverslip, six images were blindly captured and analyzed. A straight line perpendicular to the cellular membrane limits was drawn for all cells within each image. This line was drawn always at a similar distance from the nucleus. An intensity plot profile of the line

drawn was built to calculate the ratio between membrane and cytosol pixel intensity [adapted from 3]. The mean ratio of membrane/cytosol pixel intensity per condition was also calculated.

Protein Expression Analysis by Western Blot

Confluent bEnd.3 cells cultured in petri dishes were scrapped and lysed with TEN Buffer (50 mM Tris-HCl, 2 mM EDTA, 150 mM NaCl, 1 % NP-40, supplemented with phosphatases and proteases inhibitors) and then centrifuged at 14,000× g for 15 min at 4 °C. Protein concentration of the cell lysate was estimated in the supernatant by the Bradford method (Bio-Rad Protein Assay, Munich, Germany). Proteins were loaded at 40 μg per lane and resolved by SDS-PAGE on 10 to 12 % Bis/acrilamide gels and then transferred onto PVDF membranes. After blocking with dry milk 5 %, membranes were incubated with rabbit polyclonal antibodies to claudin-5 (Abcam 53765, 1:500), occludin (Invitrogen #71–1500, 2 μg/mL), *ZO-1* (Invitrogen #44–2200, 2 μg/mL), and mouse polyclonal antibody to GAPDH (glyceraldehyde-3-phosphate dehydrogenase, Hytest #5G4, 1:300000). Secondary antibody horseradish peroxidase (HRP)-conjugated were used for 1-h incubation. Chemiluminescence signal detection was performed using the traditional developer, using Immun-Star HRP (Bio-Rad Laboratories, USA). A GS800 densitometer (Bio-Rad) and Quantity One 1-D analysis software (v4.6, Bio-Rad) were used for densitometry analysis.

Subcellular Fractionation

Confluent monolayers were scrapped and lysed on fractionation buffer (250 mM sucrose, 20 mM HEPES (pH 7.4), 10 mM KCl, 1.5 mM $MgCl_2$, 1 mM EDTA and 1 mM EGTA) supplemented with 1 mM DTT and protease inhibitor cocktail, for 20 min. Lysates were aspirated at least 10 times through a 25 G needle in a 1-mL syringe and left on ice for 20 min. A 5-min centrifugation at 720 G was performed to centrifuge out the nuclear pellet, and the supernatant was re-centrifuged for 5 min at 10,000 G. The membrane and the cytoplasmic fractions were separated by ultracentrifugation at 100.000 G for 1 h (ultracentrifuge Beckman Coulter, 70.1 Ti Rotor, CA, USA). The supernatant (cytoplasmic fraction) was collected, and the pellet obtained was washed in fractionation buffer and resuspended with a 25 G needle as above. The membrane fraction was re-centrifuged for 45 min, and the final pellet was resuspended in fractionation buffer supplemented with 10 % glycerol and 0.1 % SDS. The cytoplasmic fraction was concentrated through a filter unit (Amicon Ultra Centrifugal Filters, UFC501024). All steps were carried out at 4 °C. Both membrane and cytoplasmic protein concentrations were determined as described above. Western blot was used to analyze tight junction amount in each fraction.

MMPs Gelatinolytic Assay

Culture-conditioned media from bEnd.3 cells was collected in confluent serum-free monolayers from each condition for determination of MMP-2 and MMP-9 activities. The collected medium was centrifuged (8000 g, 5 min) to remove cell debris and applied in a non-reducing SDS-PAGE containing 0.1 % gelatin. The electrophoresed gels were washed twice for 30 min in 2 % Triton X-100 at room temperature and incubated for 16 h at 37 °C in the substrate buffer (50 mM Tris-HCl, pH 7.5; 10 mM $CaCl_2$) to allow gelatin digesting by MMP-2 and MMP-9. After staining with 0.1 % Coomassie Brilliant Blue R-250, the gels were destained (in 20 % methanol and 10 % acetic acid) and the enzyme-digested regions were seen as clear bands against a blue background. The visualized bands were quantified by densitometry using GS800 densitometer and Quantity One 1-D Analysis software, v4.6.

Transfection and ILK Silencing

Integrin-linked kinase (ILK) knockdown was performed using small hairpin RNA (shRNA)-mediated silencing technology from SIGMA (Mission shRNA). The clone TRCN0000022517 was used in HEK293T cells to the lentivirus production. After 48 h, virus was collected and frozen. For infection, bEnd.3 cells were treated for 12 h at 37 °C with lentivirus diluted in DMEM (1×)/Glutamax (GIBCO®, Life Technologies, Paisley, UK), containing 5 % penicillin and streptomycin (GIBCO®, Life Technologies) and 10 % fetal bovine serum (GIBCO®, Life Technologies) containing 5 μg/mL polybrene. Afterwards, the virus containing medium was replaced by fresh medium. Selection of infected cells was done with puromycin treatment (2 μg/mL). ILK silencing (KD ILK) was monitored and confirmed by Western blot using mouse anti-ILK (BD Pharmigen #611802, 1:1000). In this experiment, cells treated with control viral DNA (empty vector) are indicated as pLKO.1 and were used as a control.

Statistical Analysis

Results from at least four independent experiments were represented as mean±SEM. Significant differences between groups were determined by one-way ANOVA followed by the Bonferroni post hoc test. When data normality was not verified, the *Kruskal-Wallis* test was used. Significance was set at $p<0.05$. All analysis was conducted using the software GraphPad Prism® 6.0 for Mac OSX (GraphPad Software, La Jolla CA).

Results

METH-Induced Loss of Viability in bEnd.3 Cells

The viability of bEnd.3 cultures under different doses of METH and ALC was evaluated both by MTT and LDH assays. MTT results showed that mitochondrial activity was only affected by METH 1 mM, which was significantly reduced when compared to the control condition ($p<0.05$) (Fig. 1a). ALC 1 mM added to the cells 30 min before METH 1 mM did not prevent the decrease in the viability of bEnd.3 cells. The results provided by the LDH assay confirmed the increased toxicity of METH 1 mM, which led to significant cell loss when compared to the control ($p<0.001$). In accordance with the data provided by the MTT assay, ALC 1 mM in combination with METH could not prevent bEnd.3 cell death (Fig. 1b).

ALC Prevented the METH-Induced Loss of F-Actin Filaments Alignment

F-actin filaments organization is characteristic of adhered and immobile endothelial cells. Using phalloidin to visualize F-actin, we observed a dose-dependent loss of stress fibers organization induced by METH (Fig. 2a). This loss of organization was quantified through measuring the directionality of the filaments within the different conditions using a derivative of the original image (Fig. 2b). In the control condition, F-actin filaments are mostly organized in a single orientation, with a high proportion of filaments aligned at the same direction. The filaments organization is progressively lost when cells are exposed to increasing doses of METH, as evidenced through directionality quantification (Fig. 2c). Importantly, pretreatment with ALC 1 mM prevented the loss of organization induced by METH 1 mM as shown in Fig. 2d and e, where the majority of filaments were in a single direction (control vs METH 1 mM $p<0.0001$; ALC/METH 1 mM vs METH 1 mM, $p<0.05$).

ALC Prevented the METH-Induced Loss and Redistribution of Claudin-5

METH-induced changes in claudin-5 were previously reported [3, 9, 10]. Here, we aimed to assess the effect of ALC 1 mM in preventing these changes. Indirect immunofluorescence results showed that while in control conditions, claudin-5 is localized in the cellular membrane, after METH-exposure claudin-5 is also present in the cytoplasm (Fig. 3a and b). The ratio membrane/cytoplasm for claudin-5 localization is significantly decreased when cells are exposed for 24 h to METH ($p<0.0001$ for both METH 0.5 and 1 mM) compared to the control (Fig. 3b). In addition, the total amount of claudin-5 was also significantly decreased after exposure to METH, as shown by Western blot analysis ($p<0.01$ for both METH 0.5 mM and 1 mM, compared to the control, Fig. 3c). To confirm the impact of METH on claudin-5 distribution, we performed a subcellular fractionation analysis, which confirmed an increase of cytoplasmatic claudin-5 content in cells treated with METH 1 mM ($p<0.01$, Fig. 3d).

Aiming to evaluate the ability of ALC to prevent the METH-induced redistribution of claudin-5, we treated cells with ALC 1 mM. The redistribution of claudin-5 after METH exposure was partially prevented when ALC 1 mM was used, as shown by immunofluorescence images (Fig. 3a) for both doses (METH 0.5 mM vs control $p<0.001$, METH 1 mM vs control $p<0.05$,

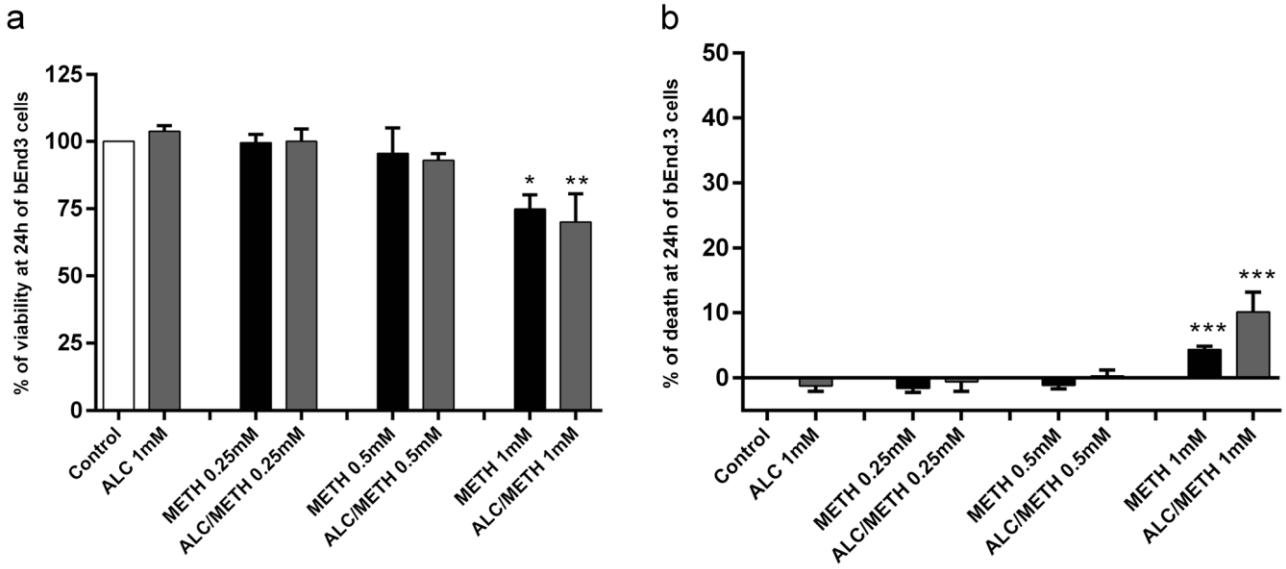

Fig. 1 Viability/cytotoxicity assays: **a** MTT assay, **b** LDH assay. Confluent bEnd.3 cells monolayers were treated with ranging concentration of METH and ALC 1 mM. **a** MTT reduction was assessed 24 h after treatment. **b** Cell death was measured by lactate dehydrogenase released on the bEnd.3 culture medium at the same time point. Data represent mean±SEM. Significant differences are marked as $*p<0.05$, $**p<0.01$, and $***p<0.001$ compared to the control group (as determined by ANOVA followed by the Bonferroni post hoc test)

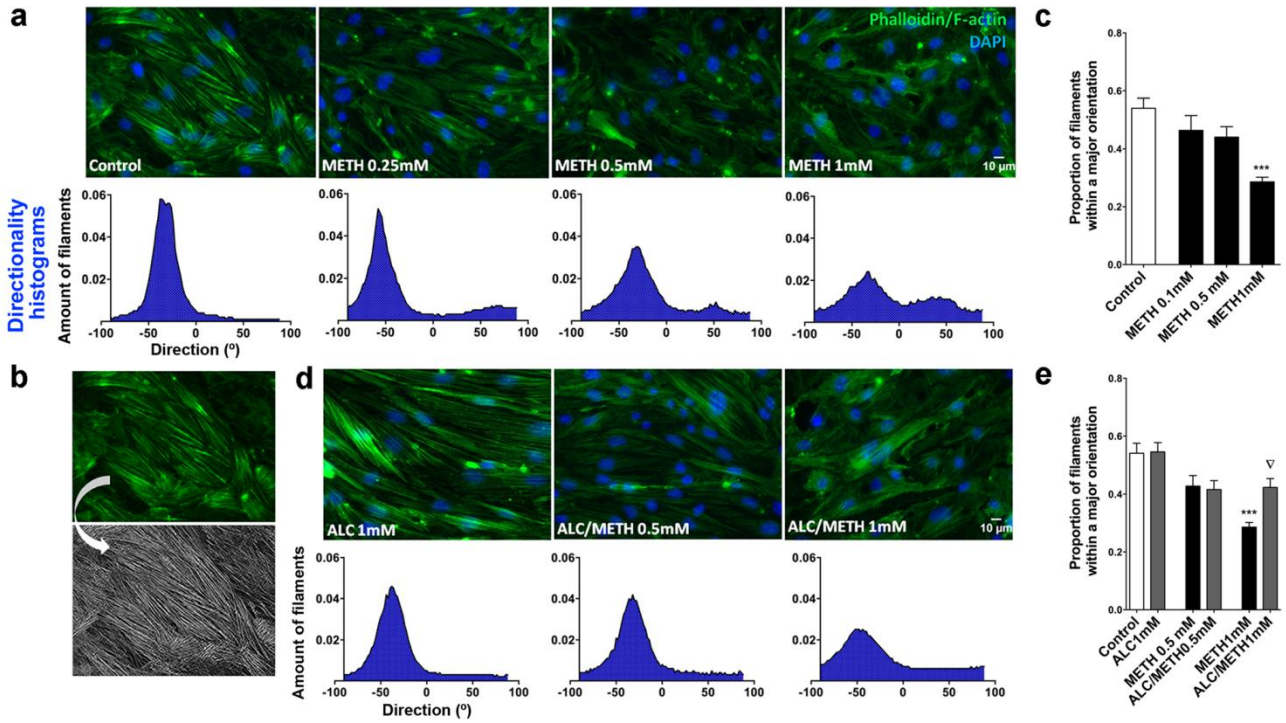

Fig. 2 F-actin filaments alignment. Confluent bEnd.3 cells monolayers were treated with METH 0.5 and 1 mM doses according to the described procedures. **a** Representative images are shown for F-actin filaments stained with Alexa Fluor® 488-Phalloidin and nuclei labeled with DAPI, after METH exposure. The mean histogram for each condition is represented below the respective image. **b** Changes on F-actin filaments alignment were analyzed by the Directionality plugin of Fiji Software, using the local gradient orientation method to derive the image. **c** Proportion of actin filaments in a preferential direction after METH exposure. **d** F-actin filaments stained with Alexa Fluor® 488-Phalloidin and labeled with DAPI, when cells were pretreated with ALC 1 mM before METH exposure. The mean histogram for each condition is represented below the respective image. **e** Proportion of actin filaments in a preferential direction in cells treated with ALC 1 mM before METH exposure. Data represent mean±SEM. ***$p<0.001$ compared to control group; ▽$p<0.05$ compared to METH 1 mM (as determined by ANOVA followed by the Bonferroni post hoc test)

Fig. 3b). Total claudin-5 quantification by Western blot also evidenced a protective effect of ALC, although significance was only reached for METH 1 mM dose ($p<0.05$, Fig. 3c). When the quantification was performed separately in both subcellular fractions, significance for the protective effect of ALC was not achieved ($p=0.22$).

METH did not Affect Occludin and *ZO-1*

We investigated also the effect of METH exposure in *ZO-1* and occludin. In our in vitro model, METH failed to induce any significant change in occludin or *ZO*-1, both when evaluated by immunofluorescence (Fig. 4a and d) or Western blot (Fig. 4b and e). To further confirm this, we performed an evaluation by subcellular fractionation, where occludin levels on the membrane and cytoplasmic fractions were shown to be unaltered after METH or ALC treatment (Fig. 4c).

ALC Prevented METH-Induced MMP-9 Activity

As activation of MMPs is a common mechanism of BBB leakiness, we investigated also if the translocation of claudin-5 mechanism could be linked to METH-triggered MMPs activation. To understand if both MMP-2 and MMP-9 gelatinases were triggered by METH, gelatinolytic assays were performed. Our results show that MMP-9 release to the medium was increased by both METH 0.5 mM and 1 mM (Fig. 5a). The increased activity was observed for METH 0.5 mM 12 h postexposure ($p<0.05$) and 16 h postexposure for METH 1 mM ($p<0.05$, Fig. 5a). This effect was higher at 24 h ($p<0.001$ for METH 0.5 mM and $p<0.01$ for METH 1 mM vs control). MMP-2 activity was not significantly affected by METH exposure (data not shown).

To test the effect of ALC at the MMP-9 level, we evaluated the release of this gelatinase in the presence of ALC added before METH exposure. As represented in Fig. 5b, ALC 1 mM was effective in preventing the activation of MMP-9 both for METH 0.5 and 1 mM ($p<0.01$ for both METH doses vs control). The broad spectrum MMP inhibitor BB-94 was also assayed resulting in the expected inhibition of the METH-triggered MMPs activity ($p<0.05$ for METH 0.5 mM and $p<0.001$ for METH

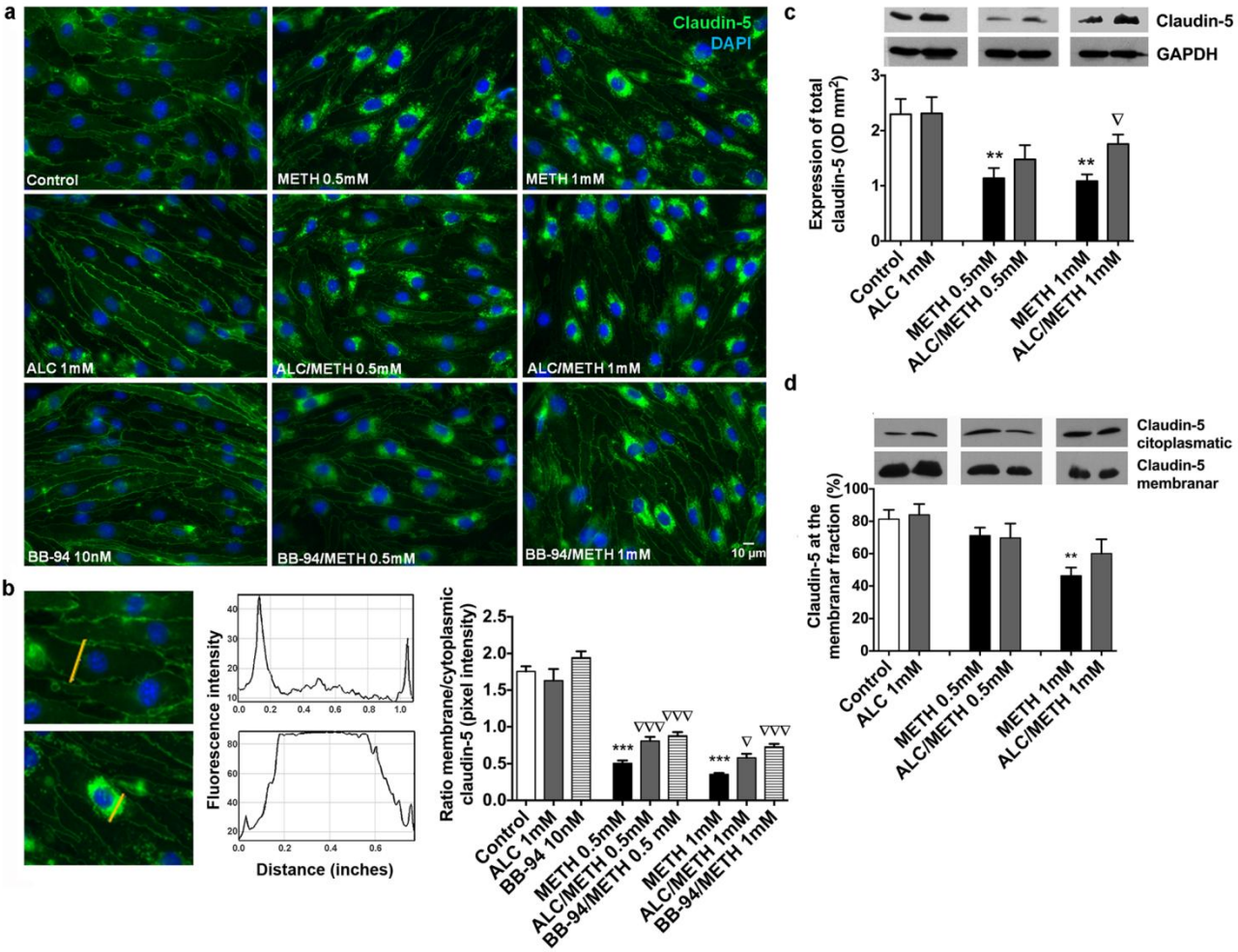

Fig. 3 Claudin-5 decrease and redistribution. Confluent bEnd.3 cells monolayers were treated with METH 0.5 and 1 mM, with or without ALC 1 mM or BB-94 10 nM. **a** Immunofluorescence representative images stained for claudin-5 and nuclei (DAPI). **b** Plot intensity profile for claudin-5 immunofluorescence obtained by drawing a straight line in each cell, always at the same position (Fiji Software), which enables to calculate the ratio between membrane and cytoplasm pixel intensity. (**c**) Total amount of claudin-5 determined by Western blot, mean ratio for each condition are represented. (**d**) Claudin-5 quantification after subcellular fractionation of the cytoplasmatic and membranar portions. Data represent mean±SEM. Significant differences are marked as $*p<0.05$; $**p<0.01$, and $***p<0.001$ compared to control; $\triangledown\triangledown\triangledown p<0.001$ and $\triangledown p<0.05$ compared to the respective METH dose (as determined by ANOVA followed by the Bonferroni post hoc test)

1 mM vs control, Fig. 5b). Importantly, ALC inhibition of MMPs activity was not significantly different from that achieved with BB-94 ($p>0.9999$).

Next, we tested if the inhibition of MMPs activity would have an impact at the level of TJs. We added the MMP inhibitor BB-94 to the bEnd.3 cell culture before METH treatment and evaluated the distribution of claudin-5 by immunofluorescence analysis. As depicted in Fig. 3a and quantified in Fig. 3b, inhibition of MMPs activity reduced METH-induced translocation of claudin-5 to the cytoplasm, as evidenced by the ratio membrane/cytoplasm for claudin-5 localization ($p<0.001$ for both METH doses vs control, Fig. 3b). These results confirm that METH-induced translocation of claudin-5 is promoted by METH-triggered activation of MMPs, which was previously shown to have a crucial role in TJ degradation in other pathologic conditions. Importantly, at this level, the effect of BB-94 was similar to that of ALC ($p=0.14$).

ALC Prevented ILK Expression Induced by METH

Since ILK increased expression has been reported to increase MMP-9 activation, we investigated the impact of METH on ILK expression in bEnd.3 cells. Our results show that METH treatment induced a significant increase in ILK expression ($p<0.05$, METH vs control), which was totally prevented when ALC was added to the medium 30 min before METH exposure ($p<0.05$, METH vs ALC/METH), (Fig. 6a). To our knowledge, the action of METH over ILK expression was never reported. Likewise, the preventive effect of ALC at this level is also a new and exciting feature for this compound.

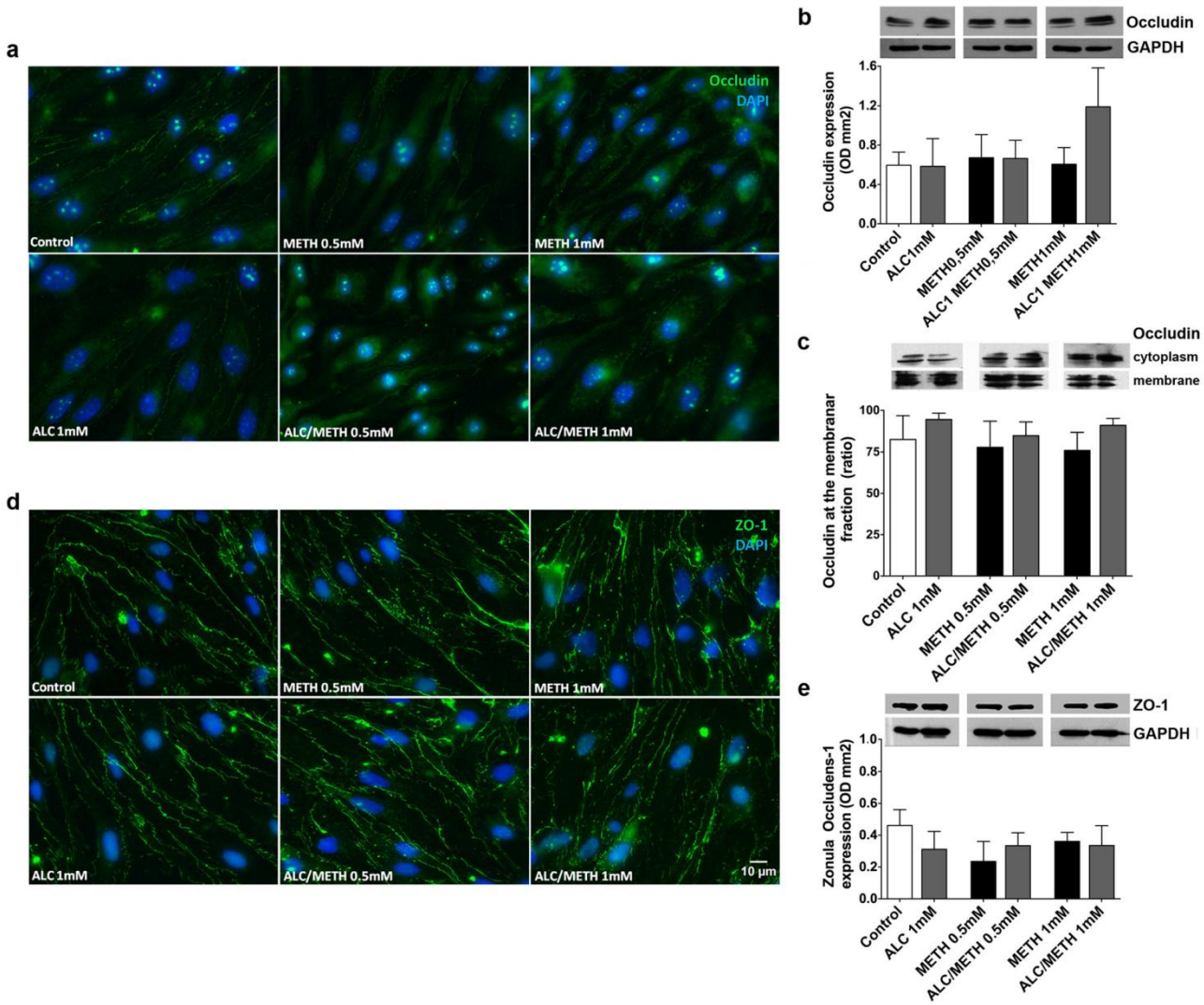

Fig. 4 METH effects on occludin and *Zonnula occludens-1*. Confluent bEnd.3 cells monolayers were treated with METH 0.5 and 1 mM, with or without the pretreatment with ALC 1 mM. **a** Immunofluorescence representative images stained for occludin nuclei (DAPI). **b** Total amount of occludin determined by Western blot. **c** Occludin quantification after subcellular fractionation of the cytoplasmatic and membranar portions; *ZO-1*. **d** Immunofluorescence representative images stained for *ZO-1* and nuclei (DAPI). **e** Total amount of *ZO-1* determined by Western blot. Data represent mean±SEM. No significant differences were observed (as determined by ANOVA followed by the Bonferroni post hoc test)

ILK Silencing Prevented METH-Triggered MMP-9 Activity

Six days after infection, ILK silencing was completed (~90 %) in endothelial cells as shown in Fig. 6b ($p<0.001$, KD ILK vs pLKO.1). When analyzed by zymography (Fig. 6c), bEnd.3 cells treated with METH showed significantly higher levels of activated MMP-9 than those where ILK was knockdown ($p<0.001$, pLKO.1/METH vs KD ILK/METH). Therefore, our results show that cells lacking ILK fail to respond to METH by increasing MMP-9 activity. As reported above, ALC was able to prevent the METH-induced activation of MMP-9 ($p<0.01$ for pLKO.1/METH vs pLKO.1/ALCMETH). In addition, the action of ALC/METH in KD ILK cells is not different from the action of METH in these cells ($p>0.9999$ for KD ILK/METH vs KD ILK/ALCMETH), showing that ILK may be a target for ALC action.

Discussion

It is commonly accepted that MMP-induced leakiness at the BBB is a critical event for the development of several neurological diseases. In the present study, we provide evidence that ALC is able to prevent the METH-triggered activation of MMP-9 via ILK increased expression, preventing changes in F-actin arrangement and claudin-5 redistribution. To our knowledge, this is the first time that ALC is shown to prevent MMP-associated

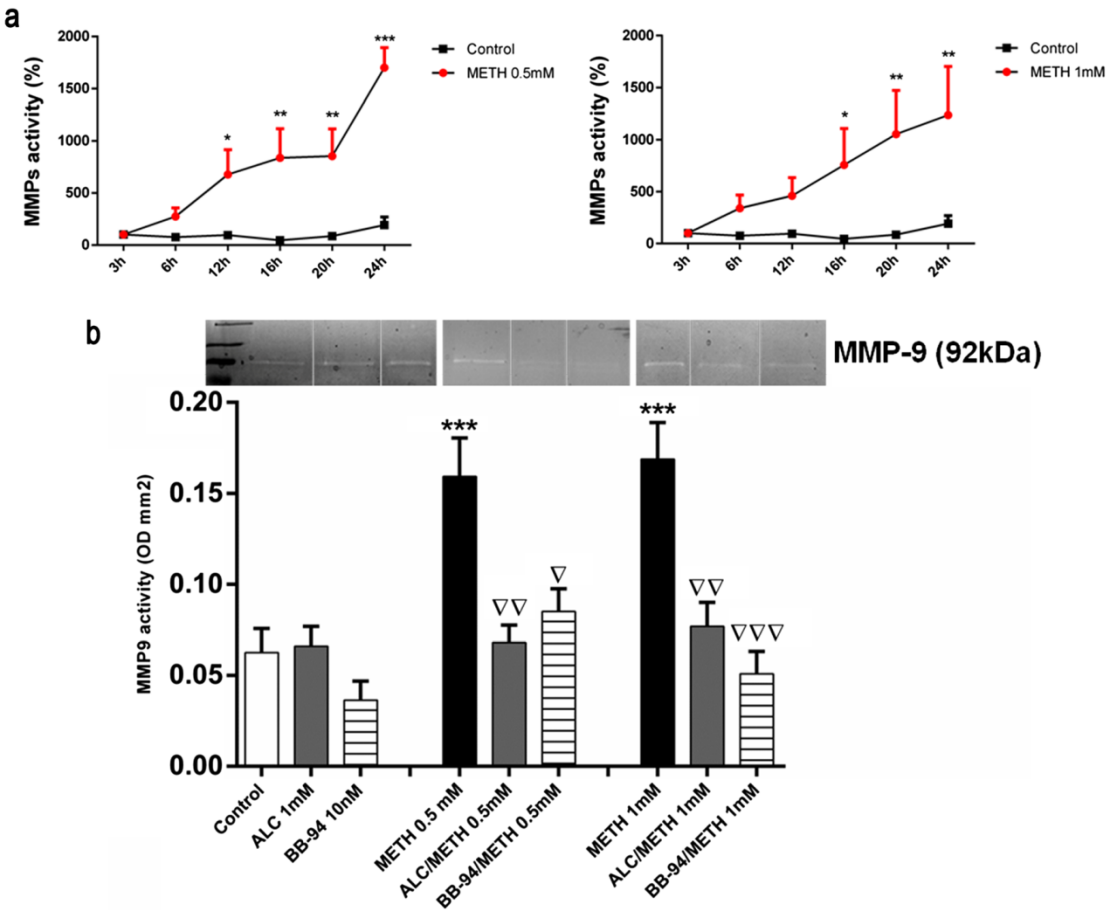

Fig. 5 METH-triggered MMP-9 activity. Confluent bEnd.3 cells monolayers were treated with METH 0.5 and 1 mM and cells; the medium was collected for determination of gelatinases activity. **a** Graphic representation of MMP-9 activity in culture mediums collected at 3, 6, 12, 16, 20, and 24 h after exposure to 0.5 mM METH (*upper left*) and 1 mM METH (*upper right*). **b** Zymography was performed to assess the effect of ALC 1 mM and BB-94 10 nM pretreatment on METH-induced MMP-9 activity at 24 h. Data represent mean±SEM. Significant differences are marked as $*p<0.05$; $**p<0.01$, and $***p<0.001$ compared to the control; $\triangledown p<0.05$, $\triangledown\triangledown p<0.01$, and $\triangledown\triangledown\triangledown p<0.001$ compared to the respective METH-dose treated cells (as determined by ANOVA followed by the Bonferroni post hoc test)

disruption of TJ and F-actin alignment, which is expected to contribute to maintain the BBB integrity.

In healthy endothelial cells, F-actin is organized along the cell axis into bright oriented bundles, forming aligned filaments that promote traction forces, adhesion, and maintain the stability of cell morphology [44]. METH impact on actin filaments was observed in previous studies that reported either actin depolymerization, altered cell shape, local accumulation of condensed actin, or disruption of the F-actin parallel strands, leading to compromised TJ function [14, 26, 45]. In our study, METH exposure led to a dramatic loss of F-actin integrity concomitant with claudin-5 redistribution and decreased expression. In endothelial cells, these events may lead to loss of adhesion and/or relevant restructuration of the endothelium, thus contributing to increase METH neurotoxicity. Interestingly, although METH-induced internalization of both claudin and occludin through endocytosis was previously seen to be concomitant with TJ fragmentation and gap formation [3, 13, 14], the functional significance of such translocation remains unclear, since it can occur also in the absence of BBB structural changes [15]. As the anchoring protein *ZO-1* and the transmembrane protein occludin are physically linked to the actin filaments, some authors have hypothesized that actin depolymerization could be secondary to the loss of these binding interactions. METH impact on ZO-1, however, is not consensual, and similarly to what we report here, other authors also could not verify any changes in this particular protein [3, 10]. Importantly, our work was the first to report ALC protection over METH-induced changes in TJ function, since a pretreatment with 1 mM ALC was effective in preventing the METH-induced loss of actin alignment, as well as claudin-5 loss and translocation to the cytoplasm. The action of ALC at the cytoskeleton level is poorly explored, but previous in vitro studies

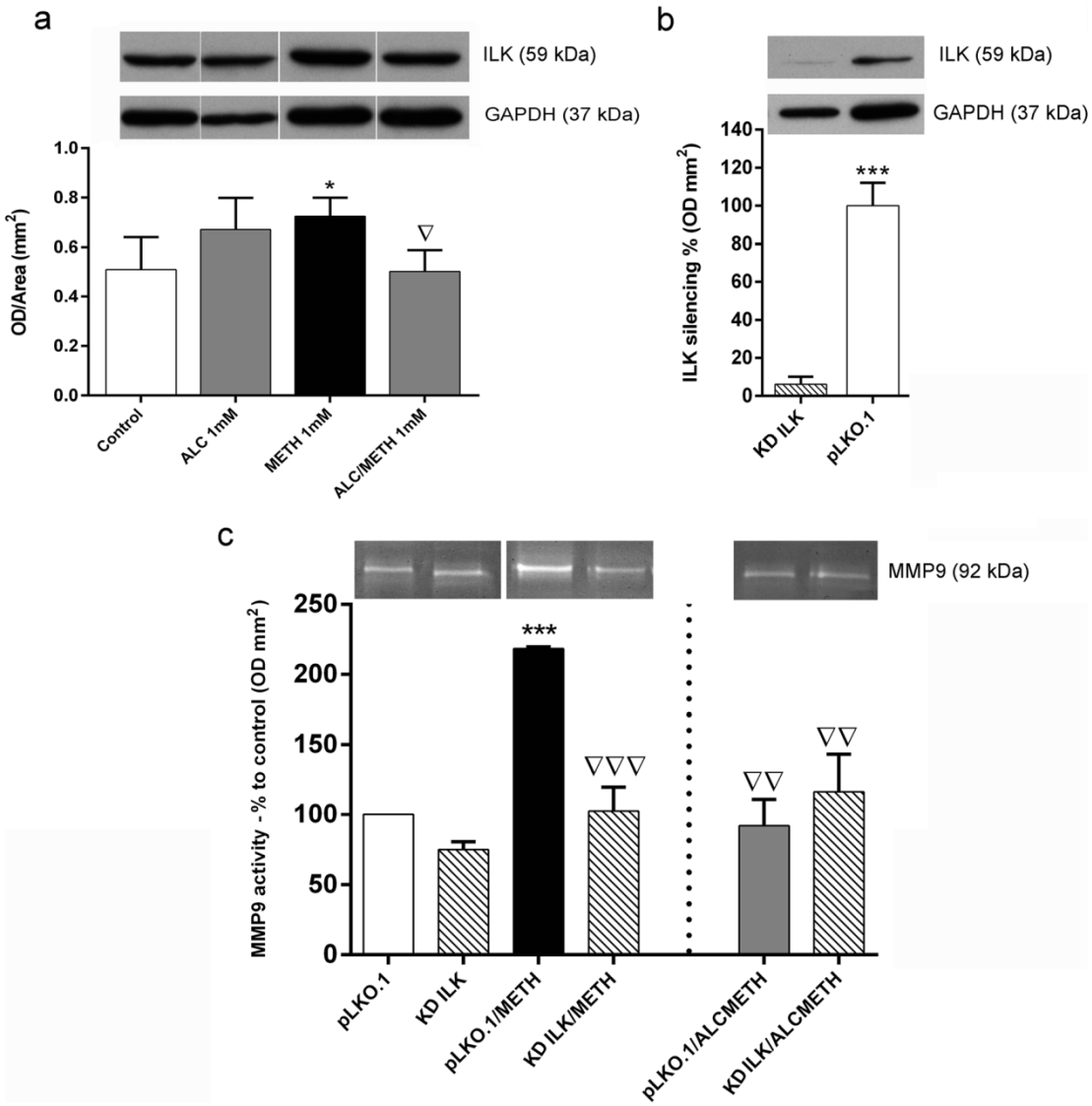

Fig. 6 ALC prevented METH-induced ILK increased expression. Confluent bEnd.3 cells monolayers were treated with METH 1 mM with or without 1 mM ALC. **a** Graphic representation of the total amount of ILK expression 24 h after METH treatment for each condition, significant differences are marked as *$p<0.05$ compared to the control and ▽$p<0.01$ compared to METH treatment. **b** ILK silencing in bEnd.3 cells at 6 days of infection (**$p<0.01$ and ***$p<0.0001$, compared to the respective non-silenced cells, pLKO.1). **c** Zymography performed in bEnd.3 culture medium after METH and/or ALC treatment in ILK knockdown cells (KD ILK) and control cells (pLKO.1) (***$p<0.001$ for pLKO.1 vs pLKO.1/METH, ▽▽▽$p<0.001$ for KD ILK vs KD ILK/METH and ▽▽$p<0.01$ for pLKO.1 vs KD ILK/METH and pLKO.1/ALCMETH). Data represent mean±SEM. All significant differences were determined by ANOVA followed by the Bonferroni post hoc test

have shown that ALC promotes microtubule stabilization which can render the cells more resistant to insults [30].

Different mechanisms have been proposed for the lack of BBB tightness after METH exposure [3, 4, 10, 11, 13, 15]. Among those, the activation and expression of MMPs, a common mechanism of BBB leakiness, was often referred after METH exposure [4, 6, 9]. Based on previous reports where L-carnitine was seen to decrease glomerular sclerosis and interstitial fibrosis after cisplatin treatment, by reducing MMP-9 activity [46], and ALC administration was shown to ameliorate MMP-related dystrophy [47], we hypothesized that ALC could prevent METH-induced MMPs activity contributing this way to maintain the integrity of the endothelial monolayer. Increased MMP-9 activity after METH exposure was previously reported in brain regions associated to the reward system [6, 9]. MMPs are proteolytic enzymes involved in the remodeling and cleavage of the extracellular matrix known to degrade TJ proteins. Our zymography results show that both METH 0.5 and 1 mM doses triggered the activity of MMP-9, but not of MMP-2. This is in accordance with former in vivo studies that reported a rapid transient increase in striatal MMP-9 expression and activity after repeated low

doses of METH, which was associated with increased degradation of extracellular matrix components and increased BBB permeability [4, 6, 9, 48]. As hypothesized, ALC 1 mM was able to prevent MMP-9 increased activity in cells exposed to METH, which prevented changes on F-actin alignment and reduced claudin-5 redistribution, contributing to maintain the integrity of the endothelial cytoskeleton. These results open new insights into ALC therapeutic use.

Another possible mechanism for METH-induced damage at the BBB level is associated to increased production of ROS by endothelial cells [3, 10, 13, 29]. In a former study, it was proposed that increased oxidative stress in METH-treated endothelial cells could lead to cytoskeleton rearrangement and TJ redistribution through RhoA activation [10]. Modulation of RhoGTPases by METH has been reported showing that RhoA, Rac, or Cdc42 can be modulated by METH, impacting the endothelial barrier [10, 13, 14]. Constitutive activation of RhoGTPases was associated with TJ endocytosis and stress fibers assembly and reorganization [14, 49, 50]. Rho-associated coiled-coil-containing kinases (ROCK) are important cytoskeleton regulators through downstream modulation of actin, myosin, and associated proteins [10, 49–51]. Previous studies have shown the involvement of the Rho/ROCK pathway on actin reorganization and verified that ROCK inhibition was able to block actin disruption [50, 52]. Aiming to evaluate the role of ROCK on METH-induced structural damage, we used the ROCK selective inhibitor fasudil. However, ROCK inhibition did not prevent METH-induced disruption of F-actin organization and led to a highly disturbed structural pattern (Online Resource 1). The influence of RhoGTPases activation and/or inactivation on TJ function is ambiguous. In Madin-Darby canine kidney (MDCK) epithelial cells expressing constitutively active or dominant-negative RhoA, Rac1, or Cdc42, it was shown that activation, as well as inactivation, of each GTPase resulted in increased paracellular permeability and dramatic reorganization of the F-actin cytoskeleton and TJ proteins [49], evidencing that Rho GTPases in epithelial junctions may regulate the barrier function through distinct mechanisms.

Several possible mechanisms were proposed for METH-triggered MMP-9 activity, involving different signaling cascades depending on stimulus, cell type, and MMP isoform [6, 53]. Mechanisms related with METH-induce glutamate [6] or dopamine [54] release are plausible in vivo, but not feasible in our bEnd.3 model. Increased phosphorylation of p38, JNK1/2, and/or ERK1/2 proteins leading to higher transcription of MMPs was also suggested [4, 47, 53]. Importantly, JNK1/2 and p38 were both reported to suffer increased phosphorylation after METH exposure in vivo [11] and decreased phosphorylation after ALC administration [47]. However, in the present study, we could not observe increased MMP transcription as a consequence of METH exposure (Online Resource 2), suggesting that METH-triggered MMP-9 activity may occur through posttranslational processes.

Cell adhesion to the extracellular matrix is an important process controlling cell shape change, migration, proliferation, survival, and differentiation. Recent studies have revealed that cytoplasmic integrin-linked kinase (ILK) and its interactive proteins play important roles in these processes [55]. ILK is directly binded to the cytoplasmic domains of β1 integrin and connects integrins to the actin cytoskeleton by interacting directly with several proteins such as paxillin and parvin, thus, coordinating actin organization [55, 56]. There is evidence that ILK expression stimulates MMP-9 activation, whereas ILK silencing inhibits invasion in several carcinomas [56, 57]. In normal epithelial cells, the loss of cell–cell adhesion is the hallmark of ILK overexpression, due to the E-cadherin downregulation and nuclear translocation [58]. ILK overexpression and clustering results in the activation of a variety of intracellular signaling processes such as Akt phosphorylation and GSK-3 inhibition, which lead to the activation of the transcription factor AP-1 resulting in the MMP-9 potentiation [55, 57]. In the present work, we show that METH-triggered activation of MMP-9 is mediated by ILK overexpression, which, to our knowledge, was never shown before. Although it was suggested that ILK may upregulate MMP-9 by promoting MMP-9 overexpression, as already mentioned, we failed to observe METH-induced increased transcription of MMP-9 (Online Resource 2). However, other authors have also reported ILK-dependent increased MMP-9 activity in the absence of significant changes in its expression, suggesting that under ILK regulation, various pathways may be involved [58].

BBB impairment after METH exposure may exacerbate drug neurotoxicity and may contribute to the long-term neurodegeneration and cognitive deficits frequently reported. This may occur by increased extravasation of neurotoxic proteins and pro-inflammatory molecules across the barrier, as well as deficits in both transcellular and paracellular transports [7, 15]. We show also that ALC was effective in preventing the increased expression of ILK, thus preventing MMP-9 activation and preserving actin structure and TJ function. The present results support the potential of ALC in preserving the BBB integrity, which was already demonstrated in vivo, since it was shown that alcohol impairment on human brain endothelium is prevented by ALC treatment [28, 29]. Of note, our results highlight ILK as a new target for ALC therapeutic use. The ongoing development of selective inhibitors of both MMP-9 and ILK as potential pharmacologic targets in several diseases may benefit from ALC investigation particularly in the oncology field, where increased activity of MMPs is long known to be associated with tumor invasion and metastatic potential [59, 60].

Despite the protection obtained at the structural level, ALC was not able to prevent cell death and reduced viability in our bEnd.3 cultures exposed to METH 1 mM. In isolated endothelial cells, loss of viability under METH exposure can be

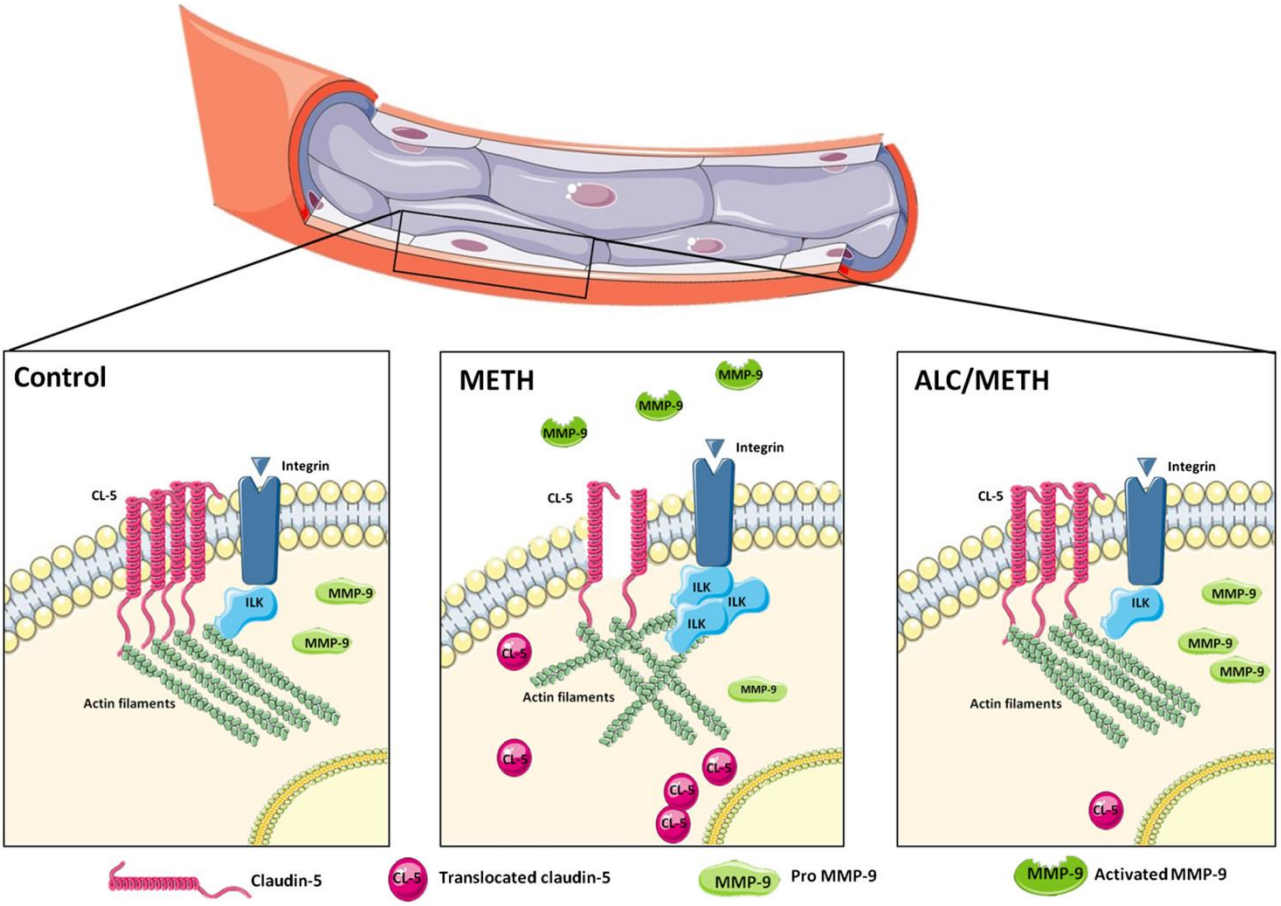

Fig. 7 Schematic representation of the ALC protective role over the molecular events triggered by METH in endothelial cells. Exposure to METH in bEnd.3 leads to disruption of the actin filaments arrangement and claudin-5 translocation to the cytoplasm (and decreased expression). We show that these events are mediated by MMP-9 activation in association with ILK overexpression and may lead to tight junction dysfunction and increased BBB permeability. Pretreatment with ALC prevented METH-induced activation of MMP-9 and preserved the arrangement of actin filaments and claudin-5 distribution. Our results highlight ILK as a nouvelle target for the ALC therapeutic use

associated with mitochondrial dysfunction caused by deficient antioxidant defense machinery accompanied by substantial lipid peroxidation, protein carbonylation, and increased ROS generation, which leads to disruption of the mitochondrial electrochemical gradient, impaired ATP synthesis, and energy deficits [for review, see 2]. In this scenario, cell death may arise as a consequence of METH-induced release of cytochrome c into the cytosol and resulting activation of caspase-mediated apoptotic pathways. The involvement of nitric oxide (NO) and peroxynitrite in METH-related apoptotic mechanisms has also been reported [61]. Moreover, it has been shown that, through ROS-signaling, METH can regulate the expression of AP-1, NF-κB, and AP-2 families that are crucial in controlling death and survival signals [for review, see 2]. Via JNK activation, ROS-signaling can also induce DNA strand break and base excision [62]. In addition, endothelial cells are important producers of several cytokines and release high amounts of interleukin-1 (IL-1) [63], which is known to be the major endogenous pyrogen [64]. Although we did not collect any data regarding METH-induced hyperthermia, changes in cellular morphology under METH exposure were shown to tightly correlate with hyperthermia and increased BBB permeability [65]. Noteworthy, we have shown in vivo that ALC neuroprotection over MDMA exposure is not related to the drug-induced thermal response [66]. We have also shown that in vivo ALC prevents DNA damage and carbonyl formation, but not lipid peroxidation [66]. Using a human endothelial cell line, other authors demonstrated that ALC prevents METH-induced loss of cell viability under glucose deprivation [67]. In such conditions, ALC may increase the availability of acyl-CoA to the citric acid cycle counteracting the decreased pyruvate dehydrogenase activity. However, under standard glucose levels, as in the present study, ALC protection against METH-induced cell loss was not shown. As such, we reason that the rate of cell loss observed for METH 1 mM is probably due to increased ROS/RNS-signaling at the mitochondrial level, through the activation of pathways that cannot be regulated by ALC.

Conclusion

In summary, we showed that in endothelial cells, exposure to METH led to disruption of actin filaments concomitant with claudin-5 translocation to the cytoplasm. These events seem to be mediated by MMP-9 activation in association with ILK overexpression and may lead to TJ dysfunction and BBB increased permeability. Our work was the first to assess the role of ALC as a neuroprotective agent over METH-induced damage via MMP-9 activity. Pretreatment with ALC prevented METH-induced activation of MMP-9, preserving claudin-5 location and the structural arrangement of the actin filaments (Fig. 7). Our results highlight ILK as a nouvelle target for ALC therapeutic use, adding to the list of ALC benefits in several neurologic conditions. Of note, this may be of particular interest in the oncology field due to the close relation between MMP-9 activity and metastatic events.

Acknowledgments This research project was funded by Programa Operacional Factores de Competitividade (COMPETE) and by National funds through FCT—Fundação para a Ciencia e Tecnologia, reference FCOMP-01-0124-FEDER-011320 (FCT PTDC/SAU-OSM/100630/2008). Joana Bravo received a research grant under this project. Teresa Summavielle was supported by Programa Ciência—Programa Operacional Potencial Humano (POPH)-Promotion of Scientific Employment, ESF and MCTES and program Investigador FCT, POPH and Fundo Social Europeu. We thank Glial Cell Biology Group as a whole and specially Dr Joana Paes Faria and Dr João Relvas for providing the lentivirus for shRNA-mediated silencing of ILK. We thank Dr Fátima Pina (INEB, University of Porto) for statistic advice in the analyses of the actin data. We thank Dr Maria José Oliveira (INEB, University of Porto) for her kind support regarding the zymography methodology. We also thank Dr Paula Sampaio and Paula Magalhães (IBMC Technical Services) for assistance with image analyses and cell culture facilities.

Conflict of Interest The authors declare that they have no conflict of interest.

References

1. Gold MS, Kobeissy FH, Wang KK, Merlo LJ, Bruijnzeel AW, Krasnova IN, Cadet JL (2009) Methamphetamine- and trauma-induced brain injuries: comparative cellular and molecular neurobiological substrates. Biol Psychiatry 66(2):118–127. doi:10.1016/j.biopsych.2009.02.021
2. Krasnova IN, Cadet JL (2009) Methamphetamine toxicity and messengers of death. Brain Res Rev 60(2):379–407. doi:10.1016/j.brainresrev.2009.03.002
3. Ramirez SH, Potula R, Fan S, Eidem T, Papugani A, Reichenbach N, Dykstra H, Weksler BB, Romero IA, Couraud PO, Persidsky Y (2009) Methamphetamine disrupts blood-brain barrier function by induction of oxidative stress in brain endothelial cells. J Cereb Blood Flow Metab 29(12):1933–1945. doi:10.1038/jcbfm.2009.112
4. Urrutia A, Rubio-Araiz A, Gutierrez-Lopez MD, ElAli A, Hermann DM, O'Shea E, Colado MI (2013) A study on the effect of JNK inhibitor, SP600125, on the disruption of blood-brain barrier induced by methamphetamine. Neurobiol Dis 50:49–58. doi:10.1016/j.nbd.2012.10.006
5. Bowyer JF, Thomas M, Schmued LC, Ali SF (2008) Brain region-specific neurodegenerative profiles showing the relative importance of amphetamine dose, hyperthermia, seizures, and the blood-brain barrier. Ann N Y Acad Sci 1139:127–139. doi:10.1196/annals.1432.005
6. Conant K, Lonskaya I, Szklarczyk A, Krall C, Steiner J, Maguire-Zeiss K, Lim ST (2011) Methamphetamine-associated cleavage of the synaptic adhesion molecule intercellular adhesion molecule-5. J Neurochem 118(4):521–532. doi:10.1111/j.1471-4159.2010.07153.x
7. Northrop NA, Yamamoto BK (2012) Persistent neuroinflammatory effects of serial exposure to stress and methamphetamine on the blood-brain barrier. J Neuroimmune Pharmacol 7(4):951–968. doi:10.1007/s11481-012-9391-y
8. Goncalves J, Baptista S, Martins T, Milhazes N, Borges F, Ribeiro CF, Malva JO, Silva AP (2010) Methamphetamine-induced neuroinflammation and neuronal dysfunction in the mice hippocampus: preventive effect of indomethacin. Eur J Neurosci 31(2):315–326. doi:10.1111/j.1460-9568.2009.07059.x
9. Martins T, Baptista S, Goncalves J, Leal E, Milhazes N, Borges F, Ribeiro CF, Quintela O, Lendoiro E, Lopez-Rivadulla M, Ambrosio AF, Silva AP (2011) Methamphetamine transiently increases the blood-brain barrier permeability in the hippocampus: role of tight junction proteins and matrix metalloproteinase-9. Brain Res 1411:28–40. doi:10.1016/j.brainres.2011.07.013
10. Mahajan SD, Aalinkeel R, Sykes DE, Reynolds JL, Bindukumar B, Adal A, Qi M, Toh J, Xu G, Prasad PN, Schwartz SA (2008) Methamphetamine alters blood brain barrier permeability via the modulation of tight junction expression: implication for HIV-1 neuropathogenesis in the context of drug abuse. Brain Res 1203:133–148. doi:10.1016/j.brainres.2008.01.093
11. ElAli A, Urrutia A, Rubio-Araiz A, Hernandez-Jimenez M, Colado MI, Doeppner TR, Hermann DM (2012) Apolipoprotein-E controls adenosine triphosphate-binding cassette transporters ABCB1 and ABCC1 on cerebral microvessels after methamphetamine intoxication. Stroke 43(6):1647–1653. doi:10.1161/STROKEAHA.111.648923
12. Haorah J, Knipe B, Leibhart J, Ghorpade A, Persidsky Y (2005) Alcohol-induced oxidative stress in brain endothelial cells causes blood-brain barrier dysfunction. J Leukoc Biol 78(6):1223–1232. doi:10.1189/jlb.0605340
13. Toborek M, Seelbach MJ, Rashid CS, András IE, Chen L, Park M, Esser KA (2013) Voluntary exercise protects against methamphetamine-induced oxidative stress in brain microvasculature and disruption of the blood-brain-barrier. Mol Neurodegener 8(1):22. doi:10.1186/1750-1326-8-22
14. Park M, Kim HJ, Lim B, Wylegala A, Toborek M (2013) Methamphetamine-induced occludin endocytosis is mediated by the Arp2/3 complex-regulated actin rearrangement. J Biol Chem 288(46):33324–33334. doi:10.1074/jbc.M113.483487
15. Martins T, Burgoyne T, Kenny B-A, Hudson N, Futter CE, Ambrósio AF, Silva AP, Greenwood J, Turowski P(2013) Methamphetamine-induced nitric oxide promotes vesicular trasnport in blood-brain barrier endothelial cells. Neuropharmacol (65):74-82. doi:10.1016/j.neuropharm.2012.08.021
16. Balda MS, Whitney JA, Flores C, González S, Cereijido M, Matter K (1996) Functional dissociation of paracellular permeability and transepithelial electrical resistance and disruption of the apical-basolateral intermembrane diffusion barrier by expression of a mutant tight junction membrane protein. J Cell Biol 134(4):1031–1049
17. Chen F, Hori T, Ohashi N, Baine AM, Eckman CB, Nguyen JH (2011) Occludin is regulated by epidermal growth factor receptor activation in brain endothelial cells and brains of mice with acute liver failure. Hepatology 53(4):1294–1305. doi:10.1002/hep.24161
18. Yamamoto M, Ramirez SH, Sato S, Kiyota T, Cerny RL, Kaibuchi K, Persidsky Y, Ikezu T (2008) Phosphorylation of claudin-5 and

occludin by rho kinase in brain endothelial cells. Am J Pathol 172(2): 521–533. doi:10.2353/ajpath.2008.070076
19. Muresan Z, Paul DL, Goodenough DA (2000) Occludin 1B, a Variant of the Tight Junction Protein Occludin. Mol Biol Cell 11: 627-634
20. Reynolds JL, Mahajan SD, Aalinkeel R, Nair B, Sykes DE, Schwartz SA (2011) Methamphetamine and HIV-1 gp120 effects on lipopolysaccharide stimulated matrix metalloproteinase-9 production by human monocyte-derived macrophages. Immunol Invest 40(5):481–497. doi:10.3109/08820139.2011.559499
21. Liebner S, Kniesel U, Kalbacher H, Wolburg H (2000) Correlation of tight junction morphology with the expression of tight junction proteins in blood-brain barrier endothelial cells. Eur J Cell Biol 79(10):707–717. doi:10.1078/0171-9335-00101
22. Kashiwamura Y, Sano Y, Abe M, Shimizu F, Haruki H, Maeda T, Kawai M, Kanda T (2011) Hydrocortisone enhances the function of the blood-nerve barrier through the up-regulation of claudin-5. Neurochem Res 36(5):849–855. doi:10.1007/s11064-011-0413-6
23. Masahiko I, Kazumasa M, Schoichiro T (1999) Characterization of ZO-2 as a MAGUK family member associated with tight as well as adherens junctions with a binding affinity to occludin and a catenin. J Biol Chem 274(26):5981–5986
24. Singh AB, Harris RC (2004) Epidermal growth factor receptor activation differentially regulates claudin expression and enhances transepithelial resistance in Madin-Darby canine kidney cells. J Biol Chem 279(5):3543–3552. doi:10.1074/jbc.M308682200
25. Forster C, Burek M, Romero IA, Weksler B, Couraud PO, Drenckhahn D (2008) Differential effects of hydrocortisone and TNFalpha on tight junction proteins in an in vitro model of the human blood-brain barrier. J Physiol 586(7):1937–1949. doi:10.1113/jphysiol.2007.146852
26. Young EJ, Aceti M, Griggs EM, Fuchs RA, Zigmond Z, Rumbaugh G, Miller CA (2014) Selective, retrieval-independent disruption of methamphetamine-associated memory by actin depolymerization. Biol Psychiatry 75(2):96–104. doi:10.1016/j.biopsych.2013.07.036
27. Mizoguchi H, Yamada K, Nabeshima T (2011) Matrix metalloproteinases contribute to neuronal dysfunction in animal models of drug dependence, Alzheimer's disease, and epilepsy. Biochem Res Int 2011:681385. doi:10.1155/2011/681385
28. Abdul Muneer PM, Alikunju S, Szlachetka AM, Haorah J (2011) Inhibitory effects of alcohol on glucose transport across the blood-brain barrier leads to neurodegeneration: preventive role of acetyl-L: -carnitine. Psychopharmacology (Berl) 214(3):707–718. doi:10.1007/s00213-010-2076-4
29. Haorah J, Floreani NA, Knipe B, Persidsky Y (2011) Stabilization of superoxide dismutase by acetyl-l-carnitine in human brain endothelium during alcohol exposure: novel protective approach. Free Radic Biol Med 51(8):1601–1609. doi:10.1016/j.freeradbiomed.2011.06.020
30. Pettegrew J, Levine J, McClure R (2000) Acetyl-L-carnitine physical-chemical, metabolica, and therapeutic properties: relevance for its mode of action in Alzheimer's disease and geriatric depression. Mol Psych 5:616–632
31. Jones LL, McDonald DA, Borum PR (2010) Acylcarnitines: role in brain. Prog Lipid Res 49(1):61–75. doi:10.1016/j.plipres.2009.08.004
32. Goo MJ, Choi SM, Kim SH, Ahn BO (2012) Protective effects of acetyl-L-carnitine on neurodegenarative changes in chronic cerebral ischemia models and learning-memory impairment in aged rats. Arch Pharm Res 35(1):145–154. doi:10.1007/s12272-012-0116-9
33. Lee NY, Choi HO, Kang YS (2012) The acetylcholinesterase inhibitors competitively inhibited an acetyl L-carnitine transport through the blood-brain barrier. Neurochem Res 37(7):1499–1507. doi:10.1007/s11064-012-0723-3
34. Yasuto K, Ikumi T, Aki O, Yoshimichi S, Toru K, Jun-ichi N, Hiroko N, Noriyoshi H, Masahide A, Akira T (2001) Functional relevance of carnitine transporter OCTN2 to brain distribution of L-carnitine and acetyl-L-carnitine across the blood-brain barrier. J Neurochem 79: 959–969
35. Kusuhara H, Sugiyama Y (2005) Active efflux across the blood-brain barrier: role of the solute carrier family. ASENT 2:73–85
36. Rump TJ, Abdul Muneer PM, Szlachetka AM, Lamb A, Haorei C, Alikunju S, Xiong H, Keblesh J, Liu J, Zimmerman MC, Jones J, Donohue TM Jr, Persidsky Y, Haorah J (2010) Acetyl-L-carnitine protects neuronal function from alcohol-induced oxidative damage in the brain. Free Radic Biol Med 49(10):1494–1504. doi:10.1016/j.freeradbiomed.2010.08.011
37. Brown RC, Morris AP, O'Neil RG (2007) Tight junction protein expression and barrier properties of immortalized mouse brain microvessel endothelial cells. Brain Res 1130(1):17–30. doi:10.1016/j.brainres.2006.10.083
38. Omidi Y, Campbell L, Barar J, Connell D, Akhtar S, Gumbleton M (2003) Evaluation of the immortalised mouse brain capillary endothelial cell line, b.End3, as an in vitro blood–brain barrier model for drug uptake and transport studies. Brain Res 990(1–2):95–112. doi:10.1016/s0006-8993(03)03443-7
39. Jin CH, Moo TT, Youn CS, Sun YJ, Joo-Il K, Sook HE, Onyou H (2002) Methamphetamine-induced apoptosis in a CNS-derived catecholaminergic cell line. Mol Cells 13(2):221–227
40. Huang H, Liu N, Guo H, Liao S, Li X, Yang C, Liu S, Song W, Liu C, Guan L, Li B, Xu L, Zhang C, Wang X, Dou QP, Liu J (2012) L-carnitine is an endogenous HDAC inhibitor selectively inhibiting cancer cell growth in vivo and in vitro. PLoS One 7(11):e49062. doi:10.1371/journal.pone.0049062
41. Wojtowicz-Praga SM, Dickson RB, Hawkins MJ (1997) Matrix metalloproteinase inhibitors. Investig New Drugs 15:61–75
42. Doug L (2000) Comparison of the LDH and MTT assays for quantifying cell death: validity for neuronal apoptosis? J Neurosc Meth 96:147–152
43. Nekouzadeh A, Genin GM (2011) Quantification of fibre polymerization through Fourier space image analysis. Proc Math Phys Eng Sci 467(2132):2310–2329. doi:10.1098/rspa.2010.0623
44. Shamloo A (2014) Cell-cell interactions mediate cytoskeleton organization and collective endothelial cell chemotaxis. Cytoskeleton (Hoboken). doi:10.1002/cm.21185
45. Shen L, Turner JR (2005) Actin depolymerization disrupts tight junctions via caveolae-mediated endocytosis. Mol Biol Cell 16(9): 3919–3936. doi:10.1091/mbc.E04-12-1089
46. Martinez G, Costantino G, Clementi A, Puglia M, Clementi S, Cantarella G, De Meo L, Matera M (2009) Cisplatin-induced kidney injury in the rat: L-carnitine modulates the relationship between MMP-9 and TIMP-3. Exp Toxicol Pathol 61(3):183–188. doi:10.1016/j.etp.2008.07.004
47. Hnia K, Hugon G, Rivier F, Masmoudi A, Mercier J, Mornet D (2007) Modulation of p38 mitogen-activated protein kinase cascade and metalloproteinase activity in diaphragm muscle in response to free radical scavenger administration in dystrophin-deficient Mdx mice. Am J Pathol 170(2):633–643. doi:10.2353/ajpath.2007.060344
48. Abdul Muneer PM, Alikunju S, Szlachetka AM, Haorah J (2012) The mechanisms of cerebral vascular dysfunction and neuroinflammation by MMP-mediated degradation of VEGFR-2 in alcohol ingestion. Arterioscler Thromb Vasc Biol 32(5):1167–1177. doi:10.1161/ATVBAHA.112.247668
49. Bruewer M, Hopkins AM, Hobert ME, Nusrat A, Madara JL (2004) RhoA, Rac 1, and Cdc42 exert distinct effects on epithelial barrier via selective strictural and biochemical modulation on junctional proteins and F-actin. Am J Physiol Cell Physiol 287:C327-C335
50. Breyer J, Samarin J, Rehm M, Lautscham L, Fabry B, Goppelt-Struebe M (2012) Inhibition of Rho kinases increases directional

motility of microvascular endothelial cells. Biochem Pharmacol 83(5):616–626. doi:10.1016/j.bcp.2011.12.012
51. Tonges L, Koch JC, Bahr M, Lingor P (2011) ROCKing regeneration: Rho kinase inhibition as molecular target for neurorestoration. Front Mol Neurosci 4:39. doi:10.3389/fnmol.2011.00039
52. Weiner JA, Fukushima N, Contos JJ, Scherer SS, Chun J (2001) Regulation of Schwann cell morphology and adhesion by receptor-mediated lysophosphatidic acid signaling. J Neurosc 21(18):7069–7078
53. Elke G, Katrin H, Yvette N, Hermann H (2000) Sustained ERK phosphorylation is necessary but not sufficient for MMP-9 regulation in endothelial cells: involvement of Ras-dependent and -independent pathways. J Cell Sci 113:4319–4330
54. Betzen C, White R, Zehendner CM, Pietrowski E, Bender B, Luhmann HJ, Kuhlmann CR (2009) Oxidative stress upregulates the NMDA receptor on cerebrovascular endothelium. Free Radic Biol Med 47(8):1212–1220. doi:10.1016/j.freeradbiomed.2009.07.034
55. Wu C, Dedhar S (2001) Integrin-linked kinase (ILK) and its interactors: a new paradigm for the coupling of extracellular matrix to actin cytoskeleton and signaling complexes. J Cell Biol 155(4):505–510. doi:10.1083/jcb.200108077
56. Rosano L, Spinella F, Di Castro V, Dedhar S, Nicotra MR, Natali PG, Bagnato A (2006) Integrin-linked kinase functions as a downstream mediator of endothelin-1 to promote invasive behavior in ovarian carcinoma. Mol Cancer Ther 5(4):833–842. doi:10.1158/1535-7163.MCT-05-0523
57. Troussard AA, Costello P, Yoganathan EN, Kumagai S, Roskelley CD, Dedhar S (2000) The integrin linked kinase (ILK) induces an invasive phenotype via AP-1 transcription factor-dependent upregulation of matrix metalloproteinase 9 (MMP-9). Oncogene 19:5444–5452
58. Matsui Y, Assi K, Ogawa O, Raven PA, Dedhar S, Gleave ME, Salh B, So AI (2012) The importance of integrin-linked kinase in the regulation of bladder cancer invasion. Int J Cancer 130(3):521–531. doi:10.1002/ijc.26008
59. Johnsen M, Lund RL, Romer J, Almholt K, Danø K (1998) Cancer invasion and tissue remodeling: common themes in proteolytic matrix degradation. Curr Opin Cell Biol 10:667–671
60. Murphy G, Ward R, Hembry RM, Reynolds JJ, Kuhn K, Tryggvason K (1989) Characterization of gelatinase from pig polymorphonuclear leucocytes. Biochem J 258:463–472
61. Sheng P, Cerruti C, Ali S, Cadet JL (1996) Nitric oxide is a mediator of methamphetamine (METH)-induced neurotoxicity. In vitro evidence from primary cultures of mesencephalic cells. Ann N Y Acad Sci 801:174–186
62. Barzilai A (2007) The contribution of the DNA damage response to neuronal viability. Antioxid Redox Signal 9(2):211–218. doi:10.1089/ars.2007.9.ft-6
63. Mantovani A, Bussolino F, Dejana E (1992) Cytokine regulation of endothelial cell function. FASEB J 6(8):2591–2599
64. Leon LR (2002) Invited review: cytokine regulation of fever: studies using gene knockout mice. J Appl Physiol (1985) 92(6):2648–2655. doi:10.1152/japplphysiol.01005.2001
65. Sharma HS, Kiyatkin EA (2009) Rapid morphological brain abnormalities during acute methamphetamine intoxication in the rat: an experimental study using light and electron microscopy. J Chem Neuroanat 37(1):18–32. doi:10.1016/j.jchemneu.2008.08.002
66. Alves E, Binienda Z, Carvalho F, Alves CJ, Fernandes E, de Lourdes BM, Tavares MA, Summavielle T (2009) Acetyl-L-carnitine provides effective in vivo neuroprotection over 3,4-methylenedioximethamphetamine-induced mitochondrial neurotoxicity in the adolescent rat brain. Neuroscience 158(2):514–523. doi:10.1016/j.neuroscience.2008.10.041
67. Abdul Muneer PM, Alikunju S, Szlachetka AM, Murrin LC, Haorah J (2011) Impairment of brain endothelial glucose transporter by methamphetamine causes blood-brain barrier dysfunction. Mol Neurodegener 6:23. doi:10.1186/1750-1326-6-23

CHAPTER III

Methamphetamine promotes α-tubulin deacetylation in endothelial cells: the protective role of Acetyl-L-Carnitine

Toxicology Letters, 234 (2015), 131-138

“Follow your heart but take your brain with you.”

(unknown author)

Toxicology Letters 234 (2015) 131–138

Contents lists available at ScienceDirect

Toxicology Letters

journal homepage: www.elsevier.com/locate/toxlet

Methamphetamine promotes α-tubulin deacetylation in endothelial cells: The protective role of acetyl-L-carnitine

S. Fernandes [a,b,c,d], S. Salta [a,b,c], T. Summavielle [*,a,b,c]

[a] Rua Alfredo Allen, Instituto de Investigação e Inovação em Saúde, Universidade do Porto, 4200-135 Porto, Portugal
[b] Rua do Campo Alegre, 823, Addiction Biology Group, Instituto de Biologia Molecular e Celular (IBMC), Universidade do Porto, 4150-180 Porto, Portugal
[c] Rua Valente Perfeito, 322, School of Allied Health Sciences – Polytechnic Institute of Porto (ESTSP-IPP), 4400-330 Vila Nova de Gaia, Portugal
[d] Alameda Prof. Hernâni Monteiro, Faculdade de Medicina da Universidade do Porto (FMUP), 4200-319 Porto, Portugal

HIGHLIGHTS

- Methamphetamine induces α-tubulin deacetylation in endothelial cells.
- Acetyl-L-carnitine prevents methamphetamine-induced deacetylation of microtubules.
- Acetyl-L-carnitine modulates the activity of HDACs at the post translational level.

ARTICLE INFO

Article history:
Received 19 December 2014
Received in revised form 16 February 2015
Accepted 17 February 2015
Available online 19 February 2015

Keywords:
Cytoskeleton
α-Tubulin
Methamphetamine
Acetyl-L-carnitine
Histone deacetylase

ABSTRACT

Methamphetamine (METH) is a powerful psychostimulant drug used worldwide for its reinforcing properties. In addition to the classic long-lasting monoaminergic-disrupting effects extensively described in the literature, METH has been consistently reported to increase blood brain barrier (BBB) permeability, both *in vivo* and *in vitro*, as a result of tight junction and cytoskeleton disarrangement. Microtubules play a critical role in cell stability, which relies on post-translational modifications such as α-tubulin acetylation. As there is evidence that psychostimulants drugs modulate the expression of histone deacetylases (HDACs), we hypothesized that in endothelial cells METH-mediation of cytoplasmatic HDAC6 activity could affect tubulin acetylation and further contribute to BBB dysfunction. To validate our hypothesis, we exposed the bEnd.3 endothelial cells to increasing doses of METH and verified that it leads to an extensive α-tubulin deacetylation mediated by HDACs activation. Furthermore, since we recently reported that acetyl-L-carnitine (ALC), a natural occurring compound, prevents BBB structural loss in a context of METH exposure, we reasoned that ALC could also preserve the acetylation of microtubules under METH action. The present results confirm that ALC is able to prevent METH-induced deacetylation providing effective protection on microtubule acetylation. Although further investigation is still needed, HDACs regulation may become a new therapeutic target for ALC.

1. Introduction

Methamphetamine (METH) is a powerful psychostimulant used worldwide for its reinforcing properties that leads to long-lasting deleterious effects (Gold et al., 2009; Krasnova and Cadet, 2009). METH toxicity is characterized by the disruption of the dopaminergic system, concomitant with terminal degeneration and eventual neuronal death (Conant et al., 2011; Krasnova and Cadet, 2009). However, METH has been increasingly recognized to impact also the blood-brain-barrier (BBB), causing the release of inflammatory mediators and astrogliosis (Gold et al., 2009; Goncalves et al., 2010; Northrop and Yamamoto, 2012; Ramirez et al., 2009). METH-induced permeability at the BBB level has been consistently reported both *in vivo* and *in vitro* (Conant et al., 2011; Martins et al., 2011; Urrutia et al., 2013), as a result of tight junction and cytoskeleton disarrangement

* Corresponding author at: Addiction Biology Group, Instituto de Biologia Molecular e Celular (IBMC), Rua do Campo Alegre 823, 4150-180 Porto, Portugal. Tel.: +351 226 074 900.
E-mail addresses: silvia.fernandes@ibmc.up.pt (S. Fernandes), sofia.salta@ibmc.up.pt (S. Salta), tsummavi@ibmc.up.pt (T. Summavielle).

http://dx.doi.org/10.1016/j.toxlet.2015.02.011
0378-4274/

(Dietrich, 2009; Kousik et al., 2012; Park et al., 2013). In endothelial cells, METH was also shown to trigger nitric oxide (NO)-mediated transcytosis (Martins et al., 2013). Recently, we showed, also in endothelial cells, that exposure to METH leads to disruption of actin filaments concomitant with claudin-5 translocation to the cytoplasm, promoted by MMP-9 activation in association with ILK overexpression (Fernandes et al., 2014).

Similarly to the actin filaments, microtubules play a critical role in cell stability and dynamics. Proper regulation of microtubule components relies on post translational modifications such as α-tubulin acetylation (Hammond et al., 2008). Microtubule deacetylation is carried out by histone deacetylase (HDAC) 6, a class II HDAC and the class III HDAC sirtuin 2 (SIRT2), which form a complex that allows them to bind to tubulin (Hubbert et al., 2002; Nahhas et al., 2007; Sadoul et al., 2011; Yang and Seto, 2008). Of note, it was recently shown that interfering with HDAC6 is sufficient to prevent microtubule deacetylation (Gold et al., 2015). There is growing evidence that HDACs inhibition is strongly associated with decreased cell mobility, which is of particular interest in the oncology field (Hrabeta et al., 2014; Ocker and Schneider-Stock, 2007). Although there are several studies showing that METH and other psychostimulants affect the expression of HDACs (Cassel et al., 2006; Host et al., 2011; Martin et al., 2012; Omonijo et al., 2014), and in particular the expression of HDAC6 (Omonijo et al., 2014), the effect of METH in microtubules acetylation was not yet explored. Therefore, we hypothesized that METH-induced regulation of HDACs activity, and in particular of HDAC6, may also mediate the structural loss observed in METH-exposed endothelial cells. Moreover, since we recently showed that a pretreatment with acetyl-L-carnitine (ALC) was able to prevent METH-induced activation of MMP-9, preserving the actin structural arrangement in the endothelial cells (Fernandes et al., 2014), and ALC was shown to have the potential to interact with HDAC activity (Huang et al., 2012), we reasoned that ALC could also preserve the acetylation of microtubules under METH action. ALC is a natural occurring compound that was seen to be protective by different mechanisms in several neurological conditions, including BBB dysfunction (Alves et al., 2009; Haorah et al., 2011; Muneer et al., 2011; Pettegrew et al., 2000).

To verify our hypothesis, we exposed the endothelial cell line bEnd.3 to increasing doses of METH and evaluated the individual and combined action of METH and ALC on α-tubulin acetylation. Trichostatin A (TSA), a natural product isolated from *Streptomyces hygroscopicus* commonly used as an inhibitor of class I/II HDACs known to promote microtubule acetylation, was also assayed (Dompierre et al., 2007; Harrison and Dexter, 2013).

2. Material and methods

2.1. In vitro model and cell culture

The immortalized bEnd.3 cells are derived from mouse brains and known to mimic some of the BBB characteristics. The cell line bEnd.3 was obtained from ATCC (American Type Cell Culture-CRL-2299, Manassas, VA) and cultures were maintained in DMEM (1×)/Glutamax (GIBCO®, Life Technologies, Paisley, UK), containing 1% penicillin and streptomycin (GIBCO®, Life Technologies) and 10% fetal bovine serum (GIBCO®, Life Technologies). Purity of the cell line was checked using an anti-CD31 antibody (Abcam 7388, rat monoclonal, 1:1000), which showed 100% enrichment of cells on the adhesion marker. For immunocytochemistry, cells were plated on 24-well plates (80,000 cells/well) containing glass cover slips. To obtain protein extracts or mRNA, bEnd.3 cells were cultured in petri dishes (1 million of cells). Cell culture media was changed every 3 days until cells were confluent.

2.2. Drug regimen

ALC-hydrochloride was kindly provided by Sigma-Tau S.p.A (Pomezia, Italy). TSA was purchased from Promega (#G6560) and METH hydrochloride from Sigma–Aldrich (St. Louis, MO, Cat. M-8750).

Immortalized bEnd.3 cells at confluence were treated with 0.5 mM and 1 mM of METH. METH doses were predetermined in our laboratory in agreement with previous studies using METH in similar cell models (Fernandes et al., 2014; Jin et al., 2002). ALC 1 mM was added 30 min before METH. TSA was used in a 100 nM concentration. The selected TSA and ALC doses were previously shown to be safe for the cells and are below the range of doses previously used in similar works (Huang et al., 2012; Hubbert et al., 2002; Tu et al., 2014).

2.3. Immunostaining procedure

For immunocytochemistry, bEnd.3 cells were cultured on glass cover slips in 24 well plates until 90–100% confluence. Cells were then treated with 0.5 and 1 mM of METH in the presence or absence of 100 nM TSA or 1 mM ALC, for 24 h. To evaluate α-tubulin, cells were washed with PBS, fixed during 10 min in methanol and permeabilized in 0.1% Triton X-100 during 10 min. After a blocking of 45 min in 10% NGS (normal goat serum), cells were incubated overnight at 4 °C with respective primary antibodies – Mouse anti-α-tubulin (Sigma, clone AA13 IgG1, #T8203, 1:500) and Mouse anti-acetyl-α-tubulin (Sigma, clone 6-11B-1 IgG2b, #T7451, 1:500). For secondary antibody incubation we used Anti-Mouse IgG Alexa-Fluor 488® Conjugate (Life Technologies, #A11001, 1:1000) for acetylated form and Anti-Mouse IgG Alexa-Fluor 568® Conjugate (Life Technologies, #A11004, 1:1000) for total α-tubulin, for 1 h at room temperature in the dark. Coverslips were then mounted onto glass slides with immunomount (Fluorescent Mounting Medium, CA, USA) containing 4′,6-diamidino-2-phenylindole (DAPI), and then fluorescence microphotographs were captured using Axio Imager Z1 fluorescence microscope (Carl Zeiss, Germany).

2.4. Morphometric analysis

Changes observed in α-tubulin acetylation by immunofluorescence assays were evaluated using the Fiji Software version 2.0. A total of four independent experiments were performed. From each coverslip, ten images were blindly captured and analyzed through measurement of fluorescence intensity.

2.5. Protein expression analysis by western blot

Confluent bEnd.3 cells cultured in petri dishes were scrapped and lysed with TEN buffer (50 mM Tris–HCl, 2 mM EDTA, 150 mM NaCl, 1% NP-40, supplemented with phosphatases and proteases inhibitors) and then centrifuged at 14,000 × *g* for 15 min at 4 °C. Protein concentration of the cell lysate was estimated in the supernatant by the Bradford method (Bio-Rad Protein Assay, Munich, Germany). Proteins were loaded at 25 μg per lane and resolved by SDS-PAGE on 12% Bis/acrilamide gels and then transferred onto PVDF membranes. After blocking with dry milk 5%, membranes were incubated with mouse anti-acetyl-α-tubulin antibody (Sigma, clone 6-11B-1 IgG2b, #T7451,1:1600). Membranes were washed in Stripping Buffer (Restore™ Western Blot, Thermo Scientific) and then incubated with mouse anti-α-tubulin (Sigma, clone AA13 IgG1, #T8203, 1:1000). Secondary antibody HRP (horseradish peroxidase)-conjugated were used for 1 h of incubation. Chemiluminescent signal detection was achieved using the Immun-Star HRP kit (Bio-Rad Laboratories, USA). A

GS800 densitometer (Bio-Rad) and quantity one 1-D analysis software (v4.6, Bio-Rad) were used for densitometry analysis.

2.6. Measurement of HDACs I/II activity

Evaluation of HDACs activity was performed using HDAC-GloTM I/II Assay and Screening System kit (Promega, USA) following provided instructions. This luminescent assay measures relative activity of HDAC enzymes using an acetylated luminogenic peptide susbstrate. When cleaved the substrate is quantified in a reaction using Ultra-Glo™ Recombinant Luciferase. Briefly, in each well of 96 multiwell plates, 10,000 bEnd. 3 cells were seeded and treated with ALC and TSA in dilution series: ALC (from 2 mM to 0.125 mM), and TSA (from 500 nM to 3.9 nM). 24 h after treatment, medium was replaced by another without phenol red and HDAC buffer was added, followed by HDAC™ I/II reagent. After an incubation of 30 min, luminescence was measured (Gen5 Data Analysis Software, Biotek Instruments, Inc., Synergy 2 (Izasa).

2.7. Real time – PCR

Total RNA was extracted from confluent bEnd.3 cells grown in petri dishes, using RNeasy® Mini Kit (Qiagen, Hilden, Germany). RNA quality was checked by Experion automated electrophoresis system (Bio-Rad Hercules, CA, USA) and cDNA synthesis was performed by Qiagen RT^2 HT First Strand cDNA kit using 2.0 μg of RNA. RT^2 SYBR Green Mastermix was used to amplify and quantify genes expression on a cycler (Bio-Rad iQ5 model). Specific primers were designed for gene relative expression of CDKN1A (F: 5′TGACAGATTTCTATCACTCCAAG3′; R: 5′ TGACCCACAGCAGAAGAG3′) and HDAC6 (F: 5′GCAGGAGGCAAGTTGATT3′; R: 5′AAGAAGGGTGTGGAGTGA3′). Data were analyzed by ΔΔCT method after normalization to GUSB (F: 5′GGTGAAGGTGACAACAACT3′; R: 5′CTGAATCCTCGTGCTTATTGA3′) housekeeping gene expression.

2.8. Statistical analysis

Results from at least four independent experiments were represented as mean ± SEM. Significant differences between groups were determined by one-way ANOVA followed by the Sidak's post hoc test. Significance was set at $p < 0.05$. All analysis were conducted using the software GraphPad Prism® 6.0 for Mac OSX (GraphPad Software, La Jolla, CA).

3. Results

3.1. METH decreased α-tubulin acetylation

The present results show that METH decreased α-tubulin acetylation. Immunofluorescence assays were done for both total and acetylated forms of α-tubulin showing that when bEnd.3 cells were exposed to METH 1 mM, the amount of the acetylated form was significantly reduced ($p < 0.01$, Fig. 1a and c). No significant differences were seen in total α-tubulin (Fig. 1b). This was confirmed by western blot analysis where METH 1 mM reduced significantly the rate of acetylated α-tubulin after 24 h of treatment ($p < 0.001$, Fig. 1d).

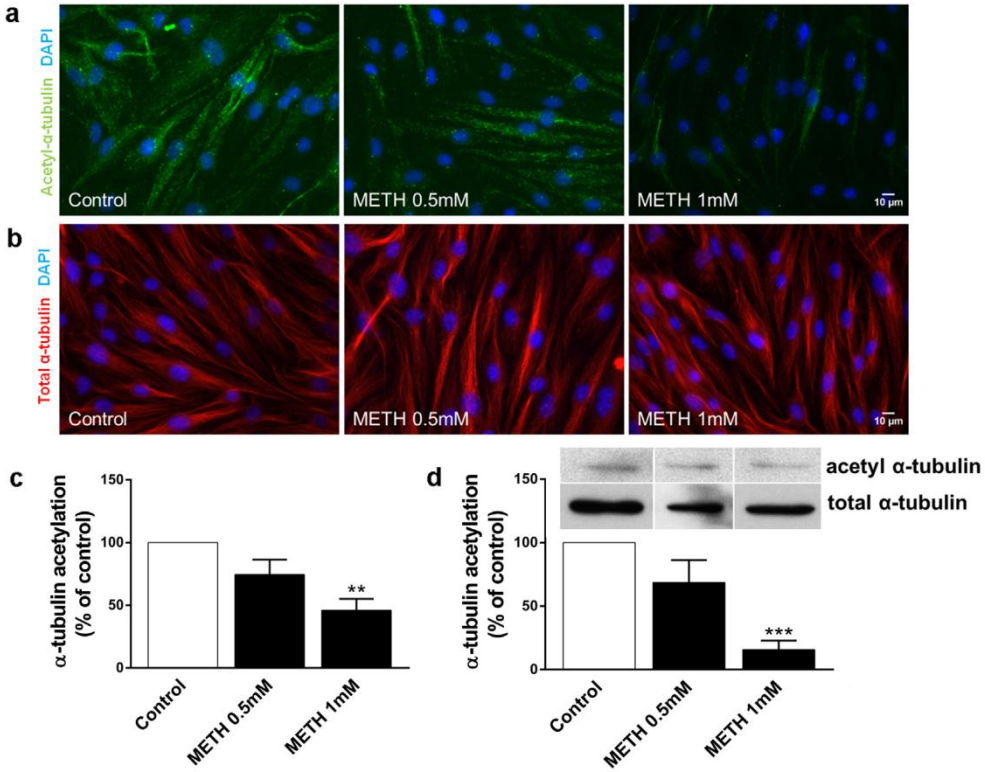

Fig. 1. Quantification of α-tubulin acetylation after METH exposure. Confluent bEnd.3 cells monolayers were treated with METH 0.5 mM and 1 mM doses according to the described procedures. Cells were stained for acetylated α-tubulin (a) and total α-tubulin (b). Nuclei were labeled with DAPI. Changes on acetylation, quantified through immunofluorescence intensity using the Fiji Software are shown in (c). Western blot was performed to assess the rate of acetylated α-tubulin, the results are represented in (d). A minimum of five independent experiments were performed. Results were expressed as mean ± SEM. $^{**}p < 0.01$ and $^{***}p < 0.001$ compared to the control group (as determined by ANOVA followed by the Sidak's post-hoc test).

3.2. ALC effectively prevented METH-induced α-tubulin deacetylation

In the present study, we addressed the effect of ALC in preventing METH-induced deacetylation. Since HDAC6 is responsible for the α-tubulin deacetylation, we used a preselected dose of TSA (see Fig. 3a), a strong inhibitor of HDACs activity. Both ALC and TSA were able to counteract METH-induced deacetylation, as shown in Fig. 2a and b. Our results show that cytoskeleton tubulin from cells pretreated with 1 mM ALC is partially protected from METH-induced damage (Fig. 2a and b, $p < 0.05$, METH 1 mM *vs.* ALC/METH 1 mM). As expected, cells treated simultaneously with TSA and METH presented significantly increased acetylation as shown in Fig. 2b ($p < 0.001$, TSA/METH 1 mM *vs.* METH 1 m or *vs.* the control group). TSA by itself also led to a strong increase in α-tubulin acetylation ($p < 0.001$, TSA *vs.* control 100 nM). Further testing through western blot analysis confirmed these results. TSA 100 nM alone or in combination with METH, resulted in a strong acetylation of α-tubulin compared to the control cells or to METH-exposed cells (Fig. 2a–c, $p < 0.001$ for control *vs.* TSA 100 nM, control *vs.* TSA/METH 1 mM, and METH 1 mM *vs.* TSA/METH 1 mM). Pretreatment with ALC 1 mM was also seen to be effective in preventing METH-induced deacetylation (Fig. 2c, $p < 0.05$, METH 1 mM *vs.* ALC/METH 1 mM). ALC by itself did not significantly differ from the control (Fig. 2b and c, $p = 0.42$).

3.3. ALC is not an effective HDACs inhibitor

Next, we investigated if ALC could act as a HDACs inhibitor. The effect of TSA, a strong inhibitor of HDACs was also assessed. As represented in Fig. 3a, a dose of 100 nM TSA inhibits half of the HDACs activity, while a dose of 500 nM reduced activity to near 20%. ALC, however does not seem to be able to prevent HDACs activity (Fig. 3b), the 1 mM dose seems to provide a slight reduction of HDACs activity, but fails to reach significance ($p = 0.513$, ALC 1 mM *vs.* control).

3.4. ALC prevents METH-induced decrease in CDKN1A gene expression

As ALC does not seem to act as a HDACs inhibitor, we investigated if it could act by down-regulation of HDAC6 expression levels. However, as represented in Fig. 4a, the expression of the HDAC6 gene was not affected by METH or ALC, which seems to indicate that METH modulation of HDAC6 occurs at a post-translational level.

A common marker of HDACs activity is the inhibition of CDKN1A gene expression due to chromatin remodeling and condensation (Xu et al., 2007). To evaluate the effect of METH and ALC over HDACs activity, we used RT-PCR to assess CDKN1A gene expression levels. As expected based on the effects described in Sections 3.1 and 3.2, METH-exposure induced a down-

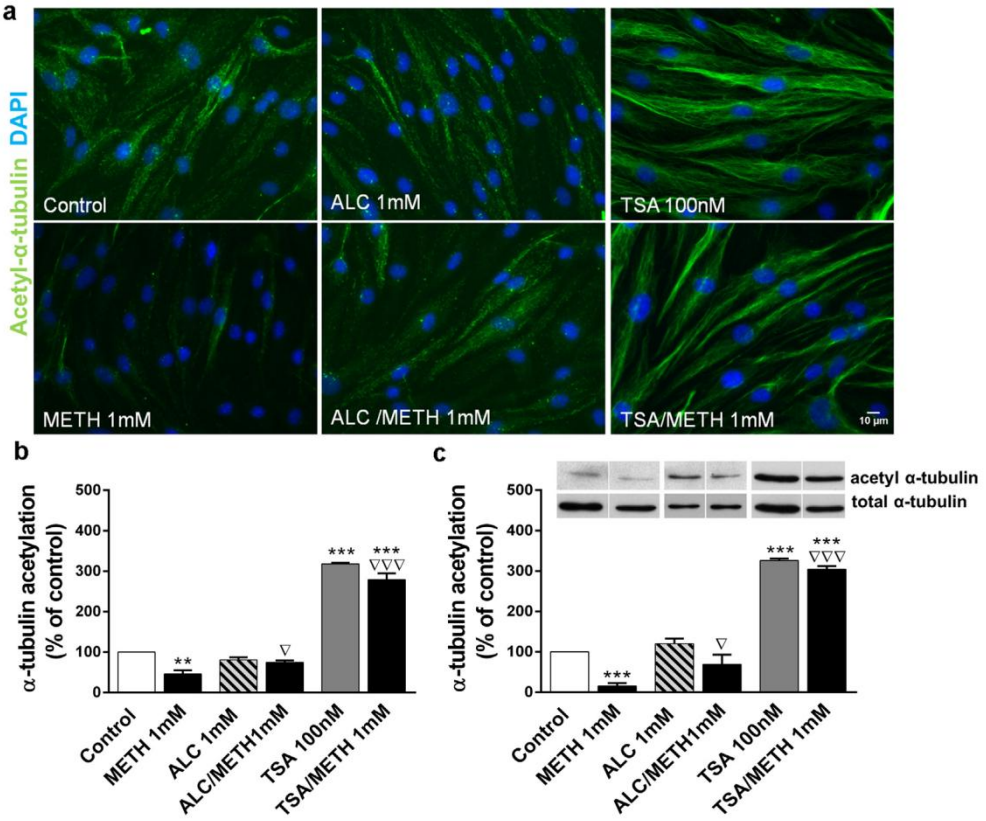

Fig. 2. Quantification of α-tubulin acetylation in cells pretreated with ALC. Confluent bEnd.3 cells monolayers were treated with METH 1 mM for 24 h, with or without a pretreatment of 1 mM ALC. TSA in a dose of 100 nM, alone or in combination with 1 mM METH was used as positive control. Cells were stained for acetylated α-tubulin and the nuclei were labeled with DAPI (a). Changes on acetylation were quantified through immunofluorescence intensity using the Fiji Software, and are represented in (b). Western blot was performed to assess the percentage of α-tubulin acetylation in each condition. The obtained results are represented in (c). A minimum of five independent experiments was performed. Results were expressed as the mean ± SEM. $^{**}p < 0.01$ and $^{***}p < 0.001$ compared to control group; $\triangledown p < 0.05$ and $\triangledown\triangledown\triangledown p < 0.001$ compared to METH-treated cells (as determined by ANOVA followed by Sidak's post-hoc test).

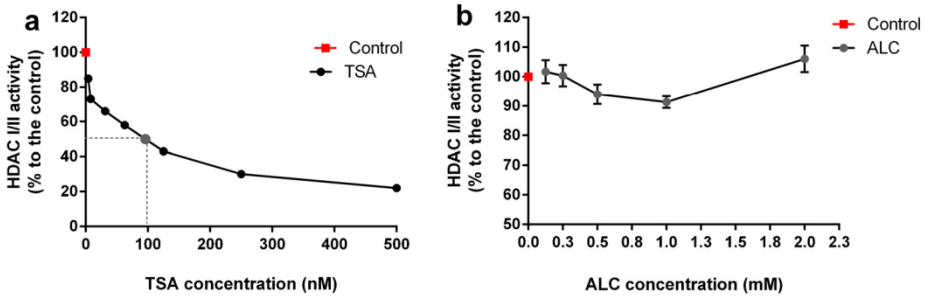

Fig. 3. Quantification of HDACs I/II class activity. Confluent bEnd.3 cells monolayers were treated with TSA in a dose ranging from from 3.9 nM to 500 nM (a) and ALC in doses ranging from 0.125 mM to 2 mM (b). HDACs I/II activity was assessed using HDAC-Glo™ I/II Assay and Screening System kit (Promega, USA) following provided instructions. Samples of ALC treated cells were evaluated in triplicate and results were measured through luminescence signal and are expressed as mean ± SEM. TSA was used as a well-known inhibitor of class I/II HDACs.

regulation of the CDKN1A gene (shown in Fig. 4b, $p < 0.001$, control *vs.* METH 1 mM). TSA on the contrary, led to an up-regulation of the CDKN1A gene (Fig. 4b, $p < 0.05$, control *vs.* TSA 100 nM) and prevents the down-regulation induced by METH (Fig. 4b, $p < 0.001$ METH 1 mM *vs.* TSA/METH 1 mM). Importantly, although ALC by itself did not affect the expression of the CDKN1A gene, a pretreatment with ALC was effective in preventing METH-induced CDKN1A down-regulation (Fig. 4b, $p < 0.001$, METH *vs.* ALC/METH 1 mM).

4. Discussion

The present work shows that METH considerably reduces α-tubulin acetylation in endothelial cells, which is likely to impact cytoskeleton stability, cell motility and polarity, and vesicle transport (Hubbert et al., 2002; Matsuyama et al., 2002). Importantly, we show that ALC partially prevents METH-induced deacetylation, protecting the endothelial cells and consequently preserving the BBB function.

Cytoskeleton microtubules are regulated by several types of conserved post-translational modifications (Song and Brady, 2014). Although the biological meaning of such mechanisms is still poorly understood, it was reported that tubulin acetylation increases its stability and half-life, rendering microtubules more resistant to drug-induced depolymerization and disassembly (Matsuyama et al., 2002; Szyk et al., 2014). Previous studies showed that METH impacts actin filaments, leading to actin depolymerization, altered cell shape and local accumulation of condensed actin, which may compromise TJs function and BBB integrity (Park et al., 2013; Young et al., 2014). Using the bEnd.3 endothelial cell model, we have previously shown that METH-exposure led to a dramatic loss of F-actin integrity concomitant with claudin-5 downregulation and redistribution (Fernandes et al., 2014). In endothelial cells, these changes at the cytoskeleton level may lead to loss of adhesion and/or relevant restructuring of the endothelium, thus contributing to METH neurotoxicity. Here, in addition, we show that METH reduces microtubule acetylation in endothelial cells. This effect is expected to contribute to BBB disruption, since it was previously shown that induced deacetylation of microtubules was associated with increased vascular permeability (Bogatcheva et al., 2007), while augmenting microtubule acetylation seems to be concomitant with the inhibition of barrier-disruptive pathways (Gorshkov et al., 2012; Saito et al., 2011).

HDACs modulation by psychostimulants was previously reported. Exposure of adult rats to METH led to altered expression patterns of several HDACs, including HDAC1 and HDAC2 (Jayanthi et al., 2014; Martin et al., 2012), and HDAC6, HDAC8-HDAC11, SIRT2, SIRT5 and SIRT6 (Omonijo et al., 2014). These expression patterns seem to depend on the METH dose and period of exposure. Similarly, cocaine self-administration was shown to induce increased expression of several HDACs (Host et al., 2011). In the present study, to verify if METH-induced deacetylation of α-tubulin was a result of HDACs modulation by METH, we used the

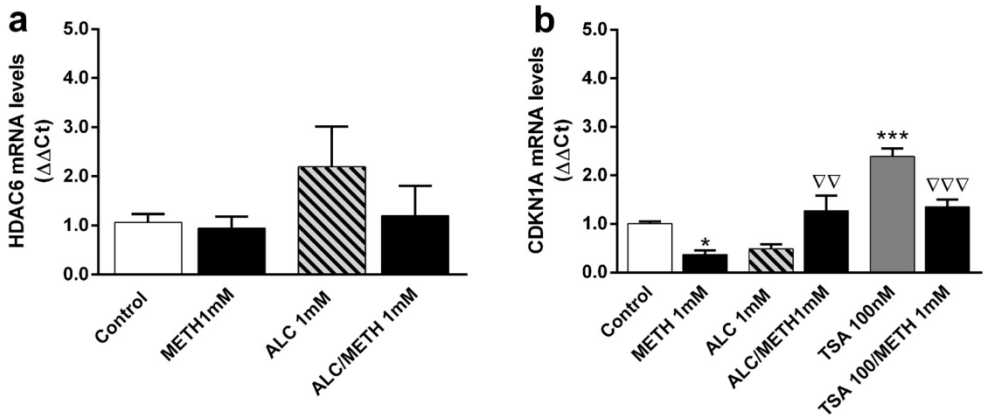

Fig. 4. Assessment of mRNA transcription. Confluent bEnd.3 cells monolayers were treated according to the described procedures. RNA was extracted from cultures treated with METH 1 mM, ALC 1 mM, TSA 100 nM or combinations of such treatments, control cultures did not receive any treatment. For each PCR a total of 2.0 μg RNA was used to determine gene expression of both HDAC6 (a) and CDKN1A (b). A total of four independent experiments were performed. Data normalization was made using GUSB gene expression. Results are expressed as mean ± SEM. $^{*}p < 0.05$ and $^{***}p < 0.001$ compared to control group; $\nabla\nabla\nabla p < 0.001$ compared to METH-treated cells (as determined by ANOVA followed by Sidak's post-hoc test).

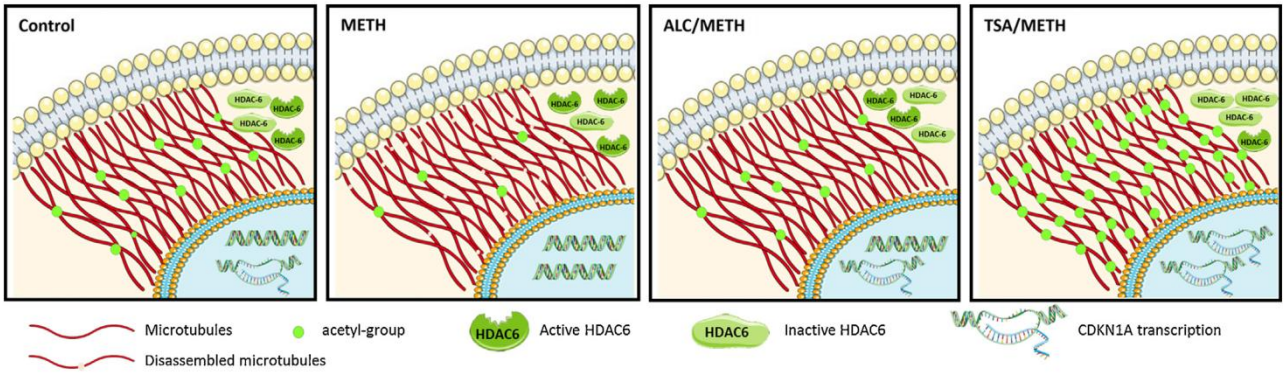

Fig. 5. Schematic representation of METH-induced deacetylation of microtubules, which is-prevented by ALC. METH induces α-tubulin deacetylation through modulation of HDAC6 activity. Microtubules deacetylation is represented by disassembly patterns previously described (Matsuyama et al., 2002; Perdiz et al., 2011). ALC pretreatment prevents METH-induced deacetylation, resulting in higher levels of α-tubulin acetylation (ALC/METH). Compared to the strong HDACs inhibition obtained with TSA, the protective action provided by ALC preserves microtubule acetylation without promoting hyperacetylation and increased transcription of CDKN1A (p21) (TSA/METH).

HDACs inhibitor TSA (Dompierre et al., 2007). Our results evidence that TSA not only prevents METH-induced deacetylation, as it strongly promotes α-tubulin acetylation also in METH-exposed endothelial cells.

TSA-mediated hyperacetylation was shown to increase the lifespan of neuronal cultures, and a number of studies reported the anti-inflammatory and neuroprotective effects of hyperacetylation both *in vitro* or *in vivo* models of ischemic stroke (Chuang et al., 2009; Harrison and Dexter, 2013) and toxicity (Agudelo et al., 2011). TSA was also used as a neuroprotective agent in several models of Parkinsonism (Harrison and Dexter, 2013), Huntington's disease, Alzheimer's disease and other neurological diseases (Chuang et al., 2009). In the oncology context, TSA has been intensively studied. Of note, a recent study showed that TSA inhibits cancer invasion through MMPs inhibition associated with HDAC2 suppression (Wang et al., 2013). As we have recently shown that METH disrupts actin integrity through MMP-9 modulation, it is possible that MMPs inhibition may also contribute to prevent METH-induced deacetylation of tubulin. However, as prolonged treatment with TSA may lead to neuronal cell toxicity, care should be taken when TSA is used for neuroprotective purposes (Chuang et al., 2009).

Since we have recently shown that ALC counteracts the effect of METH in MMP-mediated toxicity, we have also addressed the possible role of ALC in preventing METH-modulation of HDACs. As a result, in the present work, we show that 1 mM ALC was able to prevent METH-induced deacetylation of α-tubulin. A previous report postulated that ALC had the potential to directly inhibit HDACs activity in several cell types possibly by chelating and removing Zn^{2+} from the active site of the HDAC enzyme (Huang et al., 2012). However, here, we could not observe a significant effect of ALC on HDACs activity. Of note, the doses used by Huang et al. (2012) were 5 and 10 fold higher than the 1 mM dose shown here to efficiently prevent tubulin deacetylation. In addition, neither METH nor ALC led to altered levels of HDAC6 gene expression, which seems to indicate that both ALC- and METH-modulation of HDAC6 activity may occur in a post-translation way, as described for TSA (Xu et al., 2007). Despite the previously reported protective properties of ALC (Pettegrew et al., 2000), its action at the cytoskeleton level is still poorly explored. We have recently shown that ALC effectively prevents METH-induced loss of alignment in endothelial actin filaments, through ILK mediated release of MMP-9 (Fernandes et al., 2014). Of note, ILK was also shown to mediate MMP-9-release through regulation of glycogen synthase (GSK)-3β activity (for review see McDonald et al., 2008), while GSK-3β is known to interact and colocalize with HDAC6, enhancing its activity (Li et al., 2013). Since it was reported that ALC antagonizes GSK-3β, arresting microtubule-associated protein tau hyperphosphorylation in Alzheimer's disease (Jiang et al., 2011), it is possible that ALC mediation of HDAC6 activity may also occur through GSK-3β inhibition. This putative mechanism of action is essentially different from that of TSA that may inhibit HDCAs by binding to zinc in their catalytic site (Finnin et al., 1999).

In addition to hyperacetylation of the respective substrates, HDACs inhibition is also known to lead to increased histone acetylation and consequent chromatin remodeling (Li et al., 2013; Xu et al., 2007). Under TSA treatment, chromatin relaxation is known to increase the expression of CDKN1A (cyclin-dependent kinases inhibitor, or p21) gene (Blagosklonny et al., 2002; Hrabeta et al., 2014; Ocker and Schneider-Stock, 2007; Xu et al., 2007). As such, CDKN1A (p21) expression is frequently used as a marker of HDAC inhibition (Harrison and Dexter, 2013; Huang et al., 2012; Xu et al., 2007). As expected our results show that TSA promotes the overexpression of CDKN1A. Opposing to this, in METH-exposed cells, CDKN1A expression was clearly reduced, which was counteracted by ALC and TSA. These results show that in the presence of METH, both ALC and TSA seem to maintain CDKN1A expression at levels that are not significantly different from the control. However, contrarily to TSA, ALC does not trigger CDKN1A overexpression, which has been repeatedly associated with cell cycle arrest, senescence and cell death (reviewed by Xu et al., 2007). In that sense, the protection afforded through ALC may be more effective and lead to less severe side effects.

In summary, we show here for the first time that METH promotes deacetylation of α-tubulin, which is likely to impact the structure of microtubules at the endothelial cytoskeleton and disturb the BBB function. Additionally, we show also that ALC is able to prevent METH-induced deacetylation, providing effective protection of microtubules acetylation, without risking the critical consequences of HDACs inhibition (Fig. 5). Although further investigation is still needed, HDACs regulation may become a new therapeutic target for ALC.

Conflict of interest

The authors declare that there are no conflicts of interest.

Transparency document

The Transparency document associated with this article can be found in the online version.

References

Agudelo, M., Gandhi, N., Saiyed, Z., Pichili, V., Thangavel, S., Khatavkar, P., Yndart-Arias, A., Nair, M., 2011. Effects of alcohol on histone deacetylase 2 (HDAC2) and the neuroprotective role of trichostatin A (TSA). Alcohol. Clin. Exp. Res. 35, 1550–1556. doi:http://dx.doi.org/10.1111/j.1530-0277.2011.01492.x.

Alves, E., Binienda, Z., Carvalho, F., Alves, C.J., Fernandes, E., de Lourdes Bastos, M., Tavares, M.A., Summavielle, T., 2009. Acetyl-L-carnitine provides effective in vivo neuroprotection over 3,4-methylenedioximethamphetamine-induced mitochondrial neurotoxicity in the adolescent rat brain. Neuroscience 158, 514–523. doi:http://dx.doi.org/10.1016/j.neuroscience.2008.10.041.

Blagosklonny, M.V., Robey, R., Sackett, D.L., Du, L., Traganos, F., Darzynkiewicz, Z., Fojo, T., Bates, S.E., 2002. Histone deacetylase inhibitors all induce p21 but differentially cause tubulin acetylation, mitotic arrest, and cytotoxicity. Mol. Cancer Ther. 1, 937–941.

Bogatcheva, N.V., Adyshev, D., Mambetsariev, B., Moldobaeva, N., Verin, A.D., 2007. Involvement of microtubules, p38, and rho kinases pathway in 2-methoxyestradiol-induced lung vascular barrier dysfunction. Am. J. Physiol. 292, L487–L499. doi:http://dx.doi.org/10.1152/ajplung.00217.2006.

Cassel, S., Carouge, D., Gensburger, C., Anglard, P., Burgun, C., Dietrich, J.B., Aunis, D., Zwiller, J., 2006. Fluoxetine and cocaine induce the epigenetic factors MeCP2 and MBD1 in adult rat brain. Mol. Pharmacol. 70, 487–492. doi:http://dx.doi.org/10.1124/mol.106.022301.

Chuang, D.M., Leng, Y., Marinova, Z., Kim, H.J., Chiu, C.T., 2009. Multiple roles of HDAC inhibition in neurodegenerative conditions. Trends Neurosci. 32, 591–601. doi:http://dx.doi.org/10.1016/j.tins.2009.06.002.

Conant, K., Lonskaya, I., Szklarczyk, A., Krall, C., Steiner, J., Maguire-Zeiss, K., Lim, S.T., 2011. Methamphetamine-associated cleavage of the synaptic adhesion molecule intercellular adhesion molecule-5. J. Neurochem. 118, 521–532. doi:http://dx.doi.org/10.1111/j.1471-4159.2010.07153.x.

Dietrich, J.B., 2009. Alteration of blood-brain barrier function by methamphetamine and cocaine. Cell Tissue Res. 336, 385–392. doi:http://dx.doi.org/10.1007/s00441-009-0777-y.

Dompierre, J.P., Godin, J.D., Charrin, B.C., Cordelieres, F.P., King, S.J., Humbert, S., Saudou, F., 2007. Histone deacetylase 6 inhibition compensates for the transport deficit in Huntington's disease by increasing tubulin acetylation. J. Neurosci. 27, 3571–3583. doi:http://dx.doi.org/10.1523/JNEUROSCI.0037-07.2007.

Fernandes, S., Salta, S., Bravo, J., Silva, A.P., Summavielle, T., 2014. Acetyl-L-carnitine prevents methamphetamine-induced structural damage on endothelial cells via ILK-related MMP-9 activity. Mol. Neurobiol. 1–15. doi:http://dx.doi.org/10.1007/s12035-014-8973-5.

Finnin, M.S., Donigian, J.R., Cohen, A., Richon, V.M., Rifkind, R.A., Marks, P.A., Breslow, R., Pavletich, N.P., 1999. Structures of a histone deacetylase homologue bound to the TSA and SAHA inhibitors. Nature 401, 188–193. doi:http://dx.doi.org/10.1038/43710.

Gold, M.S., Kobeissy, F.H., Wang, K.K., Merlo, L.J., Bruijnzeel, A.W., Krasnova, I.N., Cadet, J.L., 2009. Methamphetamine- and trauma-induced brain injuries: comparative cellular and molecular neurobiological substrates. Biol. Psychiat. 66, 118–127. doi:http://dx.doi.org/10.1016/j.biopsych.2009.02.021.

Gold, W.A., Lacina, T.A., Cantrill, L.C., Christodoulou, J., 2015. MeCP2 deficiency is associated with reduced levels of tubulin acetylation and can be restored using HDAC6 inhibitors. J. Mol. Med. 93, 63–72. doi:http://dx.doi.org/10.1007/s00109-014-1202-x.

Goncalves, J., Baptista, S., Martins, T., Milhazes, N., Borges, F., Ribeiro, C.F., Malva, J.O., Silva, A.P., 2010. Methamphetamine-induced neuroinflammation and neuronal dysfunction in the mice hippocampus: preventive effect of indomethacin. Eur. J. Neurosci. 31, 315–326. doi:http://dx.doi.org/10.1111/j.1460-9568.2009.07059.x.

Gorshkov, B.A., Zemskova, M.A., Verin, A.D., Bogatcheva, N.V., 2012. Taxol alleviates 2-methoxyestradiol-induced endothelial permeability. Vasc. Pharmacol. 56, 56–63. doi:http://dx.doi.org/10.1016/j.vph.2011.10.002.

Hammond, J.W., Cai, D.W., Verhey, K.J., 2008. Tubulin modifications and their cellular functions. Curr. Opin. Cell Biol. 20, 71–76. doi:http://dx.doi.org/10.1016/j.ceb.2007.11.010.

Haorah, J., Floreani, N.A., Knipe, B., Persidsky, Y., 2011. Stabilization of superoxide dismutase by acetyl-L-carnitine in human brain endothelium during alcohol exposure: novel protective approach. Free Rad. Biol. Med. 51, 1601–1609. doi:http://dx.doi.org/10.1016/j.freeradbiomed.2011.06.020.

Harrison, I.F., Dexter, D.T., 2013. Epigenetic targeting of histone deacetylase: therapeutic potential in Parkinson's disease? Pharmacol. Ther. 140, 34–52. doi:http://dx.doi.org/10.1016/j.pharmthera.2013.05.010.

Host, L., Dietrich, J.-B., Carouge, D., Aunis, D., Zwiller, J., 2011. Cocaine self-administration alters the expression of chromatin-remodelling proteins; modulation by histone deacetylase inhibition. J. Psychopharmacol. (Oxford. England) 25, 222–229. doi:http://dx.doi.org/10.1177/0269881109348173.

Hrabeta, J., Stiborova, M., Adam, V., Kizek, R., Eckschlager, T., 2014. Histone deacetylase inhibitors in cancer therapy. A review. Biomed. Pap. Med. Fac. Univ. Palacky, Olomouc, Czechoslovakia 158, 161–169. doi:http://dx.doi.org/10.5507/bp.2013.085.

Huang, H., Liu N, Guo H., Liao, S., Li, X., Yang, C., Song, Liu S., W, Liu C., Guan, L., Li, B., Xu, L., Zhang, C., Wang, X., Dou Q.P, Liu J., 2012. L-Carnitine is an endogenous HDAC inhibitor selectively inhibiting cancer cell growth in vivo and in vitro. PloS One 7, e49062. doi:http://dx.doi.org/10.1371/journal.pone.0049062.

Hubbert, C., Guardiola, A., Shao, R., Kawaguchi, Y., Ito, A., Nixon, A., Yoshida, M., Wang, X.-F., Yao, T.-P., 2002. HDAC6 is a microtubule-associated deacetylase. Nature 417, 455–458.

Jayanthi, S., McCoy, M.T., Chen, B., Britt, J.P., Kourrich, S., Yau, H.J., Ladenheim, B., Krasnova, I.N., Bonci, A., Cadet, J.L., 2014. Methamphetamine downregulates striatal glutamate receptors via diverse epigenetic mechanisms. Biol. Psych. 76, 47–56. doi:http://dx.doi.org/10.1016/j.biopsych.2013.09.034.

Jiang, X., Tian, Q., Wang, Y., Zhou, X.W., Wang, Xie J.Z., J.Z, Zhu L.Q., 2011. Acetyl-L-carnitine ameliorates spatial memory deficits induced by inhibition of phosphoinositol-3 kinase and protein kinase C. J. Neurochem. 118, 864–878. doi:http://dx.doi.org/10.1111/j.1471-4159.2011.07355.x.

Jin, C.H., Moo, T.T., Youn, C.S., Sun, Y.J., Joo-Il, K., Sook, H.E., Onyou, H., 2002. Methamphetamine-induced apoptosis in a CNS-derived catecholaminergic cell Line. Mol. Cells 13, 221–227.

Kousik, S.M., Napier, T.C., Carvey, P.M., 2012. The effects of psychostimulant drugs on blood brain barrier function and neuroinflammation. Front. Pharmacol. 3, 121. doi:http://dx.doi.org/10.3389/fphar.2012.00121.

Krasnova, I.N., Cadet, J.L., 2009. Methamphetamine toxicity and messengers of death. Brain Res. Rev. 60, 379–407. doi:http://dx.doi.org/10.1016/j.brainresrev.2009.03.002.

Li, Y., Shin, D., Kwon, S.H., 2013. Histone deacetylase 6 plays a role as a distinct regulator of diverse cellular processes. FEBS J. 280, 775–793. doi:http://dx.doi.org/10.1111/febs.12079.

Martin, T.A., Jayanthi, S., McCoy, M.T., Brannock, C., Ladenheim, B., Garrett, T., Lehrmann, E., Becker, K.G., Cadet, J.L., 2012. Methamphetamine causes differential alterations in gene expression and patterns of histone acetylation/hypoacetylation in the rat nucleus accumbens. PloS One 7, e34236. doi:http://dx.doi.org/10.1371/journal.pone.0034236.

Martins, T., Baptista, S., Goncalves, J., Leal, E., Milhazes, N., Borges, F., Ribeiro, C.F., Quintela, O., Lendoiro, E., Lopez-Rivadulla, M., Ambrosio, A.F., Silva, A.P., 2011. Methamphetamine transiently increases the blood-brain barrier permeability in the hippocampus: role of tight junction proteins and matrix metalloproteinase-9. Brain Res. 1411, 28–40. doi:http://dx.doi.org/10.1016/j.brainres.2011.07.013.

Martins, T., Burgoyne, T., Kenny, B.A., Hudson, N., Futter, C.E., Ambrosio, A.F., Silva, A.P., Greenwood, J., Turowski, P., 2013. Methamphetamine-induced nitric oxide promotes vesicular transport in blood-brain barrier endothelial cells. Neuropharmacology 65, 74–82. doi:http://dx.doi.org/10.1016/j.neuropharm.2012.08.021.

Matsuyama, A., Shimazu, T., Sumida, Y., Saito, A., Yoshimatsu, Y., Seigneurin-Berny, D., Osada, H., Komatsu, Y., Nishino, N., Khochbin, S., Horinouchi, S., Yoshida, M., 2002. In vivo destabilization of dynamic microtubules by HDAC6-mediated deacetylation. EMBO J. 21, 6820–6831.

McDonald, P.C., Fielding, A.B., Dedhar, S., 2008. Integrin-linked kinase?essential roles in physiology and cancer biology. J. Cell Sci. 121, 3121–3132. doi:http://dx.doi.org/10.1242/jcs.017996.

Muneer, P.M.A., Alikunju, S., Szlachetka, A.M., Haorah, J., 2011. Methamphetamine inhibits the glucose uptake by human neurons and astrocytes: stabilization by acetyl-L-carnitine. PloS One 6, e19258. doi:http://dx.doi.org/10.1371/journal.pone.0019258.

Nahhas, F., Dryden, S.C., Abrams, J., Tainsky, M.A., 2007. Mutations in SIRT2 deacetylase which regulate enzymatic activity but not its interaction with HDAC6 and tubulin. Mol. Cell. Biochem. 303, 221–230. doi:http://dx.doi.org/10.1007/s11010-007-9478-6.

Northrop, N.A., Yamamoto, B.K., 2012. Persistent neuroinflammatory effects of serial exposure to stress and methamphetamine on the blood-brain barrier. J. Neuro. Pharmacol. 7, 951–968. doi:http://dx.doi.org/10.1007/s11481-012-9391-y.

Ocker, M., Schneider-Stock, R., 2007. Histone deacetylase inhibitors: signalling towards p21cip1/waf1. Int. J. Biochem. Cell Biol. 39, 1367–1374. doi:http://dx.doi.org/10.1016/j.biocel.2007.03.001.

Omonijo, O., Wongprayoon, P., Ladenheim, B., McCoy, M.T., Govitrapong, P., Jayanthi, S., Cadet, J.L., 2014. Differential effects of binge methamphetamine injections on the mRNA expression of histone deacetylases (HDACs) in the rat striatum. Neurotoxicology 45, 178–184. doi:http://dx.doi.org/10.1016/j.neuro.2014.10.008.

Park, M., Kim, H.J., Lim, B., Wylegala, A., Toborek, M., 2013. Methamphetamine-induced occludin endocytosis is mediated by the Arp2/3 complex-regulated actin rearrangement. J. Biol. Chem. 288 (33), 33324–33334. doi:http://dx.doi.org/10.1074/jbc.M113.483487.

Perdiz, D., Mackeh, R., Pous, C., Baillet, A., 2011. The ins and outs of tubulin acetylation: more than just a post-translational modification? Cell. Signal. 23, 763–771. doi:http://dx.doi.org/10.1016/j.cellsig.2010.10.014.

Pettegrew, J., Levine, J., McClure, R., 2000. Acetyl-L-carnitine physical-chemical, metabolica, and therapeutic properties: relevance for its mode of action in Alzheimer's disease and geriatric depression. Mol. Psychiat. 5, 616–632.

Ramirez, S.H., Potula, R., Fan, S., Eidem, T., Papugani, A., Reichenbach, N., Dykstra, H., Weksler, B.B., Romero, I.A., Couraud, P.O., Persidsky, Y., 2009. Methamphetamine disrupts blood-brain barrier function by induction of oxidative stress in brain endothelial cells. J. Cereb. Blood Flow Metab. 29, 1933–1945. doi:http://dx.doi.org/10.1038/jcbfm.2009.112.

Sadoul, K., Wang, J., Diagouraga, B., Khochbin, S., 2011. 2011. The tale of protein lysine acetylation in the cytoplasm. J. Biomed. Biotechnol. 970, 382. doi:http://dx.doi.org/10.1155/2011/970382.

Saito, S., Lasky, J.A., Nguyen, H., Danchuk, S., Sullivan, D.E., Shan, B., 2011. Pharmacological inhibition of HDAC6 attenuates endothelial barrier dysfunction induced by thrombin. Biochem. Biophys. Res. Commun. 408, 630–634. doi:http://dx.doi.org/10.1016/j.bbrc.2011.04.075.

Song, Y., Brady, S.T., 2014. Post-translational modifications of tubulin: pathways to functional diversity of microtubules. Trends Cell Biol. doi:http://dx.doi.org/10.1016/j.tcb.2014.10.004.

Szyk, A., Deaconescu, A.M., Spector, J., Goodman, B., Valenstein, M.L., Ziolkowska, N. E., Kormendi, V., Grigorieff, N., Roll-Mecak, A., 2014. Molecular basis for age-dependent microtubule acetylation by tubulin acetyltransferase. Cell 157, 1405–1415. doi:http://dx.doi.org/10.1016/j.cell.2014.03.061.

Tu, C.Y., Chen, C.H., Hsia, T.C., Hsu, H., Wei, L., Yu, M.C., Chen, W.S., Hsu, W., Yeh, H., Liu, C., Chen, Y.J., Huang, W.C., 2014. Trichostatin A suppresses EGFR expression through induction of micro RNA-7 in an HDAC-independent manner in lapatinib-treated cells. Biomed. Res. Int. 2014 doi:http://dx.doi.org/10.1155/2014/168949.

Urrutia, A., Rubio-Araiz, A., Gutierrez-Lopez, M.D., ElAli, A., Hermann, D.M., O'Shea, E., Colado, M.I., 2013. A study on the effect of JNK inhibitor, SP600125, on the disruption of blood-brain barrier induced by methamphetamine. Neurobiol. Dis. 50, 49–58. doi:http://dx.doi.org/10.1016/j.nbd.2012.10.006.

Wang, F., Qi, Y., Li, X., He, W., Fan, Q.X., Zong, H., 2013. HDAC inhibitor trichostatin A suppresses esophageal squamous cell carcinoma metastasis through HADC2 reduced MMP-2/9. Clin. Invest. Med. 36, E87–E94.

Xu, W.S., Parmigiani, R.B., Marks, P.A., 2007. Histone deacetylase inhibitors: molecular mechanisms of action. Oncogene 26, 5541–5552. doi:http://dx.doi.org/10.1038/sj.onc.1210620.

Yang, X.J., Seto, E., 2008. Lysine acetylation: codified crosstalk with other posttranslational modifications. Mol. Cell 31, 449–461. doi:http://dx.doi.org/10.1016/j.molcel.2008.07.002.

Young, E.J., Aceti, M., Griggs, E.M., Fuchs, R.A., Zigmond, Z., Rumbaugh, G., Miller, C. A., 2014. Selective, retrieval-independent disruption of methamphetamine-associated memory by actin depolymerization. Biol. Psychiat. 75, 96–104. doi:http://dx.doi.org/10.1016/j.biopsych.2013.07.036.

General Discussion and Future Perspectives

“Learn from yesterday, live for today, hope for tomorrow.

The important thing is to not stop questioning.”

Albert Einstein

1. General discussion

The interaction between the endothelium and the glial cells supporting neuronal function has gained increasing interest in the regulation of the BBB over the last few years. Impairment of BBB permeability has been strongly implicated in several pathologies such as stroke, trauma, multiple sclerosis, Alzheimer's disease, Parkinson's disease, epilepsy and brain tumors (Singh and Harris 2004; Abbott, Ronnback et al. 2006). Of particular interest is the similarity between BBB dysregulation caused by exposure to amphetamines and the neurophysiology and molecular pathology of some of the above mentioned neurological disorders (O'Shea, Urrutia et al. 2014). Psychostimulant drugs such as METH have been extensively studied in regard to their strong impact in the brain. BBB is also recognized as a target for METH action, which adds to its neurotoxicity (Dietrich 2009; O'Shea, Urrutia et al. 2014).

Due to the high prevalence of METH abuse throughout the world, it is important to unveil protection strategies to this neurotoxic compound. Among METH-induced neurotoxic effects, BBB dysfunction is a relevant one, since it can contribute to the development of other neurodegenerative pathologies and has been associated with other problems such as HIV-related dementia (Mahajan, Aalinkeel et al. 2008; Reynolds, Mahajan et al. 2011). Data provided by recent investigation show that the prevention or reversion of BBB dysfunction could be a useful therapeutic strategy in conditions in which neuronal insult is secondary to BBB damage (Abbott, Ronnback et al. 2006; Dietrich 2009).

The molecular mechanisms underlying METH effect on the BBB remain poorly explored. In this work, the *in vivo* screening of gene alteration after METH exposure was an important first step to better address METH action on signaling pathways regulating cytoskeleton and permeability events. These data provided preliminary clues on targets that could be involved in BBB dysfunction after METH exposure, allowing a more focused *in vitro* approach. This led us to explore the ILK pathway and its modulation of MMPs release on the cytoskeleton of the endothelial cells and how ALC could counteract the action of METH in this paradigm. Within the neurovascular unit, endothelial cells are the key players for the tightness of the barrier, and for that reason our experimental *in vitro* approaches were here carried out using an endothelial cell line that mimics part of the barrier properties. It is commonly accepted that MMP-induced leakiness at the BBB is a critical event for the development of several neurological diseases (Singh and Harris 2004). Adding to previous reports from other authors, we provided evidence that METH-induced MMP-9 activity is in fact regulated via ILK. Importantly, there is evidence that, at least in the case of METH, increased MMPs activity may be related to increased behavioral sensitization and reward (Mizoguchi, Yamada et al. 2004; Mizoguchi, Yamada et al. 2008; O'Shea, Urrutia et al. 2014), which are important factors for the addictive process. This effect may be related with the reshaping of the neuronal connectivity (particularly in the dopaminergic system), but may also be connected to changes at the BBB level (Mizoguchi, Yamada et al. 2008; O'Shea, Urrutia et al. 2014).

Here, as already mentioned, we show that MMP-9 activation occurs through ILK increased expression, along with structural changes in F-actin arrangement and claudin-5 redistribution in the cell. We clarify that the METH-induced decreased TEER and increased permeability previously reported by other authors (Ramirez, Potula et al. 2009; Abdul Muneer, Alikunju et al. 2011) is associated with MMP-9-induced TJs disruption. These *in vitro* data is in accordance with the data obtained in our *in vivo* assays showing an up-regulation of ILK in the brain of METH-treated animals (Fernandes, Salta et al. 2014).

Moreover, we have shown that METH also promotes deacetylation of α-tubulin, which is likely to impact the microtubule structure of the endothelial cytoskeleton and bound to further contribute to BBB dysfunction. Indeed, it was previously shown that microtubules deacetylation was associated with increased vascular permeability (Bogatcheva, Adyshev et al. 2007), while microtubule acetylation seems to be concomitant with the inhibition of barrier-disruptive pathways (Saito, Lasky et al. 2011; Gorshkov, Zemskova et al. 2012). Furthermore, we show that these events are associated with METH-regulation of HDACs. HDACs modulation by psychostimulants was previously reported and seems to be dependent on both the period and pattern of exposure (Omonijo, Wongprayoon et al. 2014). In particular, the effect of METH in microtubules acetylation at the cytoplasmatic level seems to be modulated by HDAC6 and eventually also by SIRT2, since it was recently confirmed that interfering with one of this deacetylases is sufficient to impair microtubule deacetylation (Yang, Laurent et al. 2013). In accordance we showed that METH promotes deacetylation of α-tubulin, which is likely to impact the structure of microtubules at the endothelial cytoskeleton and disturb the BBB function (Fernandes, Salta et al. 2014).

It is possible that besides our findings concerning cytoskeleton remodeling, other parallel events may occur and contribute to the pathogenesis of METH-induced BBB. This is the case of previously reported oxidative stress and ROS, leading to leukocyte adhesion and vascular endothelial dysfunction (Dietrich 2009) and eNOS activation along with endocytosis across endothelial cells (Martins, Burgoyne et al. 2013; Park, Kim et al. 2013). Importantly, the role of microglia and astrocytes in this process is yet poorly explored, but likely to promote the release of extracellular factors capable to activating integrin receptors, triggering the cascade of events above described in endothelial cells.

One important finding in this study is related with the mechanism of action of ALC in preventing BBB damage. ALC was previously shown to prevent the adverse effects of alcohol-induced oxidative stress and METH-induced decreased glucose uptake (Rump, Abdul Muneer et al. 2010; Muneer, Alikunju et al. 2011; Muneer, Alikunju et al. 2011), but the molecular mechanisms involved were not addressed. Our work was the first to assess the mechanism of ALC as a neuroprotective agent over METH-induced impairment of BBB function. In this particular issue we conclude that a pretreatment with ALC prevented METH-induced ILK expression and clustering and the consequent activation of MMP-9, preserving claudin-5 location and the arrangement of the actin cytoskeleton in an endothelial cell line.

Another important finding is the effect of ALC on acetylation processes, presumably mediated by HDAC6. In fact, more than 10 years ago, evidence already pointed toward an effect of ALC on post-translation processes, instead of an effect centered at the mitochondria. *Pettegrew* and collaborators compiled information showing that although carnitine plays a role in the β-oxidation of fatty acids, the acetyl moiety of ALC could be used to maintain acetyl-CoA levels and also to acetylate -NH_2 and -OH functional groups in amino acids and possibly modify their structure, function, and turnover (for review Pettegrew, Levine et al. 2000). Based on this hypothesis, we investigated the ability of ALC to counteract the METH-induced decrease in acetylation levels on lysine residues of the α-tubulin cytoskeleton. We confirmed that ALC is capable of preventing the deacetylation of microtubules in endothelial cells exposed to METH. We hypothesize that this may also be related with the ALC effect on ILK modulation. ILK was shown to mediate MMP-9-release through regulation of GSK-3ß activity (for review see McDonald, Fielding et al. 2008), which in turn is known to interact and colocalize with HDAC6, enhancing its activity (Li, Shin et al. 2013). As there is evidence that ALC decreases GSK-3ß expression, it seems plausible that ALC mediation of HDAC6 activity may occur through GSK-3ß inhibition. This is an interesting discussion point, because although ALC was recently proposed to be able to interact with HDACs directly by binding to zinc in their catalytic site (Huang, Liu et al. 2012), as described for TSA (Finnin, Donigian et al. 1999), in our work we could not observe a direct inhibitory effect of ALC over HDACs. Of note, the doses used by *Huang* and collaborators were much higher and led high levels of cell death which is not desirable in a protectant substance.

With the present work we add important knowledge to the list of possible clinical applications for ALC. These features of ALC action are of further importance for future developments in the clinical management not only for drug abusers but also for patients suffering from other neurological disorders related with MMPs activation. Up on that, increased activity of MMPs is long known to be associated with tumor invasion and metastasis formation in several cancer types (Murphy, Ward et al. 1989; Johnsen, Lund et al. 1998); thus, we believe that ALC may become a useful target on development of selective inhibitors for MMPs, ILK and HDACs. Although further investigation is needed, our findings also show that ALC may be effective in reducing the activity of MMPs and HDACs without leading to severe co-effects, which rends it much less toxic than other treatments, such as TSA - a common inhibitor of HDACs that was associated with p21 increased expression leading to cell cycle arrest in both tumoral and normal cells (Westendorf, Zaidi et al. 2002). The hyperacetylation stage induced by compounds like TSA is still not well-characterized and is potentially harmful for the cell (Xu, Parmigiani et al. 2007). In that sense, the protection afforded through ALC may be more effective, leading to less severe side effects and be safely used for the purpose of HDACs inhibition.

However, as mentioned above, further investigation is still needed before ALC can be safely used. Of particular relevance, is the study of the potential consequences of administrating ALC to healthy subjects, since in our lab we have seen that this may lead to altered cognitive

performance, which seems to be associated with increased synthesis of neurotransmitters as ALC is rapidly incorporated into glutamine, glutamate and GABA synthesis via the tricarboxylic acid (TCA) cycle (Scafidi, Fiskum et al. 2010). To the moment, clinical studies carried out were not conclusive and do not allow to assess the whole effect of this compound. Although ALC is being already prescribed and seems to have a promising therapeutic potential in several pathological conditions, more studies are still necessary to a better characterize its action.

2. Global conclusion

In summary, this dissertation shows that METH may affect the BBB function through regulation of ILK expression, which is associated with MMP-9 increased release and TJs dysfunction in endothelial cells. Furthermore, METH-exposure leads to HDACs activation and microtubule deacetylation, which also maybe a result of METH action at the ILK level. Importantly, we were able to show that ALC effectively prevents all these events contributing to maintain the cytoskeleton of the endothelial cells, which is essential for a proper barrier function. Despite the studies yet necessary before ALC can be used at the therapeutic level, these results provide valuable pre-clinical data with relevant translational perspectives.

3. Future perspectives

The obvious next step of this work is to obtain *in vivo* confirmation of the presented results. This can be achieved using a rat or mice model of exposure to METH and ALC, followed by evaluation of permeability parameters in brain regions of interest. Behavioral analysis can also be conducted to distinguish between the use of ALC and other pharmacologic approaches (such as the use of tubacin, a specific HDAC6 inhibitor).

The role of GSK-3ß inhibition was not assessed in our endothelial model of exposure to METH. Overexpression of GSK3β *in vitro*, could reveal valuable insight into the mechanisms by which METH leads to of BBB dysfunction, since GSK3β inhibition was associated to a sustained increase in tightness of the barrier, with an increase of TJs on the membrane fraction (Ramirez, Fan et al. 2013). Understanding METH-modulation of this particular pathway, as well as the ability of ALC to counteract it will certainly allow a better comprehension of the events reported in the present work.

Another issue that deserves further attention is the endothelial–astrocytic interaction (as well as the pericytes) in the modulation of BBB function under METH exposure. It is possible that damage to the endothelium and basal lamina may trigger the expression of signaling components that are important in barrier repair (Abbott, Ronnback et al. 2006). The cross talk between endothelial cell and microglia may also be of interest, since this may modulate MMPs release. Our preliminary data strongly suggest that microglia *per se* does not react to METH

stimulus while conditioned medium from astrocytes exposed to METH, modulates microglial reactivity to this drug. In fact, all components of the neurovascular unit will be necessary to fully explain METH-induced damage in the BBB level.

Sophisticated methodologies were already designed to better mimic the functional properties of this very complex organ (Wilhelm, Fazakas et al. 2011; Naik and Cucullo 2012), but still need optimization to combine human brain-derived primary cultures for all cell types at the neurovascular unit, with a surrounding environment arranged in a 3D and dynamic apparatus. This model, along with sophisticated imaging tools will allow the assessment in real time to the function of this artificial BBB under METH-induced damage.

Although a lot of challenges still persist, the molecular mechanisms unveiled in the present study will certainly help the design of therapies to protect the BBB function in the context of neurological injury.

4. References

Abbott, N. J., L. Ronnback, et al. (2006). "Astrocyte-endothelial interactions at the blood-brain barrier." Nat Rev Neurosci **7**(1): 41-53.

Abdul Muneer, P. M., S. Alikunju, et al. (2011). "Impairment of brain endothelial glucose transporter by methamphetamine causes blood-brain barrier dysfunction." Mol Neurodegener **6**: 23.

Bogatcheva, N. V., D. Adyshev, et al. (2007). "Involvement of microtubules, p38, and Rho kinases pathway in 2-methoxyestradiol-induced lung vascular barrier dysfunction." Am J Physiol Lung Cell Mol Physiol **292**(2): L487-499.

Dietrich, J. B. (2009). "Alteration of blood-brain barrier function by methamphetamine and cocaine." Cell Tissue Res **336**(3): 385-392.

Fernandes, S., S. Salta, et al. (2014). "Acetyl-L-Carnitine Prevents Methamphetamine-Induced Structural Damage on Endothelial Cells via ILK-Related MMP-9 Activity." Mol Neurobiol: 1-15.

Finnin, M. S., J. R. Donigian, et al. (1999). "Structures of a histone deacetylase homologue bound to the TSA and SAHA inhibitors." Nature **401**(6749): 188-193.

Gorshkov, B. A., M. A. Zemskova, et al. (2012). "Taxol alleviates 2-methoxyestradiol-induced endothelial permeability." Vascul Pharmacol **56**(1-2): 56-63.

Huang, H., N. Liu, et al. (2012). "L-carnitine is an endogenous HDAC inhibitor selectively inhibiting cancer cell growth in vivo and in vitro." PLoS One **7**(11): e49062.

Johnsen, M., L. R. Lund, et al. (1998). "Cancer invasion and tissue remodeling: common themes in proteolytic matrix degradation." Current Opinion in Cell Biology **10**(5): 667-671.

Li, Y., D. Shin, et al. (2013). "Histone deacetylase 6 plays a role as a distinct regulator of diverse cellular processes." The FEBS journal **280**(3): 775-793.

Mahajan, S. D., R. Aalinkeel, et al. (2008). "Methamphetamine alters blood brain barrier permeability via the modulation of tight junction expression: Implication for HIV-1 neuropathogenesis in the context of drug abuse." Brain Res **1203**: 133-148.

Martins, T., T. Burgoyne, et al. (2013). "Methamphetamine-induced nitric oxide promotes vesicular transport in blood-brain barrier endothelial cells." Neuropharmacology **65**: 74-82.

McDonald, P. C., A. B. Fielding, et al. (2008). "Integrin-linked kinase--essential roles in physiology and cancer biology." J Cell Sci **121**(Pt 19): 3121-3132.

Mizoguchi, H., K. Yamada, et al. (2004). "Regulations of methamphetamine reward by extracellular signal-regulated kinase 1/2/ets-like gene-1 signaling pathway via the activation of dopamine receptors." Molecular pharmacology **65**(5): 1293-1301.

Mizoguchi, H., K. Yamada, et al. (2008). "Neuropsychotoxicity of Abused Drugs: Involvement of Matrix Metalloproteinase-2 and -9 and Tissue Inhibitor of Matrix Metalloproteinase-2 in Methamphetamine-Induced Behavioral Sensitization and Reward in Rodents." Journal of Pharmacological Sciences **106**(1): 9-14.

Muneer, P. M. A., S. Alikunju, et al. (2011). "Inhibitory effects of alcohol on glucose transport across the blood-brain barrier leads to neurodegeneration: preventive role of acetyl-L: -carnitine." Psychopharmacology (Berl) **214**(3): 707-718.

Muneer, P. M. A., S. Alikunju, et al. (2011). "Methamphetamine inhibits the glucose uptake by human neurons and astrocytes: stabilization by acetyl-L-carnitine." PloS one **6**(4): e19258-e19258.

Murphy, G., R. Ward, et al. (1989). "Characterization of gelatinase from pig polymorphonuclear leucocytes. A metalloproteinase resembling tumour type IV collagenase." Biochem. J **258**: 463-472.

Naik, P. and L. Cucullo (2012). "In vitro blood-brain barrier models: current and perspective technologies." J Pharm Sci **101**(4): 1337-1354.

O'Shea, E., A. Urrutia, et al. (2014). "Current preclinical studies on neuroinflammation and changes in blood-brain barrier integrity by MDMA and methamphetamine." Neuropharmacology **87C**: 125-134.

Omonijo, O., P. Wongprayoon, et al. (2014). "Differential effects of binge methamphetamine injections on the mRNA expression of histone deacetylases (HDACs) in the rat striatum." Neurotoxicology **45**: 178-184.

Park, M., H. J. Kim, et al. (2013). "Methamphetamine-induced occludin endocytosis is mediated by the Arp2/3 complex-regulated actin rearrangement." J Biol Chem **288**(46): 33324-33334.

Pettegrew, J. W., J. Levine, et al. (2000). "Acetyl-L-carnitine physical-chemical, metabolic, and therapeutic properties: relevance for its mode of action in Alzheimer's disease and geriatric depression." Molecular Psychiatry **5**(January): 616-632.

Ramirez, S. H., S. Fan, et al. (2013). "Inhibition of glycogen synthase kinase 3beta promotes tight junction stability in brain endothelial cells by half-life extension of occludin and claudin-5." PLoS One **8**(2): e55972.

Ramirez, S. H., R. Potula, et al. (2009). "Methamphetamine disrupts blood-brain barrier function by induction of oxidative stress in brain endothelial cells." J Cereb Blood Flow Metab **29**(12): 1933-1945.

Reynolds, J. L., S. D. Mahajan, et al. (2011). "Methamphetamine and HIV-1 gp120 effects on lipopolysaccharide stimulated matrix metalloproteinase-9 production by human monocyte-derived macrophages." Immunol Invest **40**(5): 481-497.

Rump, T. J., P. M. Abdul Muneer, et al. (2010). "Acetyl-L-carnitine protects neuronal function from alcohol-induced oxidative damage in the brain." Free Radic Biol Med **49**(10): 1494-1504.

Saito, S., J. A. Lasky, et al. (2011). "Pharmacological inhibition of HDAC6 attenuates endothelial barrier dysfunction induced by thrombin." Biochem Biophys Res Commun **408**(4): 630-634.

Scafidi, S., G. Fiskum, et al. (2010). "Metabolism of acetyl-L-carnitine for energy and neurotransmitter synthesis in the immature rat brain." J Neurochem **114**(3): 820-831.

Singh, A. B. and R. C. Harris (2004). "Epidermal growth factor receptor activation differentially regulates claudin expression and enhances transepithelial resistance in Madin-Darby canine kidney cells." Journal of Biological Chemistry **279**(5): 3543-3552.

Westendorf, J. J., S. K. Zaidi, et al. (2002). "Runx2 (Cbfa1, AML-3) Interacts with Histone Deacetylase 6 and Represses the p21CIP1/WAF1 Promoter." Molecular and Cellular Biology **22**(22): 7982-7992.

Wilhelm, I., C. Fazakas, et al. (2011). "In vitro models of the blood-brain barrier." Acta Neurobiol Exp (Wars) **71**(1): 113-128.
Xu, W. S., R. B. Parmigiani, et al. (2007). "Histone deacetylase inhibitors: molecular mechanisms of action." Oncogene **26**(37): 5541-5552.
Yang, M. H., G. Laurent, et al. (2013). "HDAC6 and SIRT2 regulate the acetylation state and oncogenic activity of mutant K-RAS." Molecular Cancer Research **11**(9): 1072-1077.

Summary and conclusions

Summary and conclusions

Methamphetamine (METH) is a powerful psychostimulant drug used worldwide for its reinforcing properties. In addition to the classic long-lasting monoaminergic-disrupting effects extensively described in the literature, evidence strongly suggests the involvement of METH in cytoskeleton-mediated permeability. Indeed, METH has been consistently reported to increase blood-brain barrier (BBB) permeability, both *in vivo* and *in vitro*, leading to compromised function. As BBB dysfunction is a pathological feature of many neurological conditions, unveiling new protective agents in this field is of major relevance. Acetyl-L-carnitine (ALC) has been described to protect the BBB function in different paradigms, but the mechanisms underlying its action remain mostly unknown.

Using an *in vivo* model of METH-treated mice, we focused on the phosphatidylinositol 3-kinase/AKT signaling pathway to identify possible molecular targets in cytoskeleton-mediated permeability. We performed an array that allowed the identification of particular genes within this pathway that displayed altered striatal expression as a consequence of METH-exposure. These experiments allowed to verify that METH may alter the expression of relevant proteins that could be involved in the signaling pathways that are triggered by METH, paving the way to define which pathways deserved further attention in our study. ILK was one of those targets. Interestingly, nothing was known on how METH could affect ILK expression. We were particularly interested in exploring the modulation of matrix metalloproteinases (MMPs), since the involvement of the MMPs in the degradation of the neurovascular matrix components and tight junctions (TJs) is one of the most recent findings in METH-induced toxicity. Moreover, as there is evidence that psychostimulants drugs modulate the expression of histone deacetylases (HDACs) controlling post-translational changes in the cytoskeleton, and having in mind the impact of the tubulin cytoskeleton in critical cellular functions, we hypothesized that METH-mediation of cytoplasmatic HDAC6 activity could affect tubulin acetylation and further contribute to BBB dysfunction.

In order to assess the neuroprotective features of ALC in METH-induced damage, we used the immortalized bEnd.3 cell line. Cells were exposed to ranging concentrations of METH and the protective effect of ALC 1mM was assessed 24 hours after treatment. This dose of ALC was previously selected in our laboratory. F-actin rearrangement, TJs expression and distribution, and MMPs activity were evaluated. Integrin-linked kinase (ILK) knockdown cells were used to assess the role of ALC in ILK mediation of METH-triggered MMPs' activity. Moreover, α-tubulin acetylation and the activity of HDACs were also assessed.

Our *in vitro* results clearly show that METH led to disruption of the actin filaments concomitant with claudin-5 translocation to the cytoplasm. These events were mediated by MMP-9 activation in association with ILK overexpression. Pretreatment with ALC prevented METH-induced activation of MMP-9, preserving claudin-5 location and the structural arrangement of the actin filaments. Moreover, METH led to an extensive α-tubulin deacetylation mediated by HDACs activation, which was effectively prevented with a pretreatment with ALC.

Importantly, ILK was also shown to mediate MMP-9-release through regulation of glycogen synthase kinase (GSK)-3ß activity, which in turn seems to be necessary for HDAC6 activity, while ALC was reported to antagonize GSK-3ß, we hypothesize that ALC mediation of HDAC6 activity may occur through GSK-3ß inhibition.

Although further investigation is still needed, the present results support the potential of ALC in preserving BBB integrity, highlighting ILK and HDACs modulation as a new target for the ALC therapeutic use.

Resumo e conclusões

Resumo e conclusões

A metanfetamina (MA) é uma droga de ação psicoestimulante do sistema nervoso, usada em todo o mundo pelas suas propriedades de ação ao nível do sistema de recompensa. Para além do seu efeito clássico na integridade do sistema dopaminérgico, várias evidências sugerem o envolvimento da MA na permeabilidade mediada por alterações do citoesqueleto. De facto, tem sido frequentemente descrita a capacidade da MA em aumentar a permeabilidade da Barreira Hematoencefálica (BHE), quer *in vivo*, quer *in vitro,* resultando num comprometimento da sua função. Tendo em conta que a disfunção da BHE é uma característica de várias condições de patologia neurológica, o estudo de agentes protetores nesta área reveste-se de extrema importância. A acetil-L-carnitina (ALC) tem sido descrita como agente protetor da BHE em diferentes contextos, apesar do seu mecanismo de ação ser, ainda, praticamente desconhecido.

Através da utilização de um modelo *in vivo* de murganhos expostos a MA, este estudo focou-se na via de sinalização do fosfatidilinositol 3-cinase/AKT para identificar alvos moleculares reguladores da permeabilidade mediada por alterações do citoesqueleto. Para tal, procedeu-se à análise de um *array* que permitiu a identificação de genes pertencentes a esta via de sinalização que revelaram alterações de expressão ao nível do estriado, como consequência da exposição à MA. Estes ensaios permitiram verificar que a MA pode alterar a expressão de proteínas importantes da via sinalização sob a ação da droga, e desta forma foi possível definir quais as vias que requerem um estudo aprofundado. A cinase ligada à integrina (ILK) foi um dos alvos identificados. É importante salientar que até ao momento era completamente desconhecido o efeito da MA na expressão da ILK. Neste estudo, havia um interesse particular em explorar a modulação da atividade das metaloproteinases da matriz (MMPs), uma vez que o seu envolvimento na degradação dos componentes da matriz neurovascular e das junções de oclusão (JO) é um dos efeitos mais recentemente registados da toxicidade induzida pela MA. Para além disso, uma vez que há evidências de que as drogas de ação psicoestimulante modulam a expressão das histonas desacetilases (HDACs) que controlam alterações pós-tradução no citoesqueleto, e considerando que o citoesqueleto de tubulina desempenha funções críticas na célula, colocou-se a hipótese de que a atividade da HDAC6, citoplasmática, induzida pela MA, pudesse afetar a acetilação da tubulina e desta forma contribuir para a disfunção da BHE.

Com vista ao estudo das características neuroprotetoras da ALC nas alterações induzidas pela MA, usou-se uma linha celular imortalizada - bEnd.3. As células foram tratadas com MA em diferentes concentrações e a ação protetora de 1mM de ALC foi analisada 24 horas após o tratamento. A dose de ALC usada foi selecionada com base em estudos prévios no nosso laboratório. A organização do citoesqueleto de F-actina, a expressão e distribuição da localização das JO e a atividade das MMPs foram avaliadas. Foram igualmente usadas células onde foi induzido o silenciamento da expressão da ILK. Desta forma, foi possível estudar o papel da ALC na ILK enquanto mediadora da atividade das MMPs desencadeada pela MA.

Adicionalmente, procedeu-se à análise dos níveis de acetilação da α-tubulina, assim como da atividade das HDACs.

Os resultados obtidos nos nossos ensaios *in vitro* mostram claramente que a MA provoca a desorganização dos filamentos de actina e a translocação da claudina-5 para o citoplasma. Verificou-se, ainda, que estes eventos são mediados pela atividade da MMP-9 em associação com a sobre-expressão da ILK. Um pré-tratamento das células endoteliais com ALC previne a ativação da MMP-9 induzida pela MA, preservando a localização membranar da claudina-5 e a organização estrutural dos filamentos de actina. Para além disso, verificou-se que o tratamento com MA resulta num extensa desacetilação da α-tubulin mediada pela ativação das HDACs, processo que é efetivamente prevenido pelo pré-tratamento das células endoteliais com ALC.

É importante referir que a ILK já foi identificada como tendo um papel na ativação e libertação da MMP-9 através da regulação da atividade da glicogénio-sintase cinase 3ß (GSK-3ß), a qual, por sua vez, parece ser necessária para a atividade da HDAC6. Uma vez que já foi descrito que a ALC antagoniza a GSK-3ß, supomos que a mediação das HDACs por parte da ALC deve ocorrer via inibição da GSK-3ß.

Apesar de ser ainda necessária investigação adicional, os resultados apresentados nesta dissertação evidenciam claramente o potencial da ALC na preservação da integridade da BHE. Salienta-se a modulação da ILK e das HDACs como novos alvos para o uso da ALC a nível terapêutico.